11-9-2016

Salt-Water Aging, Bonding, and In-Service Performance of a Novel Poured Silicone Expansion Joint Sealant for Small Movement Bridges

Dominic Kruszewski
University of Connecticut - Storrs, dominic.kruszewski@uconn.edu

Salt-Water Aging, Bonding, and In-Service Performance of a Novel Poured Silicone Expansion Joint Sealant for Small Movement Bridges

Dominic Kruszewski

B.S., University of Connecticut, 2014

A Thesis

Submitted in Partial Fulfillment of the

Requirements for the Degree of

Master of Science

at the

University of Connecticut

2016

APPROVAL PAGE

Masters of Science Thesis

Salt-Water Aging, Bonding, and In-Service Performance of a Novel Poured Silicone Expansion Joint Sealant for Small Movement Bridges

Presented by

Dominic Kruszewski, B.S.

Major Advisor _____
Ramesh B. Malla

Associate Advisor_____
Montgomery T. Shaw

Associate Advisor_____
Kay Wille

University of Connecticut

2016

ACKNOWLEDGEMENTS

First and foremost, I would like to express my most sincere gratitude and appreciation to my major advisor, Dr. Ramesh B. Malla, for his unwavering guidance and support. When it seemed as though graduate school may not have been a possibility, Professor Malla granted me the opportunity to continue my studies and pursue my academic dreams. Through the toughest of times, he maintained a calm, rational and comforting demeanor with which I could not have completed my studies without. Professor Malla's unique mentorship and professionalism will resonate with me for the rest of my life.

I would also like to extend my thanks to Dr. Montgomery Shaw whose patience allowed me to push the boundaries of my work in ways I would not have thought. His experience in many fields set the standard for the experimental procedures and analysis throughout this research work. I also want to acknowledge Dr. Kay Wille, who provided positive support, insight and encouragement through many avenues.

I would like to thank the Connecticut Cooperative Transportation Research Program for sponsoring this research project and providing financial support towards the completion of this work. Additionally, I would like to acknowledge the Connecticut Department of Transportation, as well as the Technical Advisory Committee, who provided the means and professional support towards this project.

Finally, my deepest gratitude and appreciation to my family and friends who provided unwavering love, support and constant encouragement to help me complete this chapter of my life. Without them, none of this would have been possible.

TABLE OF CONTENTS

ABSTRACT

According to ASCE's 2013 Infrastructure Report Card, over 200 million trips are taken daily over a structurally deficient bridge in the United States. One of the most commonly observed degradation factors that contribute to compromising the structural integrity of bridges includes leaking expansion joints which allow water, debris and deicing corrosive materials to penetrate through to the substructure. These corrosive agents can significantly damage the bearing and other key components of the bridge, hindering the lifespan of the structure.

Currently, poured silicone sealant joint systems must be replaced every 2-3 years in Connecticut. A novel silicone foam sealant has been developed to provide a long term, cost effective sealing method for small movement expansion joints. The foam sealant, developed by chemically modifying the commercially available silicone sealant developed by Watson Bowman Acme Corp. (termed "solid sealant" herein), expands approximately 70% of its initial volume allowing for significant material savings compared to the existing product. Furthermore, the stress modulus of the foam sealant was observed to be significantly lower than that of the solid sealant, yielding reduced stresses at the interaction surface between the sealant and the substrate.

This research work presents the laboratory experiments conducted to compare the bonding properties of the foam and solid sealant, as detachment from the substrate is a major concern. Each experiment contained some combination of variables such as varying substrate materials and primer application. A five-month aging study was performed to observe the adhesion

characteristics of both sealants with and without the presence of road salt as a function of accelerated aging. The salt water aging experiment revealed that the application of primer onto the contact surface of the substrate yielded no significant difference in tensile and/or adhesion performance. The solid sealant's ultimate strain did not improve and the failure mode was almost always characteristically adhesive. Similarly, the ultimate strain of the foam sealant did not significantly change when primer was applied, and the cohesive failure mode was also consistent regardless of primer treatment. Both sealants, however, exhibited a reduced ultimate stress and while the ultimate strain increased as a function of aging.

Additionally, through the assistance of the Connecticut Department of Transportation, the foam sealant expansion joint system was installed on three bridges throughout the state to assess its performance under real conditions including environmental and vehicular effects. Both sealants were installed in a systematic manner to allow for direct comparison of their performance under the same conditions. Finally, field monitoring of the expansion joints was performed to understand the movement of each joint gap and determine whether the foam sealant can be considered as an effective sealing system under these demands while also monitoring the performance of the solid sealant. After several site visits, a few cohesive failures were observed in both sealants which were installed on the bridge with the largest joint gap. Two of these failures were located where the solid sealant was installed, while one failure occurred in the foam sealant. All three bridges are still undergoing consistent monitoring and visual inspection.

LIST OF FIGURES

LIST OF TABLES

1.0 INTRODUCTION

1.1 Background

According to the American Society of Civil Engineer's 2013 Infrastructure Report Card, about 200 million trips are taken daily over a structurally deficient bridge in the United States (ASCE, 2013). The rapidly deteriorating conditions of bridges can be largely attributed to leaky expansion joints. Expansion joints are important components in bridge structures which are used to accommodate bridge movements due to creep and shrinkage of concrete, temperature fluctuations, traffic loadings, and uneven settlement without imposing significant secondary stress to the superstructure (Dornsife 2000). Not only should expansion joints provide a watertight seal to protect the substructure from deicing chemicals and water, but they should also maintain this seal under the various movements that the bridge may experience.

Two failure modes are most often observed in bridge joints. The most common failure mode involves a compromise of the joint seal itself, allowing water and corrosive agents to flow under the deck and deteriorate the substructure. The second failure mode (which is less common) involves failure of the joint to accommodate the bridge deck movement, often due to thermal contraction and expansion. This failure is largely attributed to an improper design of the structure itself as opposed to a faulty joint. Expansion failure may result in upheaving of the road, damage to the abutment, and composite failure of the superstructure and the deck. When considering contraction failure, however, the entire deck can shift off the abutment, resulting in disaster.

Many hazards exist that, when in contact with the substructure, can degrade the integrity of the bridge itself including deicing salts and chemicals, cyclic movements due to vehicular loading, thermal contraction and expansion, vibrations of the structure, seismic hazards, and earth

pressures/settlement. In order for a bridge to accommodate induced movement, expansion joints are usually installed usually at supports or piers (although not always) to provide a seal to protect the substructure while allowing the structure to continuously move.

1.2 Research Motivation

Poured silicone sealant expansion joints are one of the more popular sealing systems used in Connecticut bridges, as most bridges found in Connecticut comprise of spans less than 120 feet. Spans this small correlate to joint gaps of less than 2 inches. The Connecticut Department of Transportation reported that the average lifespan of a poured silicone sealant expansion joint when used in new construction is approximately 7 years. However, when used for repairs or maintenance of old joints, poured silicone sealants joints last 3 years (Milner, 2014). Common issues with poured silicone sealant joints stem from inadequate surface preparation and poor installation procedures by maintenance crews. However, due to the low cost and easily installation of this type of joint, the silicone sealant remains an attractive option for transportation departments, especially when repairing small movement joints. Due to this continuous demand, the foam sealant formulation has been studied further to determine its bonding and adhesion characteristics to several substrates commonly found throughout the state of Connecticut (concrete, steel, polymer modified concrete).

1.3 Project Objectives

The objective of this research was to consider a previously developed silicone sealant for bridge expansion joints and conduct the following activities:

- Perform tension and adhesion testing to gain a better understanding of the tensile and adhesive properties of the foam sealant and compare them to those of the commercially

available silicone sealant, WaboSeal (Watson Bowman Acme, 2008). The influence of primer will be examined in order to gain a better understanding of whether it provides improved adhesion to the substrate under a laboratory setting

- Perform further laboratory testing to compare the tensile and adhesive properties of the foam and solid sealant under laboratory aging conditions. Specimens will be fabricated and submersed in warm oxygenated water to simulate extended aging. Specimens will also be exposed to deicing chemicals commonly found on Connecticut state roads in order to observe any deteriorating effects from both aging and salt.
- Develop an application procedure for in-service bridges and install the joint sealing system onto three Connecticut bridges with various traffic volumes and joint gaps. The expansion joints will be sealed in a systematic manner to allow for an in-service comparison of the performance of the commercially available sealant and newly developed foam sealant. This will determine if the foam sealant can be considered as a suitable alternative for small movement expansion joints.
- Conduct regular monitoring and observation of the foam and solid sealant under in-service conditions. Monitoring will include records of the joint gap width due to thermal contraction and expansion, acquisition of joint movement data as a function of vehicular traffic during on and off peak hours, and regular record keeping environmental conditions.

1.4 Classification of Bridge Joints

Expansion joints are commonly classified into three categories based on the range of total movement they can accommodate (Table 1). Small, medium and large movement joints should be designed to accommodate ranges up to 1.75 inches, 5 inches, and more than 5 inches, respectively.

Small range bridge joints include the butt joint (not typically used in Connecticut), the sliding plate joint, the compression seal, and poured silicone joints. Medium range joints include the strip seal and finger joint. Finally, large movement range joints include the plank seal and modular joint (and also larger finger joints).

Table 1: Classifications of Bridge Joints

Movement Range	Joint Type
Small Movement (0 - 1.75 inches)	Butt Joint Sliding Plate Joint Compression Seal Joint Asphaltic Plug Joint (APJ) Poured Silicone Seal
Medium Movement (1.75 - 5 inches)	Strip Seal Finger Joint
Large Movement (exceeding 5 inches)	Plank Seal Modular Joint

1.5 Literature Review

This section provides a literature review of the various types of bridge expansion joints used in modern construction and the advantages and disadvantages they deliver while accommodating for inherent deck movements.

The most basic type of joint, the butt joint (Figure 1), is typically used for movement less than 1 inch. The opening is provided between two rigid deck slabs which does not allow a smooth transition for traffic. Typical construction includes using a metal armoring (such as a steel angle embedded into the deck) which acts as the header. This protects the top edge of the deck from vehicle or plow impacts which may cause spalling or cracking. Advantages of the butt joint include simple and cost effective construction; the obvious downside, however, is that it easily allows penetration of water and deicing salts and chemicals, which can promote corrosion of the

substructure. This joint is often found in areas of the country that do not see snow (and therefore ice). It is also preferred that these joints be installed for very small movement bridges (i.e. less than 0.5 inches).

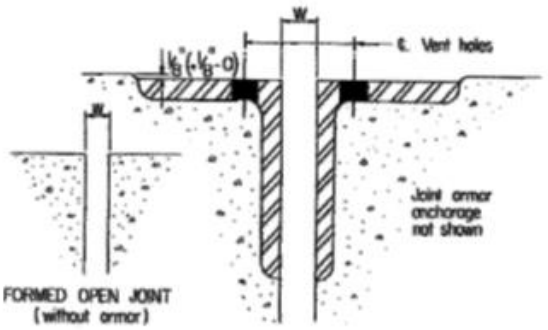

Figure 1: Typical butt joint (Burke, 1989)

Sliding plate joints (Figure 2) are typically used for movements between 1 and 3 inches and bridge deck spans up to 350 feet. They are simple in construction and are reasonably cost effective. The main idea behind sliding plate joints involves two overlapping steel plates being attached to the deck so that one of the plates is flush with the roadway. The plates slide against each other to accommodate various types of movements. These joints perform well against preventing debris from entering through to the substructure. Due to their reliable construction, they provide a good barrier for a long period of time. The down-side of the sliding plate joint, however, is that they do not provide an effective seal against water intrusion or deicing chemicals. Additionally, small particles of debris such as sand or glass can get stuck in between the plates and cause unwanted friction which may lead to wearing of the plates over time.

Figure 2: Typical sliding plate joint (Lesa Systems, 2016)

Compression seal joints (Figure 3) are comprised of continuous elastomeric sections with an internal web structure that allows for expansion and collapse of the seal to accommodate for deck movements between 0.25 to 2.5 inches. Since this seal is comprised of an elastomeric material, it is very flexible in accounting for horizontal and vertical deck movements. Additionally, the compression seal is effective in sealing the joint from water and debris infiltration. The down side of this joint, however, is that it is highly susceptible to damage from snowplows and other sharp debris. Additionally, this seal may lose its adhesion to the substrate.

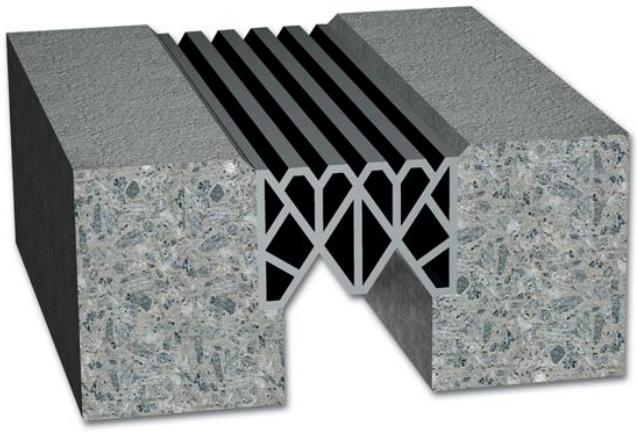

Figure 3: Typical compression seal joint (MM Systems, 2015)

Perhaps the most popular joint in New England (especially in Connecticut), the asphaltic plug joint, provides a watertight seal with essentially no traffic disruption. These joint can accommodate movement of up to 2 inches. Polymer-modified asphalt (PMA) is poured onto a backer rod which temporarily closes the gap between two bridge decks. Once the modified asphalt is sufficiently cured, it will accommodate traffic loadings and also thermal and impact loadings, as it has excellent contraction and expansion properties. The downside of APJ's is the softening and creeping of the material under high temperatures. This often leads to rutting and detachment of the asphalt from the substrate, resulting in an expensive cleaning and replacement process. In cold temperatures, the polymer-modified concrete can crack and thus allow for chemical penetration. The relaxation of the asphaltic plug joint should be sufficient to relieve the stress due to applied thermal displacement (Bramel et al., 2000). Additionally, asphaltic plug joints are not typically installed for vertical or skewed joints.

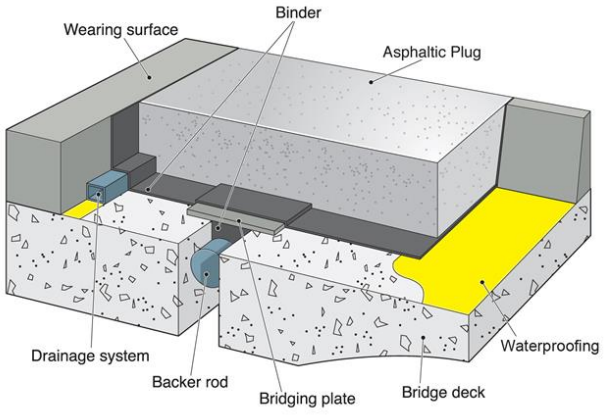

Figure 4: Typical asphaltic plug joint (Febajoint, 2015)

A typical poured silicone joint (Figure 5), which can accommodate bridge movements between 0.25 and 1.5 inches, is typically installed on shorter span bridges where the movement is minimal. Such joints consist of a backer rod inserted between two bridge decks onto which the silicone sealant is poured. The backer rod is typically made of compressible, temperature resistant, UV resistant foam to accommodate for various movements but still keep the silicone in place throughout the lifespan of the joint. Poured silicone sealant joints exhibit several advantages, including good durability, self-leveling action, strong elastic performance for a wide range of temperatures and UV exposures, and rapid curing (allowing for minimum traffic disruptions during installation). The most common down falls of the poured silicone joint, however, include detachment of the silicone from the substrate and damage to the silicone material due to accumulation of debris and salt.

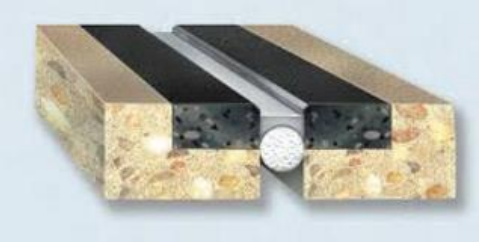

Figure 5: Typical poured silicone sealant joint (BASF, 2015)

A strip seal (Figure 6) typically consists of a "V" shape neoprene gland which is mechanically locked into a metal facing located on the header of the joint. Movement is accommodated by unfolding of the elastomeric gland. This gland provides a waterproof seal which protects the substructure of the bridge from water and road salts. However, if debris gets caught inside the gland, the joint becomes vulnerable to puncture when the gland closes during the

summer season when the bridge joint is narrowest. Additionally, faulty installation or dirty locking devices can cause pulling out of the gland from the metal rail edges.

Figure 6: Typical strip seal joint (D.S. Brown, 2015)

Finger joints (Figure 7), which are applicable for bridge movements of 3 inches or greater, are one of the most dependable expansion joints for larger movement bridges. They allow debris and water to enter, but the diaphragm that hangs between the two bridge decks catches any unwanted material and allows it to flow out to the sides of the bridge deck. Finger joints can accommodate for rotational and vertical movement, which may be crucial for medium movement bridges (especially in seismic regions). Some down sides of the finger joint, however, includes damage to the "fingers" themselves which may lead to them bending upwards. This can result in a rough bump for vehicles or puncturing of the tires. Additionally, the diaphragm that hangs below the roadway must be constantly cleaned to prevent buildup of debris. This operation may prove to be costly and time consuming.

Figure 7: Typical finger joint (Tensa, 2015)

Modular bridge joints (Figure 8), designed to accommodate bridge deck movements as large as 24 inches, are the most complex and expensive expansion joints. They are designed to provide a watertight seal while maintaining smooth wheel load transfer between decks. Since they can accommodate movement up to 24 inches, the joints themselves can be rather large, sometimes spanning over 5 feet. The system mainly comprises of a series of center beams supported atop support bars. The center beams are oriented parallel to the joint axis, while the support bars are placed parallel to the movement direction and are usually embedded into the concrete deck as a monolithic connection. Although these joints are capable of handling large thermal movements, which make them great candidates for long span bridges, the concerns raised with this type of joint include fatigue cracking of welds, damage to the neoprene sealer material, damage from snowplows, and debris getting caught in between the modules. Many departments are reluctant to use modular joints because of their high initial costs and expensive and tedious maintenance patterns.

Figure 8: Typical modular bridge joint (D.S. Brown, 2015)

1.6 Design of Bridge Expansion Joints

The American Association of State Highway and Transportation Officials (AASHTO) is the standards setting body which establishes protocols and guidelines which are used in the design and construction of highways in the United States. The 2012 version outlines procedures for the design and installation of expansion joints to accommodate movements due to temperature changes, creep and shrinkage, elastic shortening due to pre-stressing, traffic loading, construction tolerances, or other effects. The joints must be detailed to prevent damage to the structure from water, deicing chemicals, and roadway debris (AASHTO 2012). In order to determine the most applicable expansion joint, the anticipated movement of the bridge must be examined. Additionally, the designer must select the criteria for the joint regarding desired performance, durability, service life, maintenance requirements, joint details at the interface, initial costs, climate condition, installation procedures, life-cycle costs, and service level (Purvis 2003).

The most basic procedural step when selecting a suitable type of expansion joint is to assess the anticipated movement of the bridge deck due to thermal contraction and expansion, as this

phenomenon is inherent and must be accommodated for from the start. Thermal contraction and expansion will most likely produce the largest joint gap movement throughout the course of a year, especially in regions that experience seasonal temperature swings. The Connecticut Department of Transportation typically designs bridge joints to accommodate anticipated thermal movements due to temperature ranging from -10 to 110 degrees Fahrenheit (ConnDOT, 2015). This temperature range varies for each state, especially for states which experience more consistent climates than states which see all four seasons. Equation 1 shows the most common method of estimating total anticipated deck movement between a specific temperature range based on the material and span of the bridge.

$$\Delta_T = \alpha \cdot L_{deck} \cdot (T_{max} - T_{min}) \quad (1)$$

Table 2: Coefficient of Thermal Expansion for Various Materials

Material	Coefficient of Thermal Expansion (m/m/K)
Aluminum	22.2
Concrete	12
Iron	10.4
Rubber	77
Silicone	3
Steel	11

Table 2 shows that the coefficient of thermal expansion for steel and concrete is 11 and 12, respectively. These materials, the primary ones used in bridge construction throughout Connecticut, share a rather similar coefficient of thermal expansion, which results in a uniform movement of the composite section.

1.7 Structure of Report

Chapter 1 introduces the importance of expansion joints and bridges and outlines the various types of joints that can accommodate for a range of movements. This chapter also outlines the motivation behind the work presented in this thesis. Chapter 2 presents the laboratory tests that were conducted to gain a better understanding the silicone sealants' properties under tensile loadings. The tests were designed in such a way to evaluate the performance of both sealants with and without the presence of primer and road salt under controlled curing and accelerated aging. Several experiments are also outlined in this chapter which provide scientific information about the foam sealant. Chapter 3 describes the field implementation phase of the projects, where both sealants (foam and solid) were installed onto three in-service bridges throughout the state of Connecticut. The installation procedure was designed to allow for comparison of the performance of both sealants in a real-life scenario. Consequently, chapter 4 shows the field monitoring phase of the project which sheds light on the demands on the sealing system. A traffic counter was installed on one bridge to determine the vehicular demand on the joint, and displacement measuring devices were installed on two of the bridges in order to assess the movement of the structure itself.

2.0 LABORATORY TESTING

2.1 Background

Previous experiments conducted by Malla et al. (2007, 2011) included extensive laboratory testing on the foam sealant using the same formulation to understand better the mechanical behavior of the sealant. Mechanical properties such as shear strength and tensile strength have been assessed and compared to a commercially available solid sealant. Once basic properties were established, a closer examination of the results showed that the foam sealant typically failed cohesively (i.e. ripping of the silicone material) as opposed to the solid sealant, which failed adhesively (detachment from the substrate). Results also showed that the foam sealant exhibited a smaller modulus of elasticity while maintaining a comparable ultimate strain capacity. Because of the lower modulus of elasticity, the ultimate stress capacity was also lower than that of the solid sealant. Although a lower capacity may not be favorable in civil engineering materials, the ultimate capacity was achieved at an elongation of approximately 900%, which is much larger than what an average bridge gap will expand.

2.2 Experimental Motivation

Several state Department of Transportation agencies (Illinois, Connecticut among others) encourage the application of primer onto the substrate prior to installation of the silicone sealant, as it promotes a cleaner, oil-free surface onto which the sealant will bond (Temco, 2014). However, some manufacturers claim that no primer is needed with their product (Watson Bowman Acme, 2008). Little research has been conducted on the effectiveness of primer on the adhesion of silicone sealant joint systems, especially in bridge structure applications. Therefore, the inclusion of primer in laboratory experiments is of high interest.

In addition to the inclusion of primer, a primary concern for the degradation of silicone sealant joint systems is the effect of deicing chemicals, which are prevalent in Connecticut during the winter months. It has been well established that road salt corrodes and deteriorates concrete and steel. Due to silicone's excellent chemical resistance however, a key aspect of laboratory testing is to determine whether the bond between the silicone and concrete (typical header material) degrades under the presence of deicing chemicals such as sodium chloride and magnesium chloride, the two most common chemicals found on state roads during the winter (Connecticut Department of Transportation, 2015).

The motivation behind conducting laboratory testing was to observe the behavior of the foam sealant in contrast to the solid sealant with and without the presence of primer. Currently, specifications regard primer as being optional but encouraged; the true effect of the primer, however, is unknown. Therefore, the tension and adhesion test included specimens containing primer to determine how the sealant bonds to the substrate when primer is applied. Additionally, the aging experiment contained specimens with primer as well. A density test was conducted to determine the density of the foam sealant, as it is suspected that the foam sealant exhibits a lower density compared to the solid sealant because of the expansion effect. An expansion test was also conducted in order to quantify how much the foam sealant expands as a function of initial volume. Finally, a prototype joint was fabricated to test larger scale mixing and application to prepare for field installation. The results of all experiments are presented in the following section.

2.3 Overview of Foam Sealant Formulation

A poured silicone sealant expansion joint system previously developed by Malla et al. (2006, 2007, 2010, 2011) is considered as a suitable, cost effective joint sealing system that allows

for a long term sealing solution for smaller movement bridges. The sealant, termed "foam sealant" herein, is comprised of Wabo SiliconeSeal (a brand commonly used by the Connecticut Department of Transportation), water, crosslinker (Momentive Materials), and a platinum catalyst (Gelest, Inc.).

Without any additives, Wabo SiliconeSeal (termed "solid sealant" herein) produces a solid, rubber-like material; with the addition of the remaining ingredients, however, foaming of the silicone occurs due to the reaction of water with the added hydrosilane, producing silanol groups and hydrogen gas. As the foam sealant cures over time, the hydrogen gas evaporates out of the mixture and produces bubbles within the microstructure of the silicone, while the silanol groups condense and expedite the polymerization (and thus curing) of the material. A schematic of the chemical reaction is shown in Figure 9.

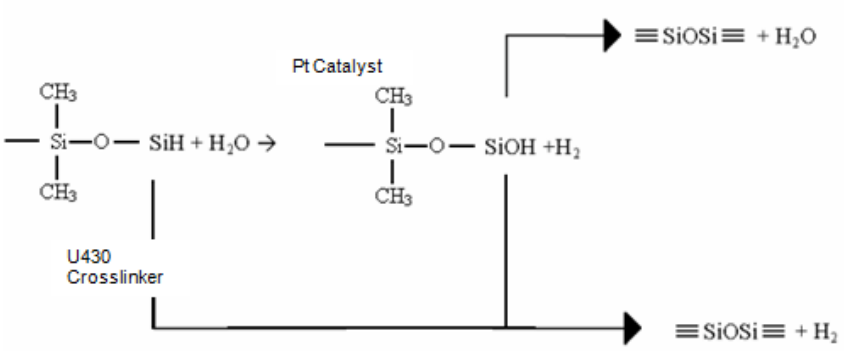

Figure 9: Schematic of Foam Sealant Reaction

The modified formulation produces a foam-like silicone sealant, which has been observed to expand approximately 70% of its initial volume (Malla et al. 2006). Previous studies have shown the foam sealant to exhibit a smaller stress modulus and much larger ultimate strain when compared to the commercial product. However, the results presented in this study may vary from previous experiments as the crosslinker supplier used in previous experiments no longer offers the

same product. Therefore, the crosslinker used throughout this work, although it is similar to the one used previously, may generate different behavior of the sealant.

2.4 Mixing Protocol for Experiments

A consistent mixing process was established in order to maintain consistency for all experiments. As with many materials that require mixing such as concrete, the quality of the sealant often depends on the skill and experience of the user; therefore, several trial mixes were conducted prior to the experiments to establish a feel for the material and produce the same consistency of material for each subsequent mix. The mixing process for the foam sealant consisted of combining equal parts by weight of the commercially available Wabo SiliconeSeal in accordance with the manufacturer's specifications. A mixing paddle was used to stir all ingredients together as outlined by the Watson Bowman specifications for mixing their commercial sealant. Before beginning, all components were weighed out by mass and placed aside to minimize wasted time between adding ingredients. Once both Wabo SiliconeSeal parts (A and B) were combined and thoroughly mixed, platinum catalyst was slowly added, followed by water. These components were added while continuously stirring the sealant. Once the added components were mixed in with the solid sealant, the crosslinker was added to initiate the chemical reaction. Mixing continued until the entire mixture exhibited a uniform texture. Component parts are outlined in Table 3.

Table 3: Mix Proportions for Foam Sealant

Component	Density (g/cm^3)	Percent Volume (%)
Wabo White	1.08	54.43
Wabo Grey	1.45	40.54
Crosslinker	0.98	2.77
Water	1	1.8
Platinum Catalyst	0.98	0.46

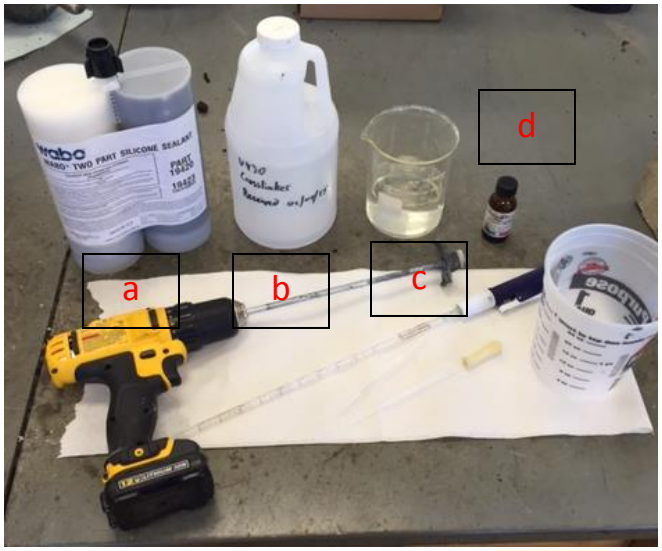

Figure 10: Wabo (a), Crosslinker (b), water (c), platinum (d)

A consistent mixing procedure is important, especially because a small deviation in quantities added or mixing technique can alter the properties of the foam sealant. Care was also taken to mix enough material to ensure the same batch of material was used for each experiment without mixing more material for the same set of specimens. The mixing procedure is illustrated in Figure 11.

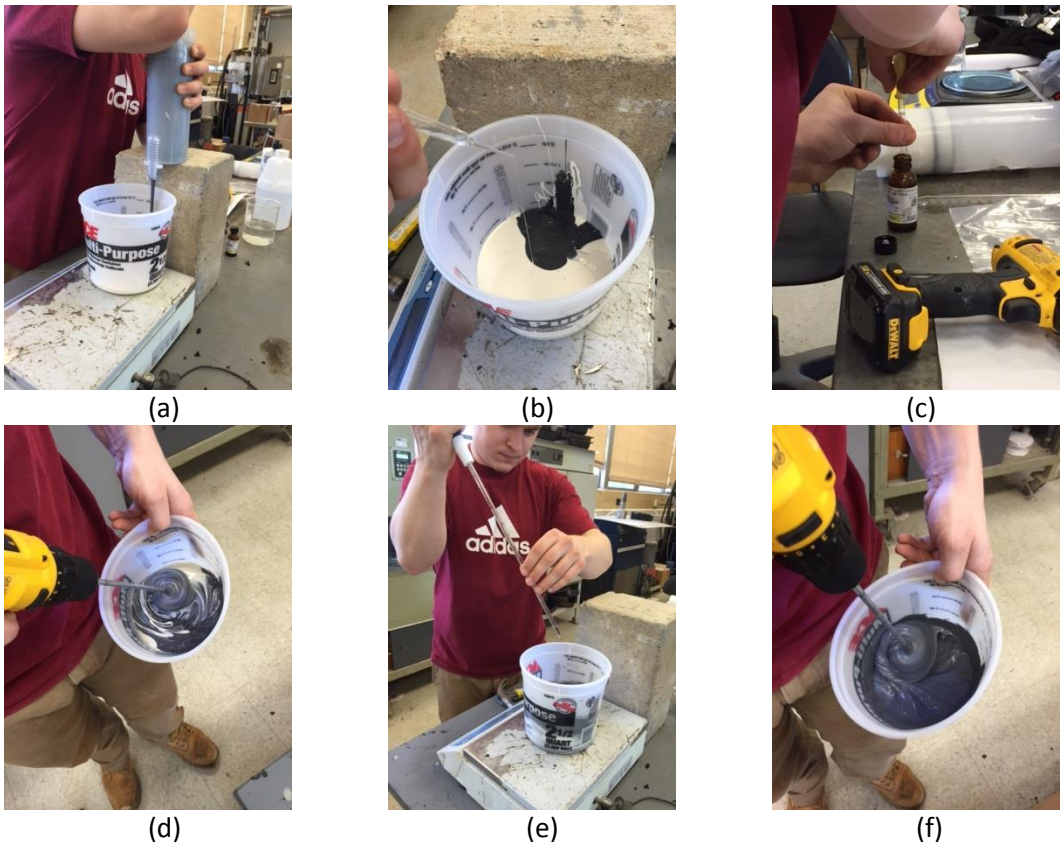

(a) Pouring equal parts by volume of Wabo black and grey
(b) Addition of water through dropper
(c) Addition of platinum catalyst through dropper
(d) Mixing of first four ingredients for about 45 seconds (time varies with initial volume)
(e) Addition of crosslinker with pipette
(f) Mixing of all five ingredients for about 45 seconds (time varies with initial volume)

Figure 11: Mixing procedure

2.5 Fabrication of Test Coupons

All laboratory tests involving evaluation of mechanical properties consisted of creating specimens containing solid or foam sealant. These specimens were used for the tension/adhesion

experiment and also for the aging experiment. Specimens were cast and fabricated similar to those used in previous studies by Malla et al. (2006, 2007) as shown in Figure 15.

The tension/adhesion experiment's test coupons were made of concrete and steel, the two most common substrates found in newly constructed bridges. First, the appropriate materials were obtained to adequately replicate those present in the field. With the assist of the Connecticut Department of Transportation, a large piece of concrete was salvaged from a local bridge undergoing replacement. This was done to reflect the type of concrete in joint headers typically found throughout the state. Steel was also obtained with the assistance from the University of Connecticut's Civil Engineering machine shop. Blocks were fabricated using typical A36 steel, the material commonly found at the joints of bridge decks with angle headers. Each specimen contained a 12.7 x 50.8 x 12.7 mm (0.5 x 2 x 0.5 in.) volume of sealant applied in between two substrate blocks measuring 76 x 50.8 x 12.7mm (3x2x0.5 in.) (LxWxH).

Figure 12: Fabrications of coupons for experimental testing

The substrate chosen for specimens in the aging experiment was a polymer modified concrete (WaboCrete), selected specifically because of its common use in bridge header repair throughout the state of Connecticut. This concrete mix, manufactured by Watson Bowman Acme

Corporation, is comprised of three components: the activator (part A), the resin (part B), and the aggregate. The aggregate contains a particle size distribution between 0.08 and 15mm, having 30-65% passing through a 2mm screen, 12-15% passing through a 0.08mm screen, and 100% passing through a 15mm screen. Per manufacturer specifications, the resin was premixed separately for about 20 seconds before being mixed with the activator in a 5 gallon bucket for approximately 30 seconds. The aggregate was then added until every particle was coated in the mixture. The components are shown in Figure 6.

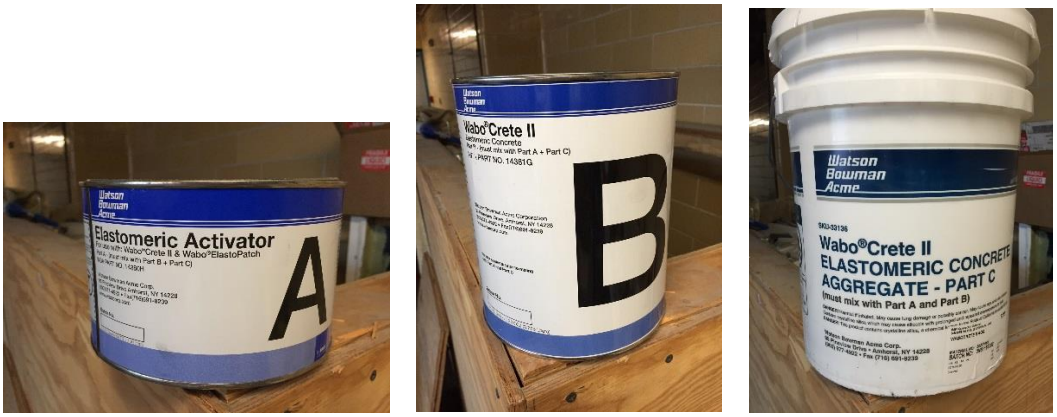

Figure 13: Components of Watson Bowman polymer modified concrete

Forms for the concrete were fabricated and treated with four coats of mineral oil which acted as a release agent. The concrete was poured into forms measuring 317.5 x 50.4 x 12.7 mm (12.5 x 2 x 0.5 in.) (LxWxD); these forms allowed for the concrete to be shaped into 317.5 mm (12.5 in.) bars which would later be cut into individual blocks for specimens (Figure 14). Each bar was shaped up using an angle grinder and sanded to match the exact desired dimensions. Upon 28-day curing of the concrete, the bars were cut into 25.4 x 76.2 mm (2x3 in.) blocks to assemble the specimens. Each bar would yield two specimens since two blocks were needed to assemble once specimen. Once all specimens were cut and cast, they were left to cure at room temperature (23 ± 2^0C) for 14 days as shown in Figure 14.

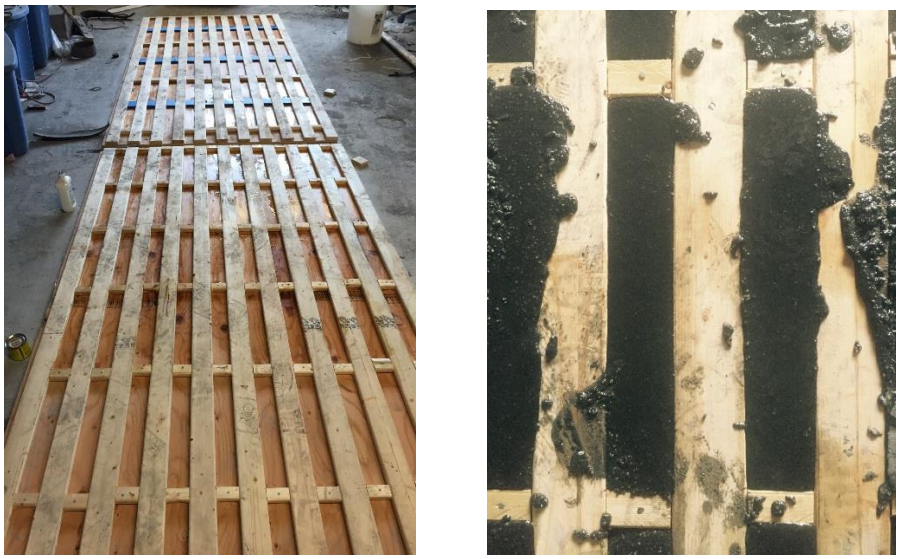

Figure 14: Formwork for polymer modified concrete casting

Care was taken to cast the specimens with exact dimensions (including sealant dimensions). Due to the expansion effect of the foam sealant, and inherent imperfections, some specimens contained sealant with slightly varying heights; therefore, exact dimensions of each specimen were recorded using a caliper for any anticipated adjustments in future calculations.

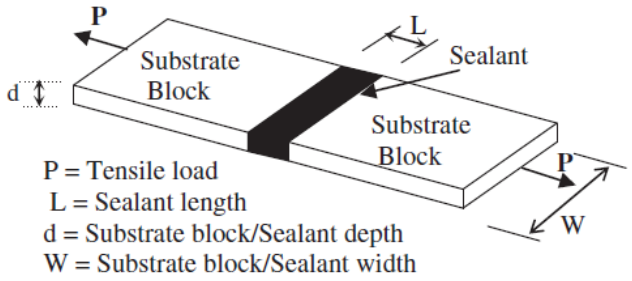

Figure 15: Typical test specimen

2.5 Application of Primer

Some specimens contained substrate blocks treated with primer in order to compare the adhesion characteristics of each sealant under the influence of primer. The primer, manufactured

by Dow Corning, was selected in accordance to the appropriate substrate. Dow Corning 1200 OS was used for specimens containing a concrete substrate. Dow Corning Primer P was used for specimens containing a steel substrate (Figure 16). Per Dow Corning specifications, the substrate was first cleaned with a lint-free cloth to remove any dust or residue. A light coating of primer was applied using a brush. After approximately 90 minutes of drying, the sealant was cast into the gap between the substrate blocks.

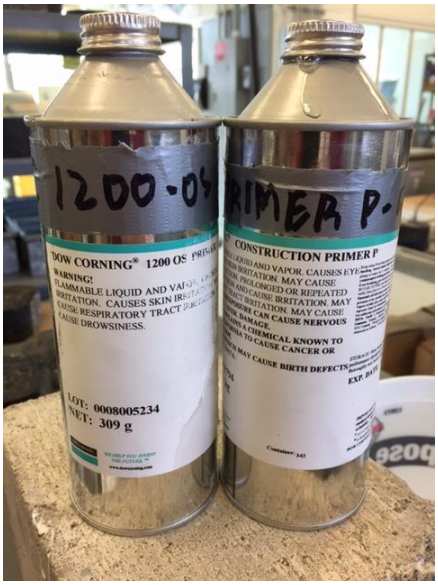

Figure 16: Primer for steel and concrete

2.6 Tension/Adhesion Test and Results

The tension and adhesion test was designed to observe the effect of primer application on each type of sealant (foam and solid) while evaluating the tensile and adhesive properties of each sealant. Additionally, the effect of the substrate was included, as specimens were cast using steel and concrete substrate.

2.6.1 Experimental Setup

Five (5) specimens were fabricated for each variable tested; foam sealant with primer, foam sealant with no primer, solid sealant with primer, and solid sealant with no primer. Since two substrates (concrete and steel) were considered, a total of forty (40) specimens, similar to the one shown in Figure 1, were fabricated for this test. Twenty (20) specimens contained sealant applied in between two concrete blocks, and the other twenty specimens contained sealant applied in between two steel blocks with the same dimensions.

Figure 17: Concrete and steel coupons

Upon casting, all forty specimens cured at room temperature (23 ± 2^0C) for 14 days. Upon completion of curing, each specimen was labeled and installed at random onto the Intron Model 1011 machine and pulled until failure using a 500 N (100 lb.) load cell. The testing procedure followed specifications outlined by ASTM C1135-00, Standard Test Method for Determining Tensile Adhesion Properties of Structural Sealants (ASTM, 2000). As shown in Figure 18, both substrate blocks were gripped using the mechanical clamps attached to the machine. The lower

end of the specimen's concrete block was fixed while the other concrete block was extended at a rate of 10 mm/min. Using displacement control, the machine recorded the tensile force required to extend the specimen over a specific displacement. From this data, stress and strain information was extracted and computed.

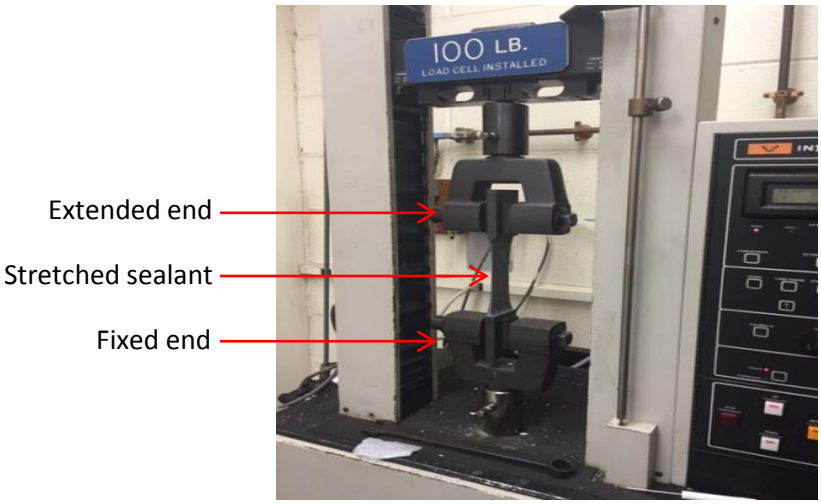

Figure 18: Tensile testing using Instron machine

2.6.2 Results

After testing five specimens per variable for each substrate (concrete and steel), both results revealed the foam sealant has a smaller elastic modulus, as illustrated in Figures 19 and 20. This can be observed by comparing the ultimate stresses between specimens containing foam sealant and those containing solid sealant. Specimens containing foam sealant exhibited an average ultimate stress of 155 kPa while maintaining an average ultimate strain of 922.5%. Meanwhile, the solid sealant exhibited an average ultimate stress of 312 kPa with a corresponding average ultimate strain of 1027%. The foam sealant showed a larger average strain, corresponding to an ultimate stress about 49% that of the solid sealant's ultimate stress capacity. While typical civil engineering materials are characterized by their ultimate capacity, this reduction in stress modulus

is actually favorable to reducing the stresses at the interface of the silicone sealant and the bridge header. There was no significant difference observed in maximum stress or strain properties of the specimens between steel and concrete substrates.

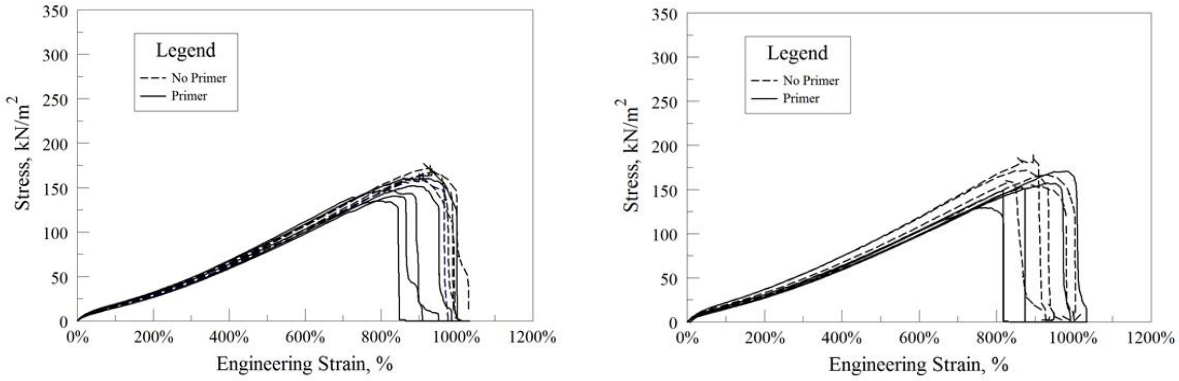

(a) (b)

Figure 19: Results for specimens containing (a) foam sealant, steel substrate and (b) foam sealant, concrete substrate

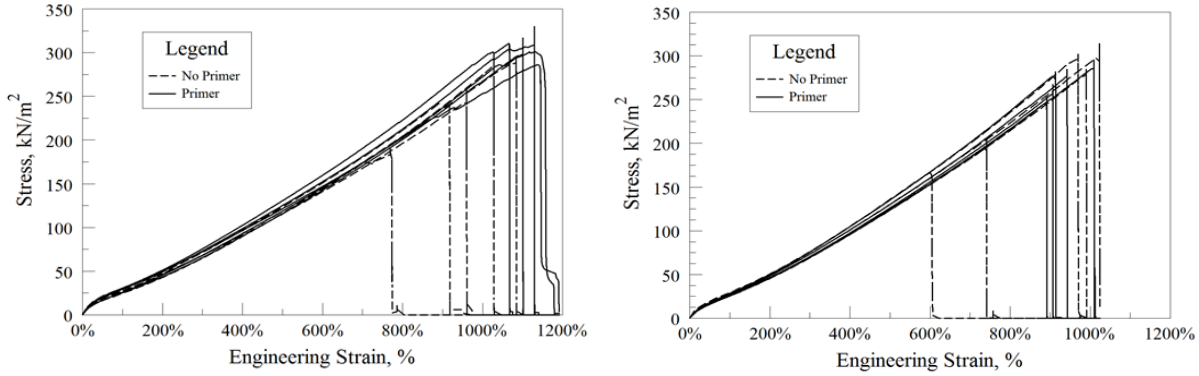

(a) (b)

Figure 20: Results for specimens containing (a) solid sealant, steel substrate and (b) solid sealant, concrete substrate

The key characteristic that can be taken from this experiment is the failure mode of each specimen. Figures 19 and 20 show the stress vs. strain curves of each specimen; although the strain

ranges are comparable, and an obvious reduction in modulus is observed in the specimens containing foam sealant, all solid sealant specimens exhibited an adhesive failure, while the foam sealant specimens failed via cohesive failure. Adhesive failure is characterized by detachment of the sealant from the substrate prior to material failure. Cohesive failure, on the other hand, pertains to ripping or shearing of the silicone material itself while maintaining its attachment to the substrate. Both failure modes can be observed in Figures 19-20, as a cohesive failure is characterized by a smooth, rolling peak as the stress approaches its ultimate limit state. Adhesive detachment, however, can be seen when the stress peak sharply drops, indicating a sudden failure under tension. Cohesive failure was observed in 100% of the specimens containing foam sealant for both substrates (concrete and steel). For specimens containing solid sealant, however, 90% of the specimens failed via adhesive failure.

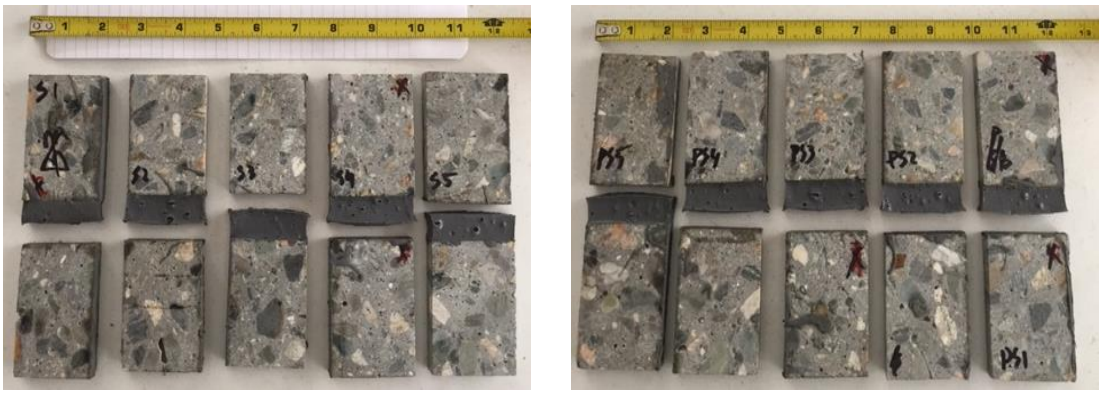

(a) **(b)**

Figure 21: Concrete specimens containing (a) solid sealant with no primer; (b) solid sealant with primer.

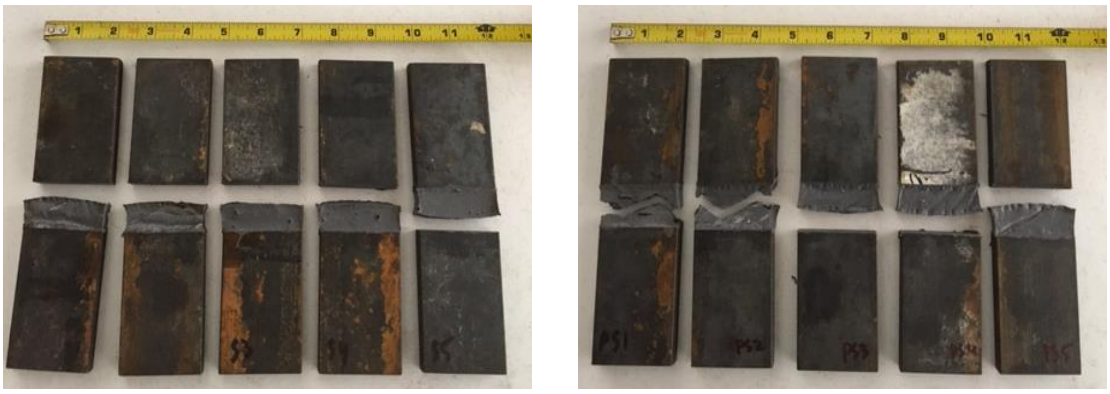

(a) **(b)**

Figure 22: Steel specimens containing (a) solid sealant with no primer; (b) solid sealant with primer.

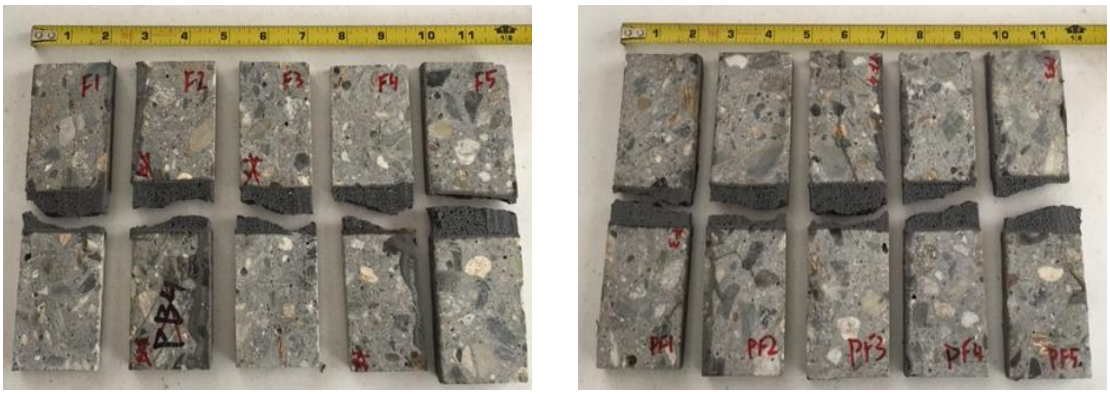

(a) **(b)**

Figure 23: Concrete specimens containing (a) foam sealant with no primer; (b) foam sealant with primer

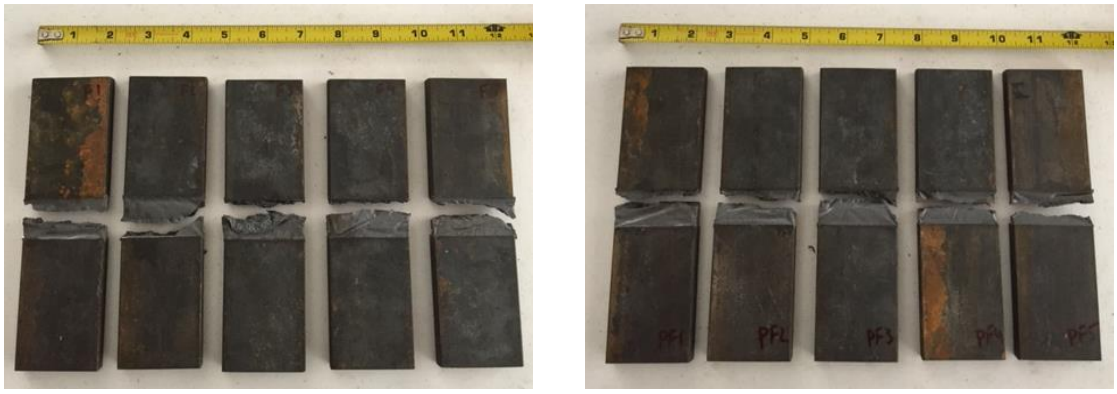

(a) **(b)**

Figure 24: Steel specimens containing (a) foam sealant with no primer; (b) foam sealant with primer

These failure modes were very similar for specimens containing primer. When primer was applied to solid specimens, 20% of them failed via cohesive failure, while 80% still failed by means of detachment from the substrate. Although primer was applied, the conclusion that primer improves bonding of the sealant to the substrate cannot be made from these results. Specimens containing foam sealant and primer still exhibited excellent bond as all specimens failed cohesively, as expected.

Table 4: Tension and Adhesion Results

Substrate	Sealant Type	Primer Presence	Average Ultimate Stress (kPa)	Average Ultimate Strain (%)	Average Modulus at 100% Strain (kPa)	Failure Mode	
						Cohesive	Adhesive
Concrete	Foam	Yes	161	906	16.06	5	0
	Foam	No	158	952	19.62	5	0
	Solid	Yes	318	933	24.1	0	5
	Solid	No	246	866	26.6	0	5
Steel	Foam	Yes	149	939	16.81	3	2
	Foam	No	164	998	17.01	5	0
	Solid	Yes	306	1121	28.38	0	5
	Solid	No	265	953	28.03	0	5

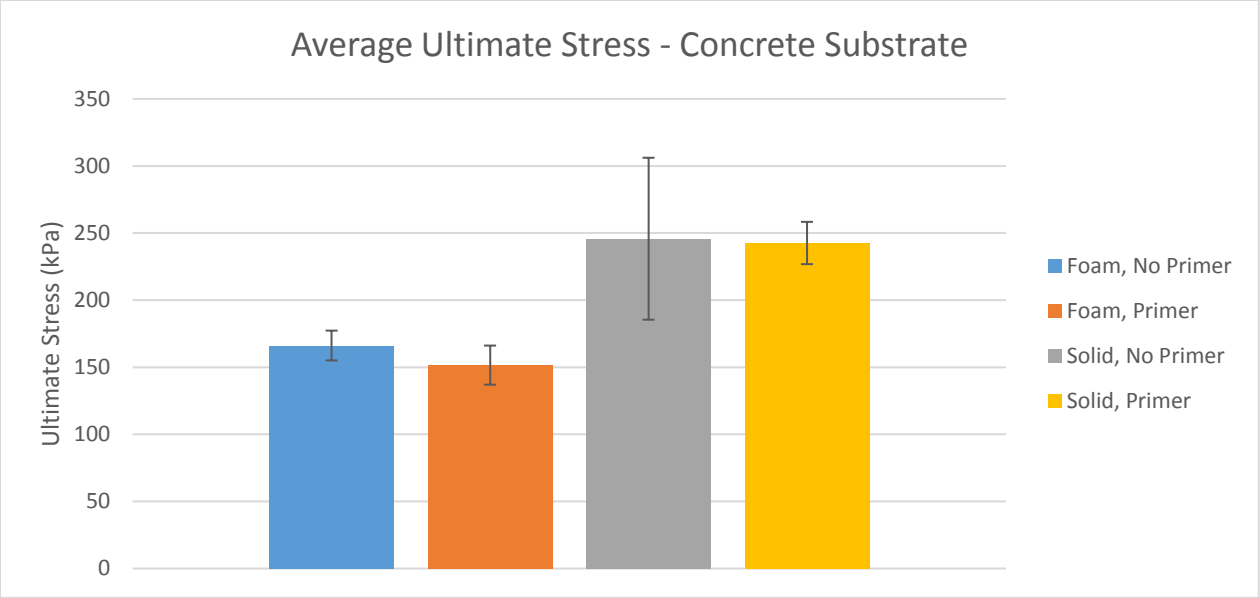

Figure 25: Average ultimate stress for specimens with a concrete substrate

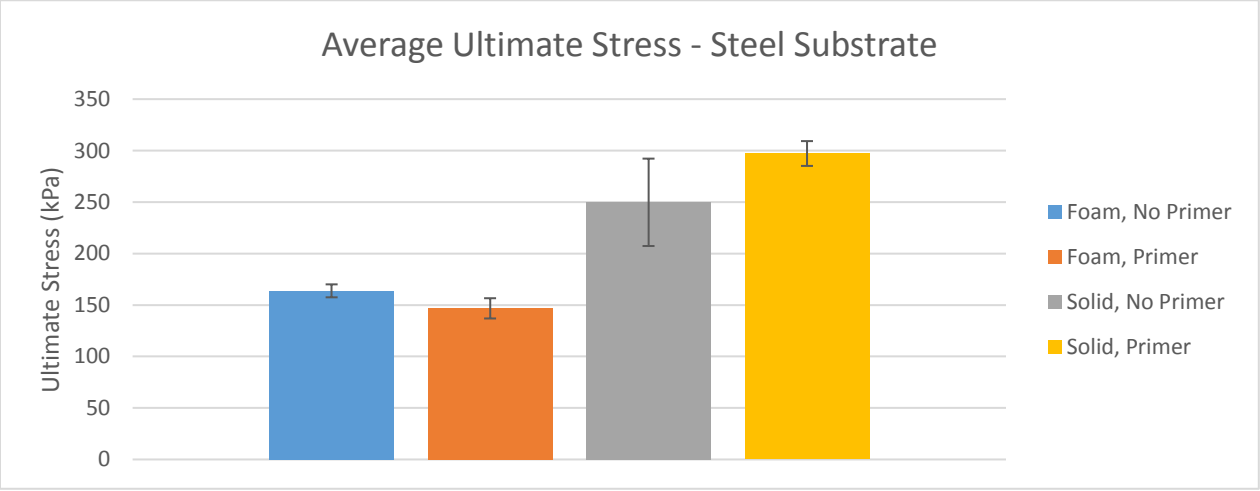

Figure 26: Average ultimate stress for specimens with a steel substrate

2.7 Aging/Salt Water Test and Results

Similar specimens were used for the aging/salt corrosion test as the ones used in the tension and adhesion experiment. Motivation to conduct an aging study stemmed from the potential degradation of the bond between the sealant and substrate over time.

2.7.1 Experimental Setup

Real time aging was simulated by utilizing hot water aging methods as specified in ASTM C1560-03 (ASTM, 2003). It was envisioned that specimens would be extracted at various time intervals and tested for adhesion and tensile strength by pulling them to failure at each respective aging period. Seven testing periods, or durations of accelerated aging, were established: 0 and 14 days, and 1, 2, 3, 4, and 5 months. Five (5) specimens per variable (foam sealant with primer; foam sealant without primer; solid sealant with primer; solid sealant without primer) were cast for each testing period. Therefore, one hundred and forty (140) samples were fabricated to be tested at each time interval including zero days aging. Since the effect of road salt exposure on aged specimens is also of interest, another set of 140 specimens were cast, yielding a total of two hundred and eighty (280) specimens in total.

Figure 27: Curing of specimens for aging experiment

Each tank was heated to 35°C (95°F) using a 400-Watt submersible water heater with a sensor and activator. Due to the large volume of water, care was taken that the entire tank was heated to the desired temperature prior to submerging the specimens. This was to ensure an even temperature distribution for all submerged specimens regardless of their position in the tank. Three temperature probes were placed inside the tank to monitor the temperature at difference locations throughout the volume of the tank. Since the heater was placed on the bottom of the tank, two probes were attached towards the top of the surface, and one was attached adjacent to the heater. Once all three temperature readings were at 35°C, the specimens were placed into the tanks. The temperature for both tanks was kept to a strict deviation tolerance of ± 0.55°C (± 1°F). Temperature profiles of each tank were recorded regularly (Figure 28). The low temperature in each tank observed on day 10 was due to a power outage of the building in which the tanks were located; however, power was restored within 6 hours and the target temperature was regained shortly afterwards.

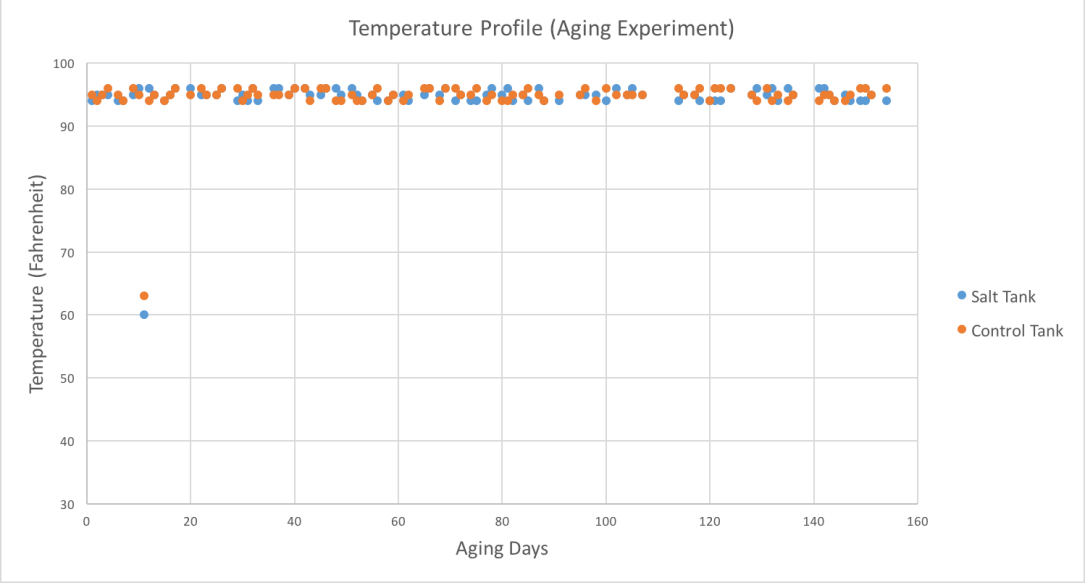

Figure 28: Temperature profile of water tanks

One tank contained water with no additives and the other tank contained a saturated solution of water mixed with sodium chloride and magnesium chloride. This experimental design enabled for observation of the effects of aging and also the effects of aging with the influence of road salt. Concentrations of sodium chloride and magnesium chloride per total solution volume were 38.72% and 2.03%, respectively. These proportions are specified by the Connecticut Department of Transportation as mandatory minimum dispensing ratios for chemical treatment of state roads. (Connecticut Department of Transportation, 2015). After thorough mixing, the pH of the solution was measured to be 8.519.

To simulate adequate aging, oxygen was delivered to the specimens through two air pumps located at the bottom of each tank. The purpose of these pumps was twofold; they supplied oxygen to the specimens and also provided circulation to the water to ensure an even temperature distribution and prevent any residual salt particles from settling to the bottom of the test tanks. The specimens were arranged on five open area racks per tank, allowing for maximum exposure to the water. Since the water heaters were placed at the bottom of the tanks, the specimens closer to the heater may experience a warmer aging environment. To reduce the proximity bias, the racks were rotated systematically on a regular basis to ensure all specimens experience the same aging environment. Throughout the course of the experiment, the tanks were covered on all sides with insulation to reduce heat loss. The experimental set up is shown in Figure 29.

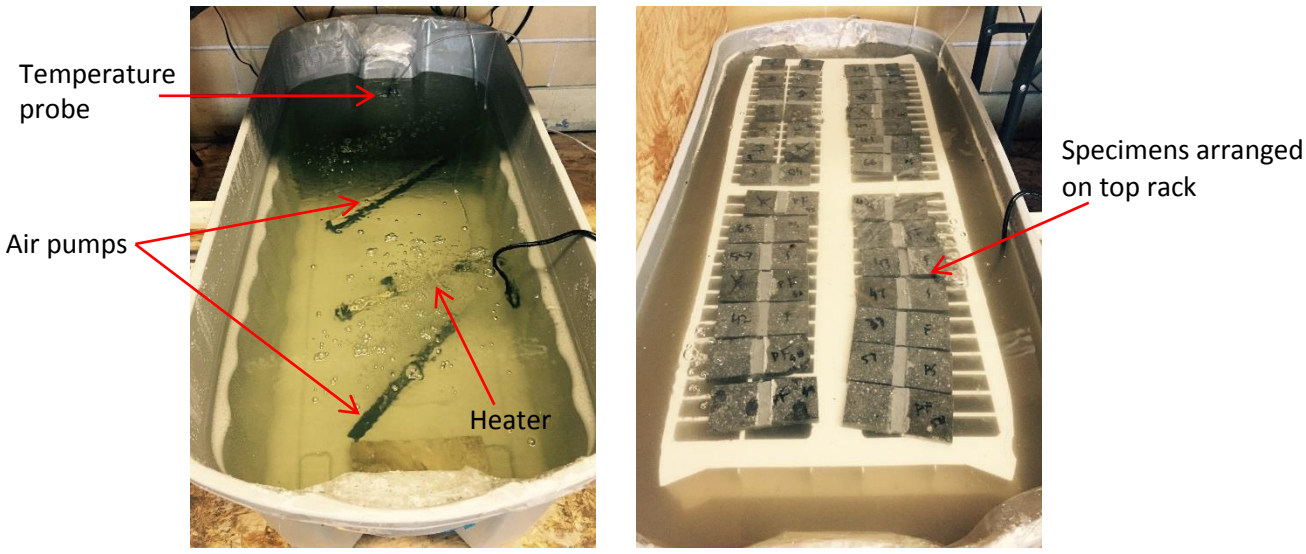

(a) (b)

Figure 29: Placement of heater and air pumps (a), water tank containing 140 specimens (b)

Due to the large number of specimens, the testing protocol was designed to minimize any changes in procedure throughout the course of five months. Therefore, upon each aging period, the specimens were removed from the tanks and rinsed with warm water to remove any salt or residue that may have accumulated over time. The specimens were then stored in a refrigerator at 42 degrees Fahrenheit to ensure a cold, dark and consistent environment. This significantly slowed down any additional aging, especially for the specimens extracted at early aging durations. After the completion of five months, all specimens were removed from the refrigerator and tested at the same time. However, due to the large number of specimens (280), the last specimen was tested six days after the first.

2.7.2 Testing Protocol

Upon extraction from the refrigerator, the specimens were labeled according to a random number generator. These numbers represented the order in which they would be tested (this minimized the bias in testing certain types of specimens before others). Since there was a large

number of specimens, this also ensured that the testing procedure was not different for a specific bundle of specimens than for others.

The testing procedure was designed in accordance with ASTM C1135 (Standard Test Method for Determining Tensile Adhesion Properties of Structural Sealants). However, the procedure deviated slightly from the specified standard because a lower rate of extension was implemented (10 mm/min instead of 50mm/min). Similar to the tension/adhesion test, the specimens were installed onto the Intron model 1011 and, using a 1000-pound load cell, pulled to failure. Because of the shape and dimensions of the substrate blocks (the dimensions of the substrate blocked exactly matched the dimensions of the grips), the specimens were mounted in the same way for each test. This was important, as a slight angle offset can induce undesirable shear stresses in the sealant and ultimately result in a different load transfer than what a pure tensile load would induce. Since inherent imperfections existed within each specimen due to the expansion of the foam sealant and general casting method, each specimen's dimensions were measured using a digital caliper, allowing for future adjustments in calculations. Per ASTM standards, the mode of failure, ultimate extension, and ultimate force were recorded upon failure. From these results, stress and strain properties were calculated and tabulated. The test setup is shown in Figure 30.

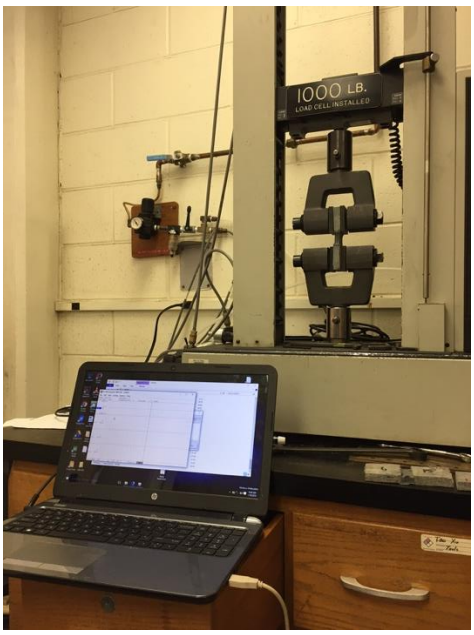

Figure 30: Experimental setup of the aging study

During testing, several observations were made. One significant observation was the presence of larger air pockets of the foam sealant, especially when the specimen was extended to a strain beyond 500%. These air pockets seemed more pronounced for specimens that were aged for a longer period of time in the salt water tank. Salt was also observed inside and around the perimeter of the air pockets, suggesting that it the salt particles settled into the air pockets located on the exposed surface of the sealant. However, upon visual inspection of these specimens after failure, no salt was detected within the inner structure of the sealant. Figure 31 shows the extent of the air pockets formed for specimens containing foam (compared to the containing solid sealant).

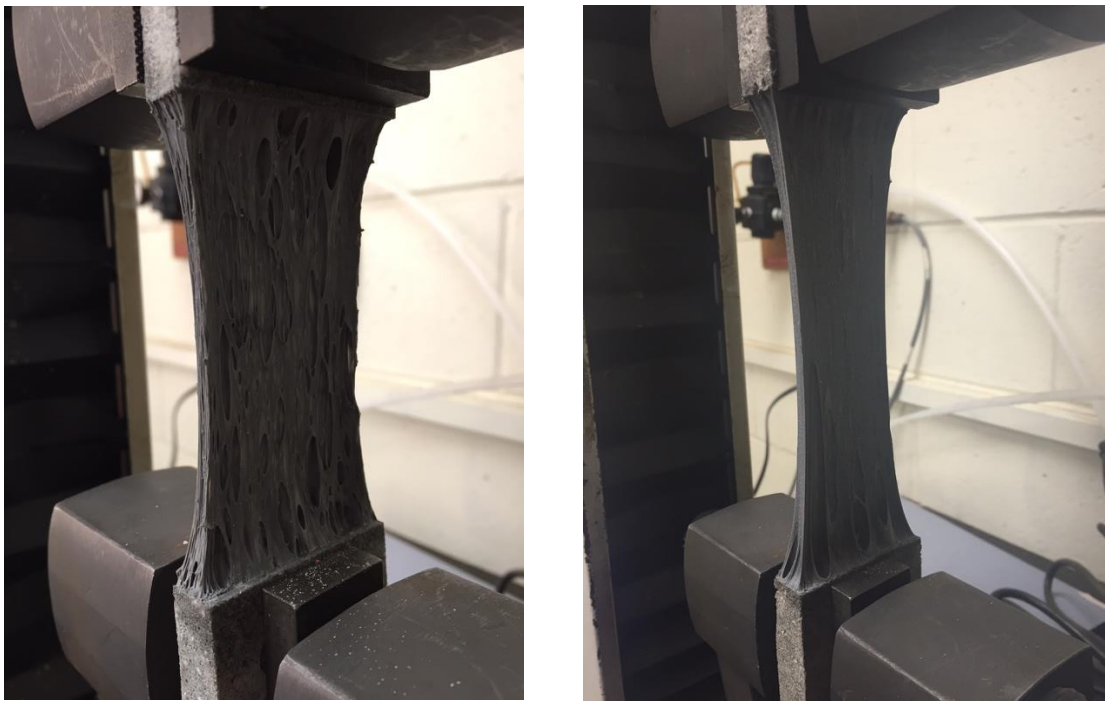

(a) (b)

Figure 31: Condition of extended specimens containing (a) foam sealant and (b) solid sealant

A common observation among foam specimens was that the cohesive mode of failure initiated at regions where large air pockets were stretched. Upon further stretching, these air pockets began to tear longitudinally, creating weak points in the structure of the sealant. Upon even further extension, the sealant grew thin and eventually yielded, creating a hole in the sealant. Once this hole developed, the remaining sections of the sealant were forced to resist further stretching with a smaller area of sealant. Additionally, stress concentrations were created around the hole where the sealant initially ripped. These regions also began to slowly tear longitudinally, eventually ripping the entire cross sectional area (resulting in a cohesive failure).

2.7.3 Results

Similar to the tension and adhesion test, stress vs. strain curves were generated for the aging/salt test. Although data was collected at time intervals of 0 days, 14 days, and 1, 2, 3, 4, and 5 months, figures 32-39 show the stress characteristics for specimens with and without salt treatment and primer treatment at 0 days, 14 days, 2 months and 5 months. The full data set can be found in appendix A.

Figure 32 shows the stress vs. strain curves for specimens tested at 0 days with no exposure to salt. Since these specimens serve as the benchmark prior to any aging, they did not receive any salt exposure. Therefore, only 20 specimens were tested for the benchmark. The curves show that the foam sealant's ultimate stress was more consistent, peaking at just under 150 kPa. The solid sealant, although it achieved a higher ultimate stress, displayed a more scattered ultimate stress at failure, most likely due to imperfections at the interface of the sealant and the substrate blocks.

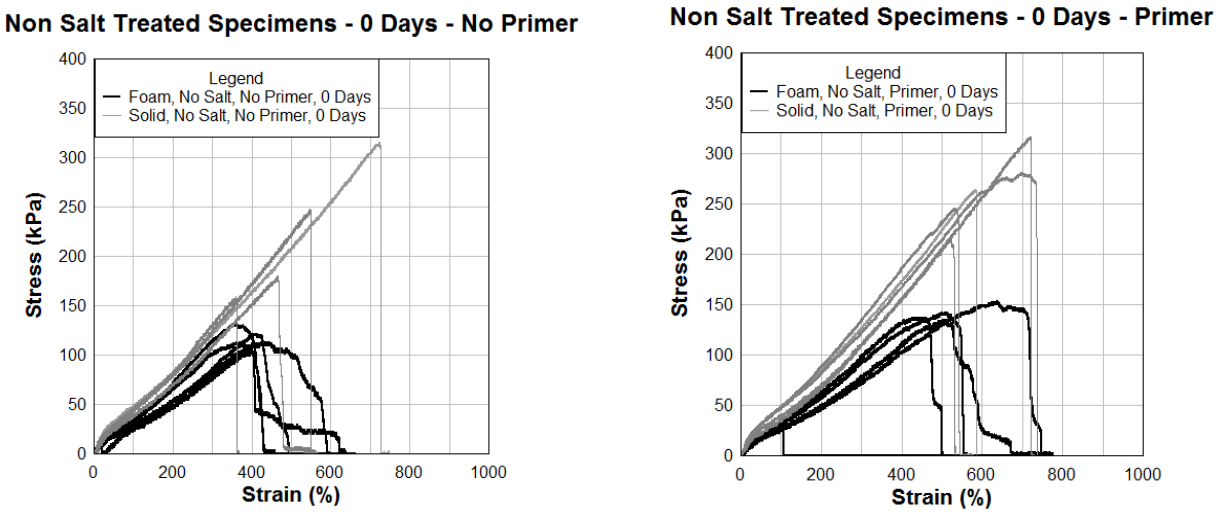

Figure 32: Non salt treated specimens at 0 days with no primer (left) and primer (right)

Figures 33-34 show the stress vs. strain curves for specimens after 14 days of aging. The average ultimate stress for solid specimens is just under 300 kPa, while the foam sealant failed at stresses ranging from 120-150 kPa. Almost all solid specimens show a higher modulus of elasticity, even at early loading stages. Almost all foam specimens fail around 600% strain.

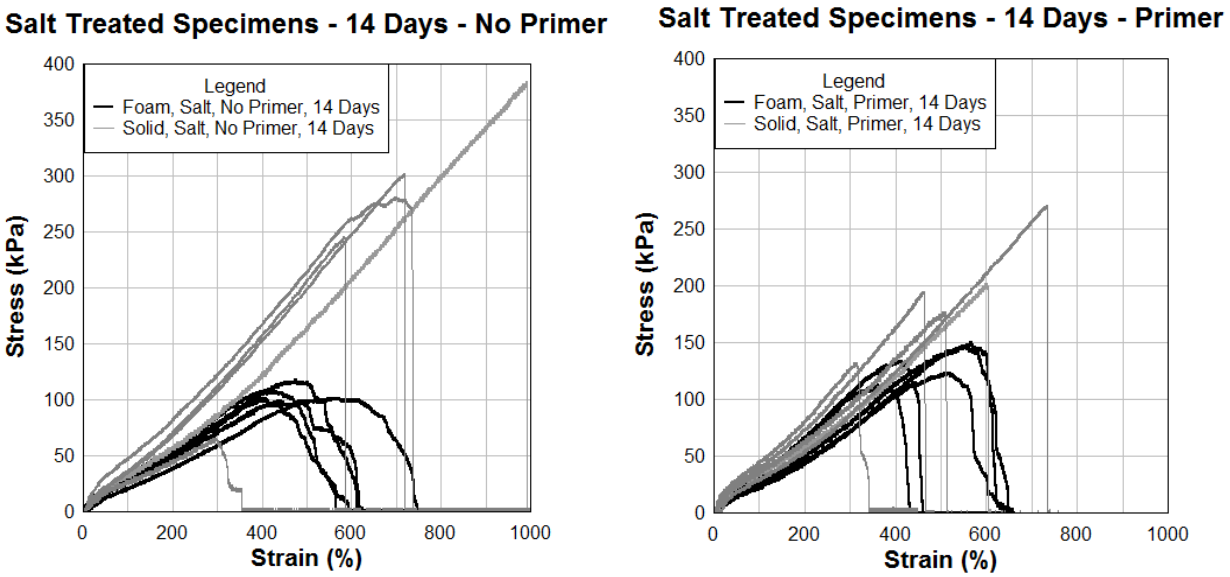

Figure 33: Salt treated specimens at 14 days with no primer (left) and primer (right)

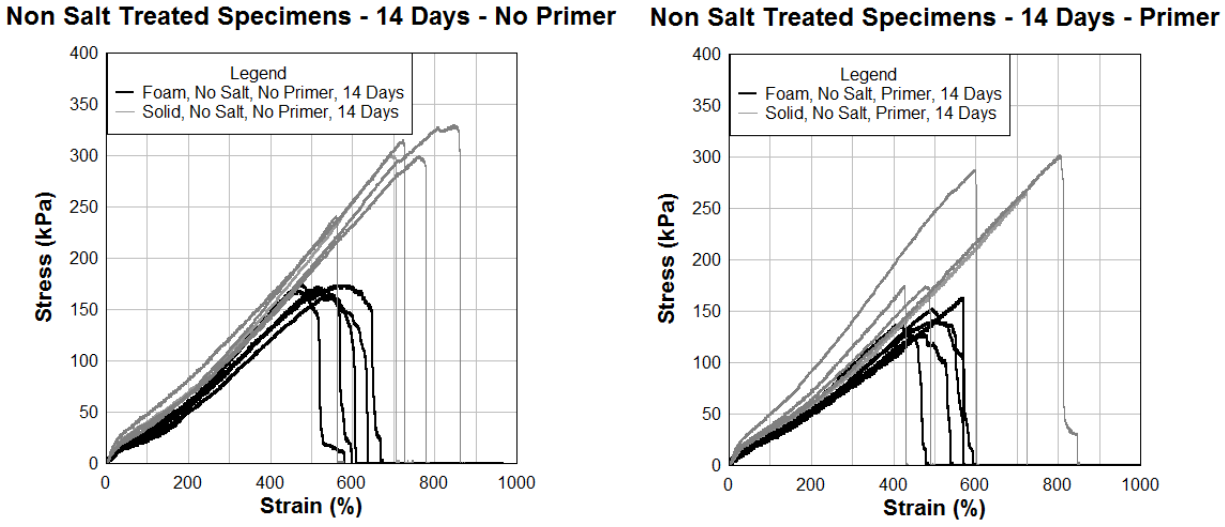

Figure 34: Non salt treated specimens at 14 days with no primer (left) and primer (right)

Figures 35-37 show the stress vs. strain curves for specimens after 60 days of aging. The average ultimate stress for solid specimens is just under 300 kPa, while the foam sealant failed at stresses ranging from 120-150 kPa. Almost all solid specimens show a higher modulus of elasticity, even at early loading stages. Again, almost all foam specimens fail around 600% strain.

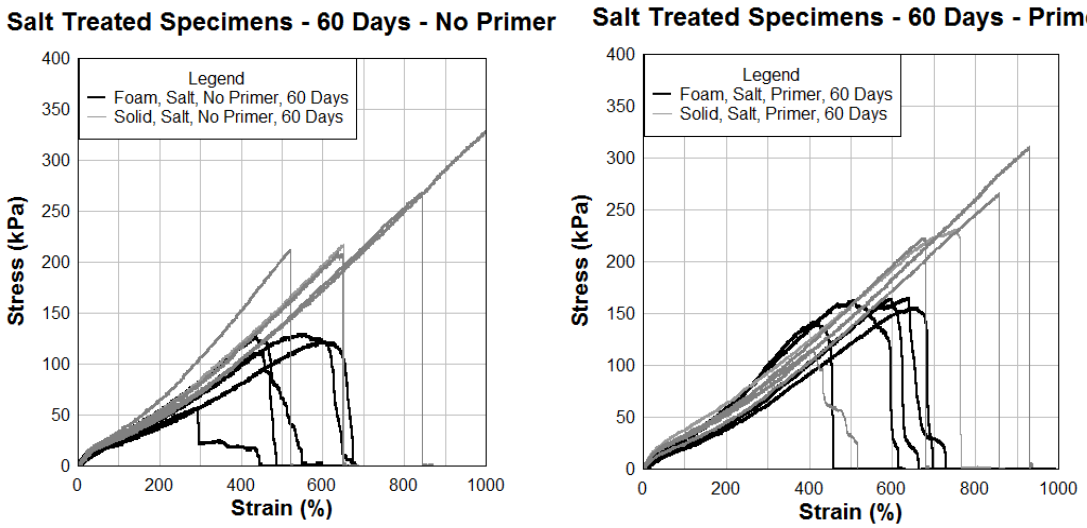

Figure 35: Salt treated specimens at 60 days with no primer (left) and primer (right)

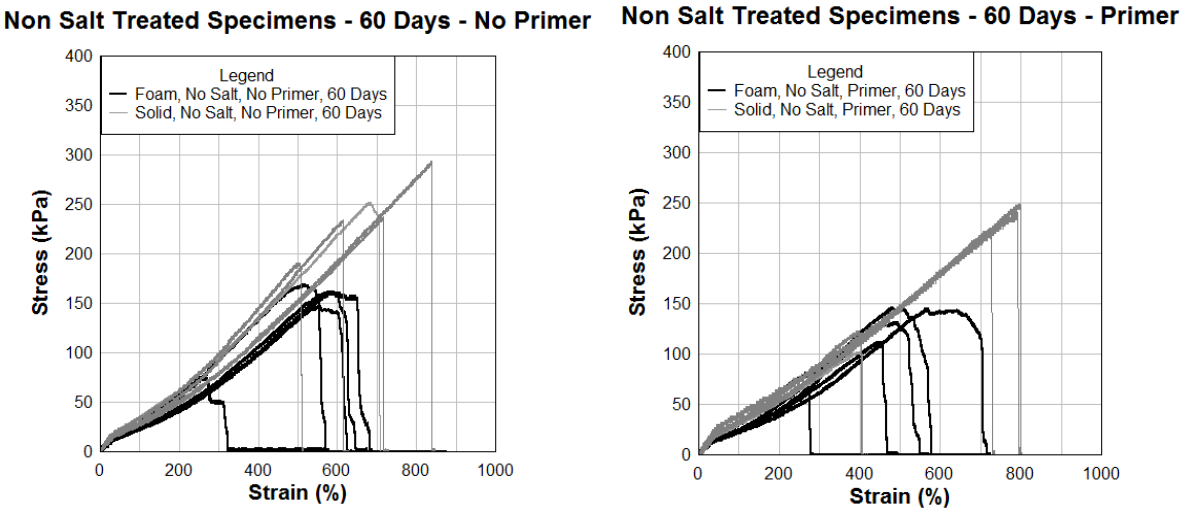

Figure 37: Non salt treated specimens at 60 days with no primer (left) and primer (right)

Figures 38-39 show the stress vs. strain curves for specimens after 150 days of aging. The average ultimate stress for solid specimens is just under 230 kPa for specimens exposed to salt. However, the specimens with solid sealant not exposed to salt experienced a larger drop in ultimate stress, peaking at around 170 kPa while the foam sealant failed at stresses ranging from 120-150 kPa.

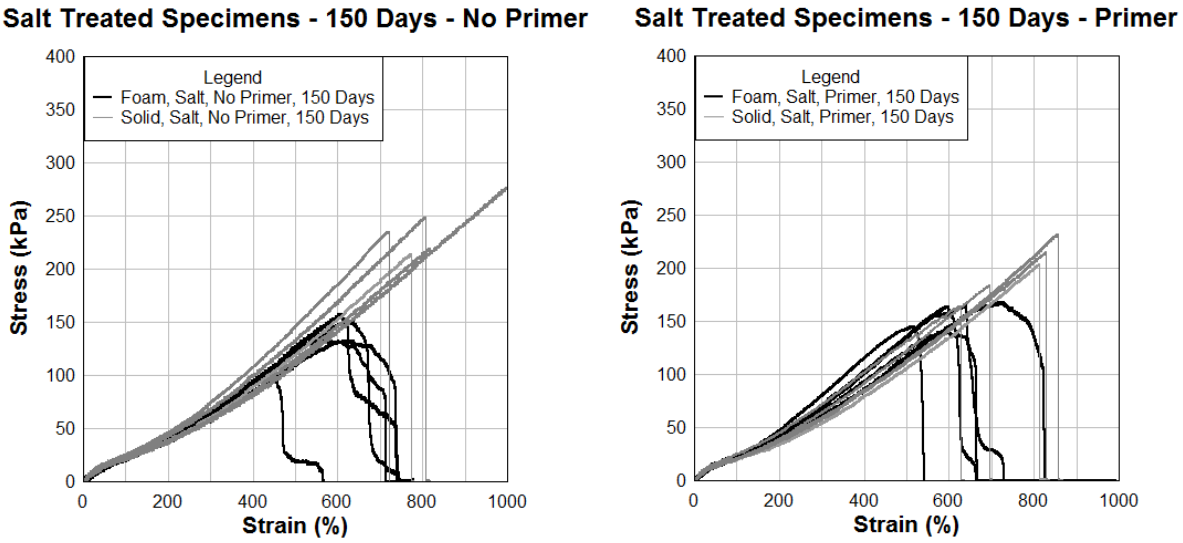

Figure 38: Salt treated specimens at 150 days with no primer (left) and primer (right)

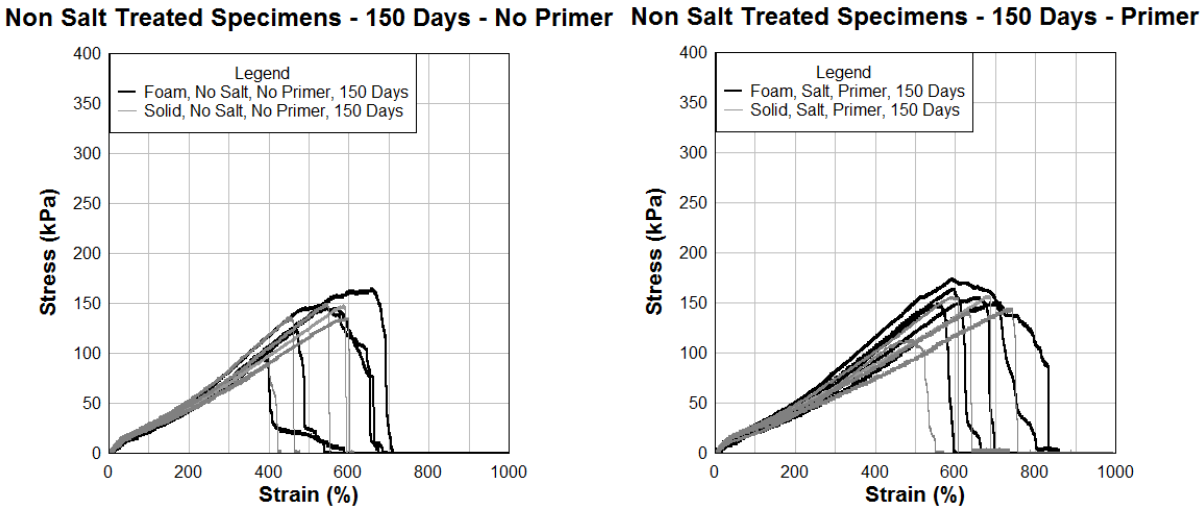

Figure 39: Non salt treated specimens at 150 days with no primer (left) and primer (right)

Figures 40-51 show the scatter of ultimate stress, stress at 100% strain, and ultimate elongation as a function of aging. The graphs are separated according to salt treated non-salt treated specimens with and without primer. Since the scatter for this graphs was quite prominent, a two-tail t-test was performed to determine if the observed difference in trend lines through these scatter points was statistically significant, or just different by chance. Since there were 33 degrees of freedom for each set of data, a significant t-value is considered as larger than 1.96 and a significant probability of the null hypothesis being correct, according to a 95% confidence interval, must be smaller than 0.05.

Figure 40 shows the ultimate stress values for specimens exposed to salt and primer treatment. Judging by the trend lines, it can be observed that the stress at failure for both the foam and solid sealants reduces over time, indicating a possible reduction in modulus. To distinguish a difference in slopes between the foam and solid, a t-test was run and generated a t-value of 3.395 and a probability of 0.001, indicating a statistical difference between the two slopes. This indicates that the rate of deterioration of the solid sealant is greater than that of the foam.

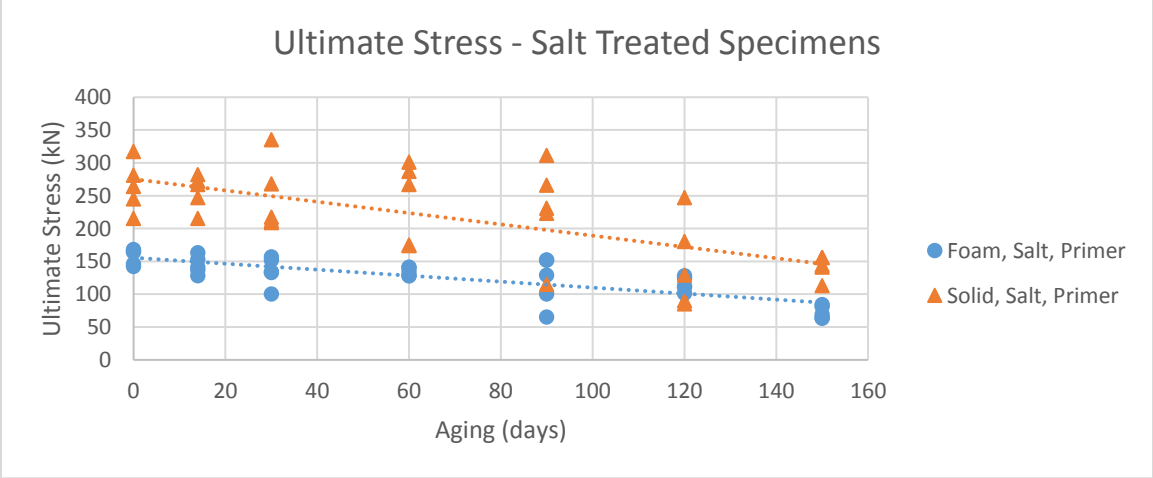

Figure 40: Ultimate Stress for specimens exposed to salt and primer treatment

Figure 41 shows the ultimate stress values for specimens exposed to salt but no application of primer. Again, it can be observed that the stress at failure for both the foam and solid sealants reduced over the duration of the experiment. When running a t-test to determine whether the difference in slopes is significant, the t-value generated was 2.23 with a probability of 0.03, suggesting a statistical difference between the foam and solid sealant's slopes. This confirms the visual observation of trend lines, as the solid sealant seems steeper.

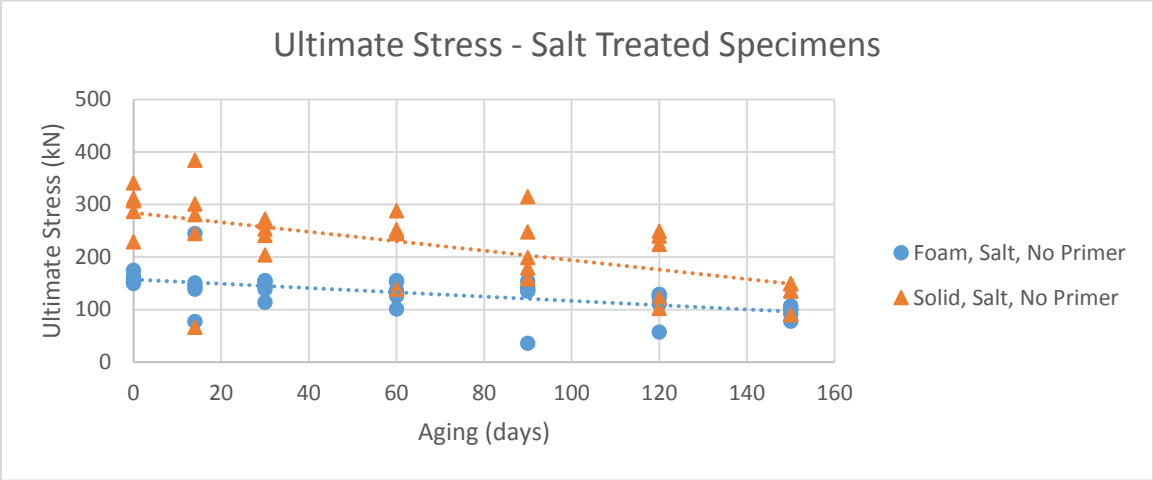

Figure 41: Ultimate Stress for specimens exposed to salt and no primer treatment

Figure 42 shows the ultimate stress values for specimens not exposed to salt but treated with primer. The ultimate failure stresses for the solid sealant is consistent with the other specimens at the start of the experiment (0 days), measuring approximately 280 kN. After 150 days of aging, the ultimate stress of the solid sealant measured consistently at approximately 140 kN, an overall reduction of about 50%. However, the foam sealant's stress at failure dropped approximately 33% over the same time period and aging conditions. The t-test confirmed that the difference in these slopes is statistically significant, as the t-value generated was 2.675 with a probability of 0.011.

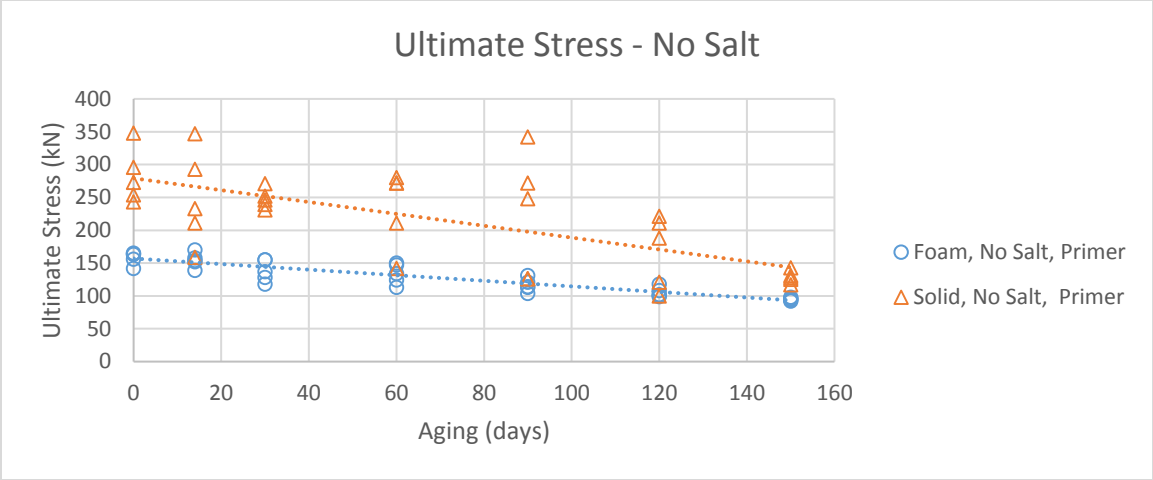

Figure 42: Ultimate Stress for specimens not exposed to salt and primer treatment

Figure 43 shows the ultimate stress values for specimens not exposed to salt and also not treated with primer. The ultimate failure stresses are consistent with the previous results. Again, the solid sealant exhibits a sharper decline in tensile capacity, indicating its vulnerability to aging itself. The t-test again confirms that the solid sealant's drop in ultimate stress is significant, yielding a t-value of 3.907 with a probably of less than 0.001.

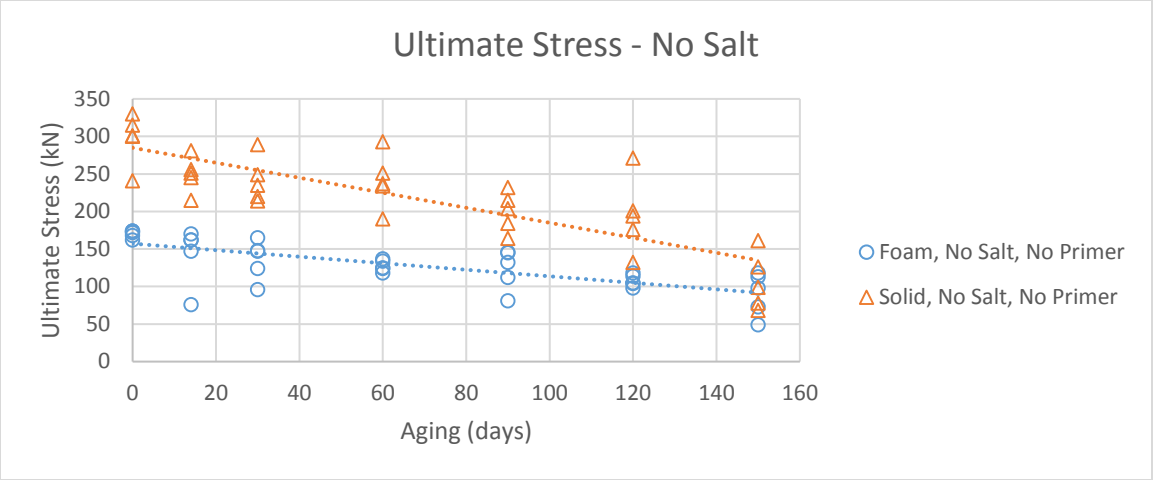

Figure 43: Ultimate Stress for specimens not exposed to salt and no primer treatment

From Figure 44, it can be observed that the modulus of the solid sealant decreases at a higher rate when exposed to salt water aging. The stress at 100% strain of specimens containing primer at 0 days (no aging) was measured to be approximately 39 kN. Over an aging period of 5 months, however, the stress dropped to about 21.5 kN, a reduction of 44.9%. The foam sealant, however, exhibited a more consistent modulus throughout the course of aging. The initial stress at 100% strain was observed to be about 26.9 kN, dropping to about 21 kN after 5 months aging. This represents a reduction in stress of approximately 21.9%. The changes in slope of these points was deemed significant with a t-value of 3.19 and probability of 0.002.

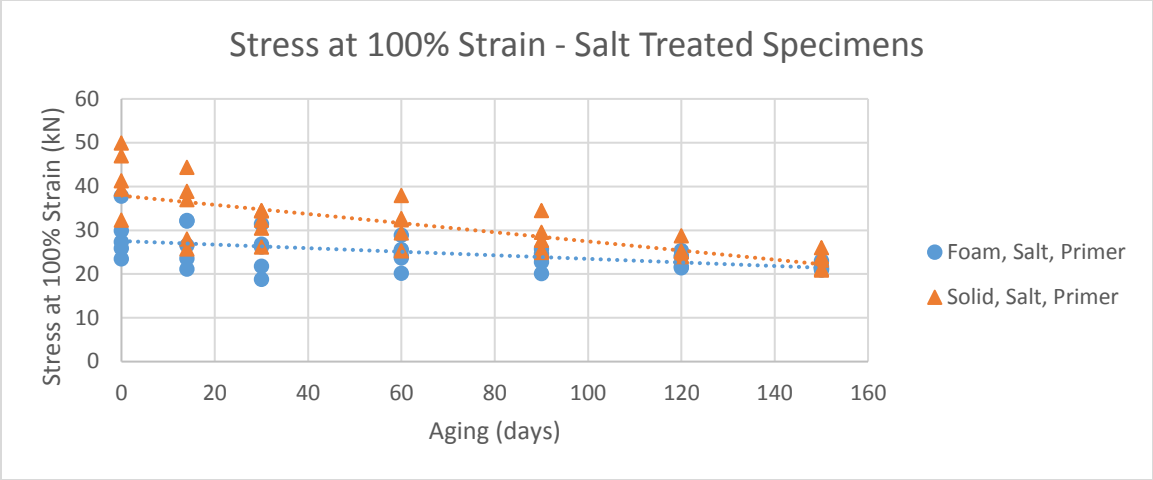

Figure 44: Stress at 100% Strain for specimens exposed to salt and primer treatment

Figure 45 shows the behavior of the stress at 100% strain observed in specimens that were aged in the salt water tank, but did not receive primer treatment prior to immersion. Once again, the modulus of the solid sealant appears to decrease at a higher rate than that of the foam sealant. The stress at 100% strain of specimens containing primer at 0 days (no aging) was measured to be approximately 39 kN. Over an aging period of 5 months, the stress dropped to about 21 kN, a reduction of 46.1%. The foam sealant also exhibited a decrease in stress, but not as sharp as the solid sealant. The foam sealant's initial stress at 100% strain was observed to be about 27 kN, dropping to about 23 kN after 5 months aging. This represents a reduction in stress of approximately 14.8%. Again, the t-test confirmed the difference in these slopes, generating a t-value of 4.305 and probability of less than 0.001.

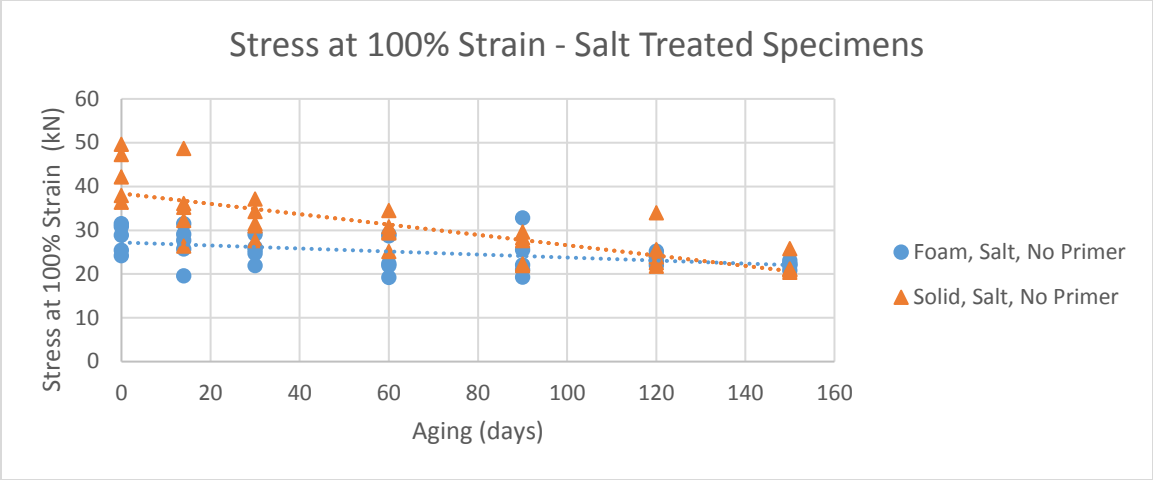

Figure 45: Stress at 100% Strain for specimens exposed to salt and no primer treatment

Figure 46 also shows that the modulus of the solid sealant appears to decrease at a higher rate than that of the foam sealant, even without the presence of salt. The stress at 100% strain of specimens containing primer at 0 days (no aging) was measured to be approximately 40.1 kN. Over an aging period of 5 months, however, the stress dropped to about 23.5 kN, a reduction of 41.4%. The foam sealant, however, exhibited a more consistent modulus throughout the course of aging. The initial stress at 100% strain was observed to be about 26.9 kN, dropping to about 21 kN after 5 months aging. This represents a reduction in stress of approximately 21.9%. The difference in slopes due to aging generated a t-value of 4.305 with a probability of less than 0.001, suggesting a significant difference in slopes.

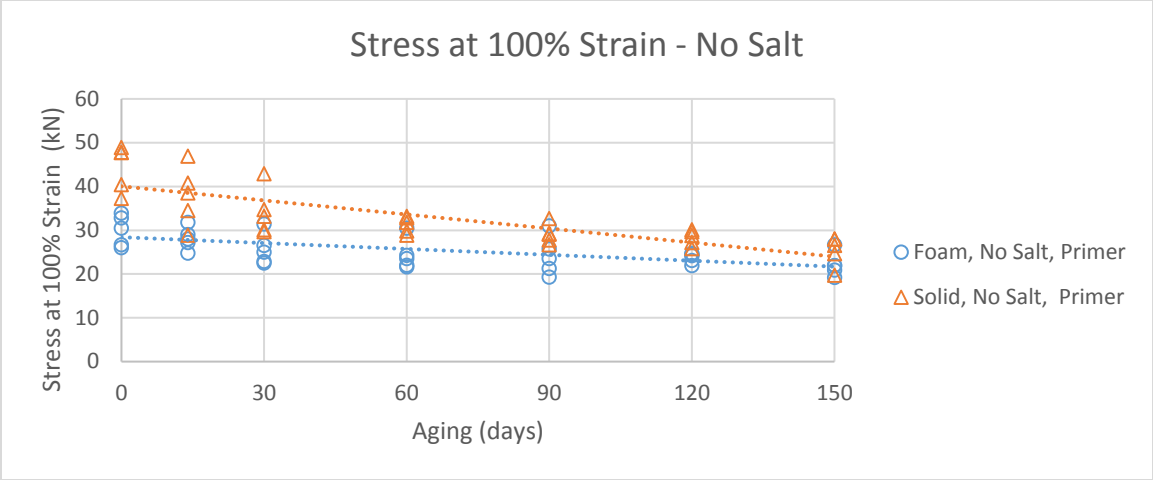

Figure 46: Stress at 100% Strain for specimens not exposed to salt and primer

Figure 47 shows the stress at 100% strain for specimens not exposed to salt or treated with primer. Again, it can be observed that the stress at 100% strain drastically reduces after 150 days of aging, even to the point where the foam and solid stresses at 100% strain are almost equal at 150 days. Although the foam sealant also exhibits a reduction in stress at 100% strain as a function of aging, the drop is not as significant. Comparing these slopes using the t-test generated a statistical difference with a t-value of 4.325 and probability of less than 0.001, suggesting that the solid sealant's stress at 100% strain dropped at a faster rate throughout the course of aging.

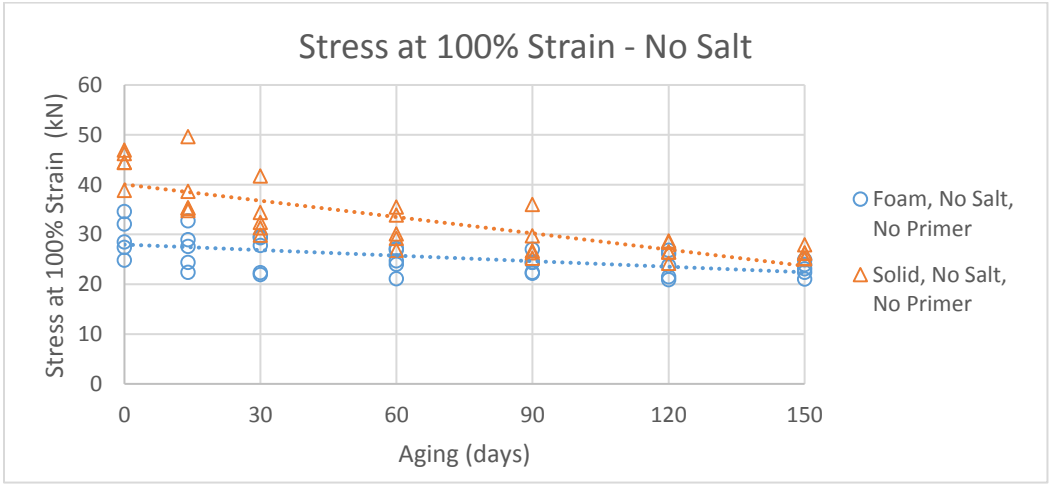

Figure 47: Stress at 100% Strain for specimens exposed to salt and no primer treatment

Figure 48 shows the ultimate strain of the specimens treated with salt but not with primer. It can be observed that the average elongation for the solid sealant appears to be almost the same over time, judging by the trend line. However, the foam sealant's elongation tends to increase over time, possibly suggesting a reduction in stiffness (and therefore an increase in ductility). Although visually these trend lines appear to differ, the t-test generates a t-value of 0.061 with a probability of 0.952. With values generated below the acceptable threshold, a conclusion cannot be reached regarding difference in slopes.

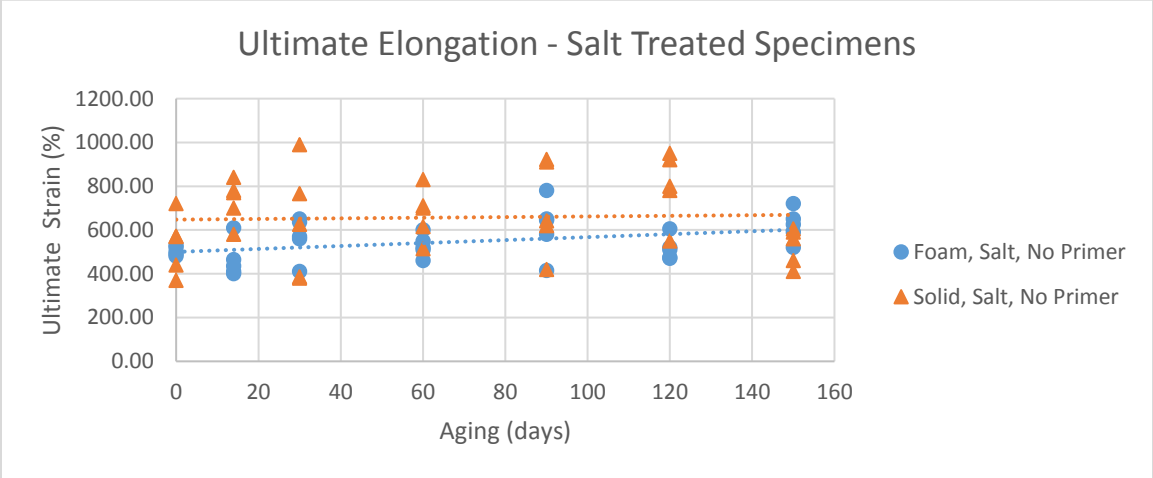

Figure 48: Ultimate strain for specimens exposed to salt and no primer treatment

Figure 49 also shows the ultimate strain for salt treated specimens that received primer treatment to the substrate. Although the initial few elongations are rather scattered, both sealants show a more consistent elongation at failure towards the longer aging durations (90, 120 and 150 days). This result may suggest that the deteriorative effects of the salt may affect both sealants in a similar fashion, resulting in more consistent failure strains. When comparing the two slopes, the

t-test generated a t-value of 0.114 and a probability of 0.909; these values are not sufficient to conclude that the difference in elongation development is significant between the two sealants.

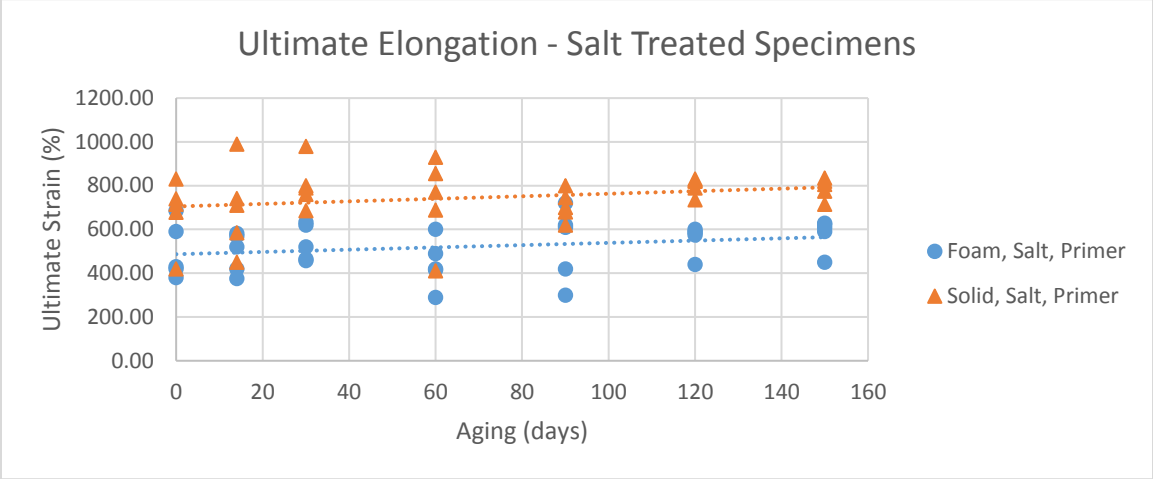

Figure 49: Ultimate strain (elongation) for specimens exposed to salt and primer treatment

Figure 50 shows the ultimate strain for specimens not exposed to salt or primer. Again, the elongations are rather scattered due to imperfections in the material, casting, and a small coupon size. However, the general trend suggests that both sealants exhibit a fairly consistent ultimate elongation, with a slight increase over a duration of 150 days. Again, no conclusion can be reached regarding the difference in slope as the t-value was 0.235 with a corresponding probability of 0.815.

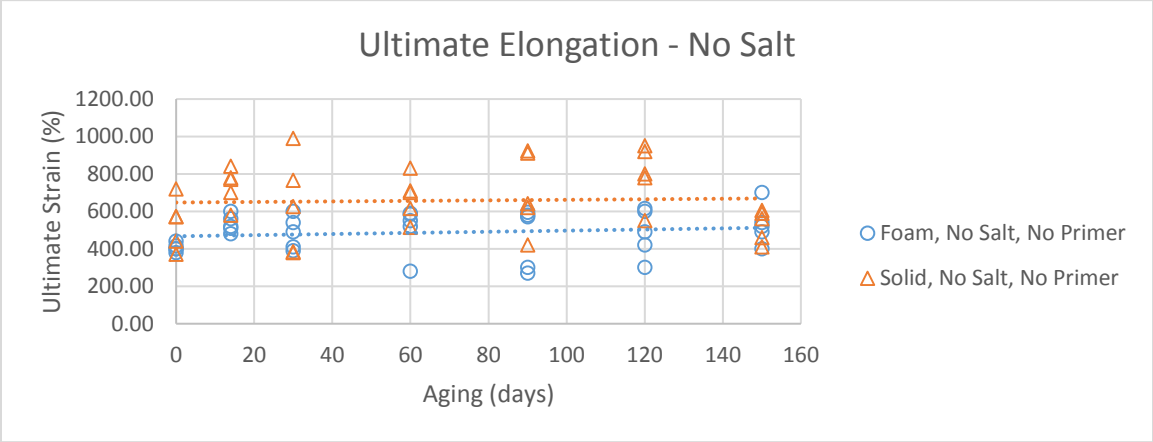

Figure 50: Ultimate strain for specimens not exposed to salt and no primer treatment

Figure 51 shows the ultimate strain for specimens not exposed to salt but treated with primer. The initial elongation of the foam specimens is relatively low compared to the other specimens (most likely due to the one specimen that failed at less than 200% elongation due to some weakness in the material). However, the general trend shows that the foam exhibits a larger elongation over the duration of aging, whereas the solid sealants elongation stays approximately the same. The t-value for the significance in slope difference is 1.515 with a probability of 0.135, values too high to determine statistical difference.

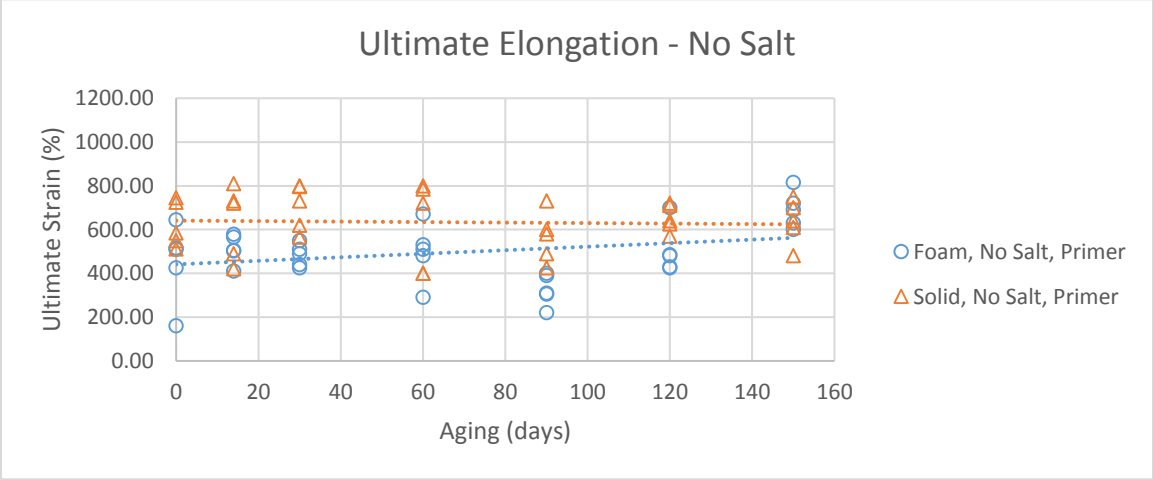

Figure 51: Ultimate strain for specimens not exposed to salt and primer treatment

Tables 5 and 6 show the average ultimate stress, average ultimate strain, and adhesive failure fraction for all specimens as a function of aging. Five specimens were tested for each parameter (i.e. 5 specimens containing foam sealant with primer at 0 days' duration, and another 5 specimens containing foam sealant without primer for the same aging period). The average values reflect the measured average of all five specimens for that particular parameter. The

ultimate stress for each specimen was recorded when the sealant could no longer sustain a higher load, regardless of continuous deformation. The ultimate strain for each specimen was considered as the maximum sustained strain before complete detachment from the substrate or the sealant itself. The raw data set from which these tables were generated can be found in Appendix B.

Table 5: Saltwater Aging Test – Average Ultimate Stresses and Strains (Salt Treated Specimens)

Salt Treated Specimens						
Age (days)	**Sealant Type**	**Surface Prep**	**Average Ultimate Stress (kPa)**	**Average Stress at 100% Strain (kPa)**	**Average Ultimate Strain (%)**	**Adhesive Failure Mode (%)**
0	Foam	Primer	157[a] ± 9.6[b]	28.8 ± 5.5	501 ± 130.7	20
		No Primer	159 ± 8.2	28.2 ± 3.2	504 ± 20.74	20
	Solid	Primer	264 ± 30.6	41.9 ± 6.8	676 ± 154	100
		No Primer	295 ± 33.4	42.6 ± 5.7	679 ± 90.58	100
14	Foam	Primer	144 ± 11	27.0 ± 5.0	493 ± 91.9	20
		No Primer	152 ± 48	26.7 ± 4.5	464 ± 85.4	0
	Solid	Primer	256 ± 21.2	34.8 ± 7.7	695 ± 200.9	100
		No Primer	255 ± 94	35.7 ± 8.1	522 ± 159.2	100
30	Foam	Primer	135 ± 17.8	25 ± 4.8	539 ± 83.6	20
		No Primer	141 ± 13.2	25.4 ± 2.5	565 ± 95.1	0
	Solid	Primer	248 ± 43.2	31.5 ± 3.4	803 ± 108.7	100
		No Primer	247 ± 21.6	32.3 ± 3.5	380 ± 117.2	100
60	Foam	Primer	134 ± 5	24.5 ± 3.1	443 ± 113.5	0
		No Primer	134 ± 17.6	24.2 ± 4.4	528 ± 51.6	0
	Solid	Primer	240 ± 49.4	31.5 ± 4.6	730 ± 200.8	100
		No Primer	234 ± 44.8	29.8 ± 3.35	731 ± 200.7	80
90	Foam	Primer	119 ± 29.8	23.4 ± 2.1	534 ± 169.9	0
		No Primer	120 ± 38.4	24.1 ± 5.3	614 ± 132.8	0
	Solid	Primer	229 ± 58	28.4 ± 3.8	709 ± 67.8	80
		No Primer	219 ± 50.2	25.9 ± 3.5	485 ± 67.6	80
120	Foam	Primer	115 ± 8.8	23.3 ± 1.69	558 ± 66.5	0
		No Primer	109 ± 24.2	23.6 ± 1.2	516 ± 54.2	0
	Solid	Primer	146 ± 54.4	25.4 ± 1.8	800 ± 39.5	60
		No Primer	187 ± 55.8	25.5 ± 4.9	527 ± 193.9	80
150	Foam	Primer	72 ± 7.8	21.6 ± 0.8	579 ± 74.0	0
		No Primer	95 ± 9	22.0 ± .84	621 ± 73.8	0
	Solid	Primer	142 ± 14	23.0 ± 2.1	790 ± 47.4	80
		No Primer	131 ± 19.4	21.8 ± 2.22	751 ± 95.8	80

[a]: Average of five samples tested (complete specimen information found in Appendix A)
[b]: 95% confidence interval for the average

Table 6: Saltwater Aging Test – Average Ultimate Stresses and Strains (Non-Salt Treated Specimens)

Non-Salt Treated Specimens						
Age (days)	**Sealant Type**	**Surface Prep**	**Average Ultimate Stress (kPa)**	**Average Stress at 100% Strain (kPa)**	**Average Ultimate Strain (%)**	**Adhesive Failure Mode (%)**
0	Foam	Primer	158[a] ±7.6[b]	29.9 ± 3.5	451 ± 180.6	0
		No Primer	170 ±4	29.4 ± 3.8	407 ± 22.2	20
	Solid	Primer	282 ±33.2	44.4 ± 5.2	623 ± 105	100
		No Primer	297 ±27	44.1 ± 3.1	534 ± 135.1	100
14	Foam	Primer	154 ±9	28.1 ± 2.5	512 ± 66.9	0
		No Primer	143 ±30.8	27.2 ± 4.0	534 ± 46.6	20
	Solid	Primer	248 ±58.4	34.8 ± 7.7	634 ± 168.9	100
		No Primer	249 ±19	35.7 ± 8.1	734 ± 99.4	100
30	Foam	Primer	138 ±13	25 ± 4.8	483 ± 51.1	0
		No Primer	136 ±21.2	25.4 ± 2.5	486 ± 87.9	0
	Solid	Primer	247 ±12	31.5 ± 3.4	702 ± 105.2	100
		No Primer	241 ±23.8	32.3 ± 3.5	629 ± 259.9	100
60	Foam	Primer	133 ±12.4	24.5 ± 3.1	496 ± 136.3	0
		No Primer	127 ±6.2	24.2 ± 4.4	505 ± 128.9	0
	Solid	Primer	235 ±47.2	31.5 ± 4.6	621 ± 203.8	100
		No Primer	241 ±29.6	29.8 ± 3.35	674 ± 117.3	100
90	Foam	Primer	116±8	23.4 ± 2.1	325 ± 73.31	0
		No Primer	123 ±21.8	24.1 ± 5.3	463 ± 163.0	0
	Solid	Primer	222 ±75.8	28.4 ± 3.8	565 ± 116.0	100
		No Primer	199 ±21.2	25.9 ± 3.5	702 ± 213.0	100
120	Foam	Primer	105 ±2	23.6 ± 1.1	504 ± 112.9	0
		No Primer	107 ±6.4	23.8 ± 2.6	485 ± 130.8	0
	Solid	Primer	168 ±43.6	28.3 ± 1.7	653 ± 62.4	80
		No Primer	194 ±40.2	26.8 ± 1.8	800 ± 157.9	100
150	Foam	Primer	95 ±1.8	22.1 ± 2.7	691 ± 83.9	0
		No Primer	90 ±23.2	23.0 ± 1.4	530 ± 109.1	0
	Solid	Primer	128 ±7.6	25.3 ± 3.4	636 ± 102.6	80
		No Primer	106 ±30.2	26.1 ± 1.1	525 ± 85.6	80

[a]: Average of five samples tested (complete specimen information found in Appendix A)
[b]: 95% confidence interval for the average

In order to investigate the effect of each individual parameter (salt, primer application, foam, and age) on the ultimate stress, ultimate strain, stress at 100% strain and adhesive failure fraction, a multiparameter linear model was applied to the entire data set using PSI-Plot (PSI-Plot). In spite of being linear, a non-linear fitting method, the Levenberg-Maquardt LSQ method (Lourakis), was used as the software was more convenient. Each parameter that influenced the specimens was assigned a variable, which was multiplied by a "parameter term" which defines how significant that parameter is. Variables such as x_1, x_2, x_3 and x_4 were used for salt, primer, foam and age, respectively. All results were tabulated according to age and each specimen was coded using a binary system. For example, a specimen containing foam exposed to salt, aging, and primer application would be identified as $x_1 = 1$, $x_2 = 1$, $x_3 = 1$ and x_4 ranging from -3 to 3 to define all 7 aging periods. The aging parameter was set from -3 to 3 so that the model would intercept 0 at 2 months aging. When solid sealant was used, x_3 was set to 0. This terminology allowed for including the global effect of all parameters when using the fitting model, shown below.

$$y = a_0 + a_1x_1 + a_2x_2 + a_3x_3 + a_4x_4 + a_{12}x_1x_2 + a_{13}x_1x_3 + a_{14}x_1x_4 + a_{23}x_2x_3 + a_{24}x_2x_4 + a_{34}x_3x_4$$

The model also included terms for interaction between two or more parameters, since specimens exposed to salt and age may have performed differently than specimens exposed to just aging. These parameters, for example, are defined by x_{12}, which would represent the interaction between salt and primer application. The parameter values, labeled as a_0, a_1, etc., were generated once the model was run. All parameter and interaction terms are defined in Table 7.

Table 7: Parameter and Interaction Terms for LSQ Model

Variable	Parameter	Interaction
x_1	Salt	--
x_2	Primer	--
x_3	Sealant	--
x_4	Age	--
a_{12}	--	Salt and Primer
a_{13}	--	Salt and Sealant
a_{14}	--	Salt and Age
a_{23}	--	Primer and Sealant
a_{24}	--	Primer and Age
a_{34}	--	Sealant and Age

The model provided parameters values and uninvariant 95% confidence intervals, which were used to generate p-values. These p-values indicate the probability of error in rejecting the null hypothesis, i.e., the factor (aging time, salt concentration, etc.) is not significant. P-values less than 0.05 were considered to be an acceptable threshold of reliability for this study. A sample output summary of this analysis is provided in Appendix C.

As expected, the specimens with foam sealant instead of solid sealant had a significant influence on the reduction of ultimate stress, yielding a p-value of less than 0.001 ($t = 16.20$). Likewise, the model showed that the influence of age also had a statistically significant effect on the reduction of the ultimate stress, yielding a p-value less than 0.001 ($t = 14.09$). The interaction between these two parameters (foam and age) confirmed these conclusions, as the yielded p-value was also less than 0.001 ($t = 6.23$). Interestingly, the interaction between salt and primer yielded a p-value of 0.008 ($t = 2.73$), which may suggest a deteriorative property of these two parameters on the ultimate stress.

Due to large variations in the ultimate strains, the statistical analysis for ultimate strain only yielded a significance when foam specimens were tested, which is expected (p-value generated was less than 0.001 and the t-value was 4.74). When considering the adhesive failure fraction, which is the fraction of adhesive failures (clean detachment from the substrate) out of five specimens tested for a particular parameter, several parameters generated a statistically meaningful effect. The inclusion of salt generated a p-value of 0.0013 ($t = 3.41$), indicating that the effect of salt may have an effect on the bond between the sealant and the substrate. However, when examining the effect of primer on the failure fraction, the yielded p-value was 0.79 ($t = 0.25$), suggesting that the effect of primer on the bond is likely to be small. Interestingly, the interaction between salt and primer generated a p-value of 0.054 ($t = 1.97$), which is slightly higher than the acceptable threshold to draw a reasonable conclusion. However, this result suggests a possible deteriorative effect due to a combination of salt and primer application. Additionally, the model results suggest that the effect of aging time has a statistically significant effect on the adhesive failure fraction, generating a p-value of 0.003 ($t = 3.877$).

2.8 Volume Expansion Test and Results

Previous studies conducted by Malla et al. have indicated that the foam sealant exhibits significant expansion after casting, often between 50% and 70%. In order to better understand the characteristics of expansion and determine the cause for such variations, the expansion experiment was established to examine the influence of initial volume of sealant on the total expansion. This concept was formulated from observations in the laboratory when certain specimens with varying amounts of sealant exhibited different expansion characteristics. Motivation to understand the behavior of expansion in this foam sealant stemmed from specifications for poured silicone sealant

joints by Watson Bowman Acme, which suggest a 12.7 mm (0.5 in.) layer of silicone to be applied above the backer rod. The top surface of the silicone seal should also be recessed at 12.7 mm (0.5 in.) from the roadway. This is primarily to prevent damage to the joint itself due to repeated vehicular loading and reduce the likelihood of snow plows tearing the sealant. Since the foam sealant exhibits significant expansion upon initial set, understanding the behavior of the expansion would provide insight to the quantities needed to prevent expanding over the roadway and instead expand to the appropriate height above the backer rod.

In order to study the expansion as a function of initial volume, the foam sealant was cast into forms resembling a small section of a typical small movement bridge joint. The dimensions of each form were 152.4 x 25.4 x 38.1 mm (6 x 1 x 1.5 in.) (LxWxD). As shown in Table 8, the initial thickness of sealant applied in each form ranged from ¼" to 1", representing typical minimum and maximum thickness of sealant that would be applied into an in-service bridge joint.

Table 8: Initial thicknesses of specimens for expansion test

	Specimen Thickness (mm)									
Specimen No.	**1**	**2**	**3**	**4**	**5**	**6**	**7**	**8**	**9**	**10**
	3.175	3.969	7.938	7.938	7.144	7.938	9.525	11.90625	12.700	13.494

The thickness of each joint was measured every minute for the first 20 minutes after initial casting, and then every 5 minutes until the sealant exhibited no further expansion for three consecutive measurements. A laser based distance measurement device was used to measure the thickness of the sealant at each time interval. The device was placed 2 inches above each set of blocks in order to ensure a consistent reference point for each specimen. A schematic of the experimental set up is shown in Figure 52.

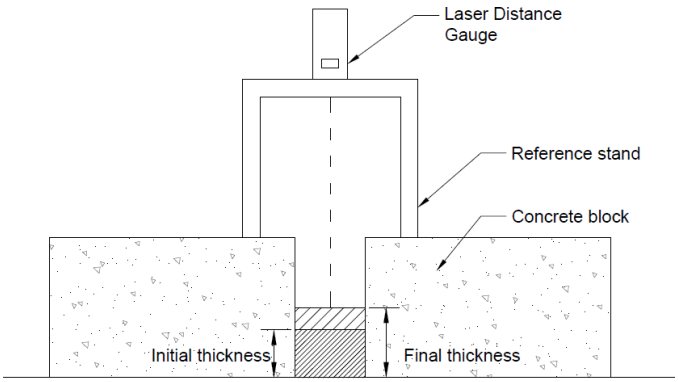

Figure 52: Expansion test assembly

As shown in Figure 53, the initial volume of sealant applied directly correlates to the final thickness of the sealant. For example, an initial thickness of 0.25” produced a final thickness of 0.375”, while an initial thickness of 1” produced a final thickness of almost 1.75”. The total exact expansion for these trials was 50% and 74%, respectively. The difference in expansion from one specimen to another may stem from lesser amounts of hydrogen gas being emitted from the specimen containing less sealant. Additionally, it can be observed that specimens containing a smaller initial amount of sealant experienced slower expansion in a step-like manner. The specimens containing a thicker amount of sealant expanded more frequently over time with larger steps.

These results indicate that applying the appropriate initial thickness of sealant into an expansion joint is crucial to ensure no sealant expands over the top edge of the substrate. Moreover, care must be taken to avoid applying conservative amounts of sealant as this may results in too thin of a layer of sealant. If the joint is too thin, it may puncture or allow water/debris to penetrate through to the substructure.

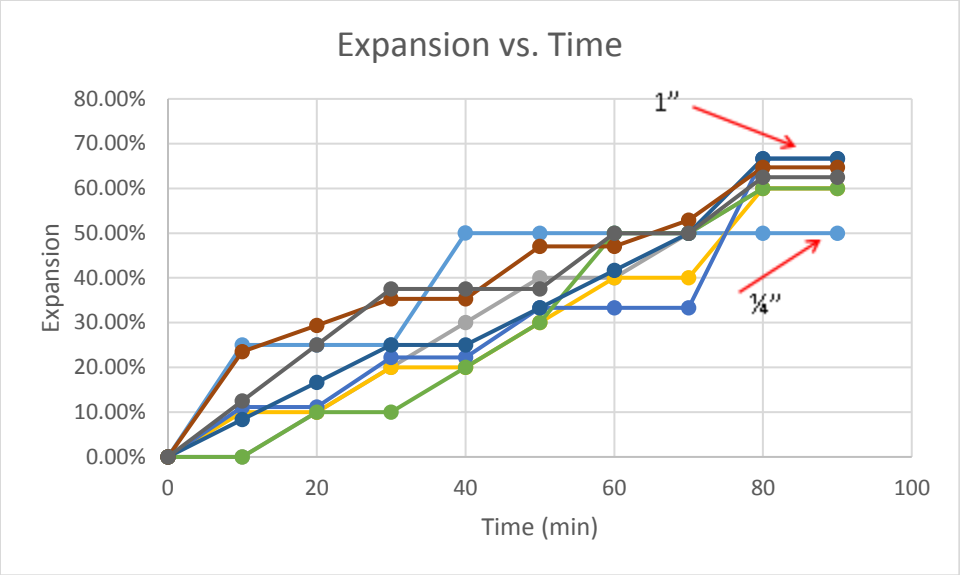

Figure 53: Expansion vs. time for foam sealant.

2.9 Conclusions

The silicone foam sealant was developed and further tested in the laboratory to gain a better understanding of the adhesion and bonding characteristics when compared to the solid sealant. Adhesion and tensile properties were obtained by pulling the specimens to failure. Expansion properties were characterized by observing expansion of various initial thicknesses of sealant. Finally, aging and road salt corrosion testing was conducted to determine the degradation of the bond and modulus of elasticity between the sealant and the substrate when subject to laboratory accelerated aging.

- Under a pure tensile load, the foam sealant exhibited a reduced modulus when stretched to its ultimate elongation. This indicates smaller stresses being transferred between the sealant material and the bridge header. This characteristic may be considered favorable when aiming to improve the adhesion properties of poured silicone joints, as the most common mode of failure is detachment from substrate (material failure was much less common).

- The application of primer onto the specimens yielded no significant difference in tensile and adhesion performance. Although 2 out of 10 specimens containing solid sealant failed via cohesive failure under the influence of primer, it cannot be said that primer significantly improves the bonding as the ultimate elongation was comparable to the specimens with no primer. The foam sealant showed no change in performance, as all specimens failed cohesively.
- The expansion of the foam sealant varies depending on the initial thickness of the sealant applied. When applying a thick coating of 1", the foam sealant expanded nearly 75%; meanwhile, a coating of 0.25" produced a total expansion of approximately 50% for a final thickness of 0.375". This may be attributed to the volume of additives in the foam sealant, as smaller quantities of foam sealant will contain less crosslinker. The evaporated hydrogen gas may tend to emit from the sealant as a whole, instead of creating air bubbles within the microstructure. For sealants with a larger thickness, however, more energy may be needed to fully evaporate the gas from the sealant; this may result in an increased foaming effect as more bubbles may stay trapped inside the structure of the sealant.
- The 100% secant modulus was observed to drop significantly for the solid sealant over an aging period of 5 months. The rate of deterioration of the solid sealant was on average 3 faster than that of the foam sealant. The specimens treated with primer did not show any noticeable change in stress modulus as a function of aging. The inclusion of road salt did not have a significant effect in the reduction of the stress modulus of either sealants.

3.0 FIELD INSTALLATION

3.1 Route 6 Bridge

Through the coordination of the Connecticut Department of Transportation, the experimental expansion joint was installed on three bridges throughout the state of Connecticut. Each bridge was chosen appropriately so that the foam sealant could accommodate the induced movements.

The first bridge is located in Windham, CT, comprising of two 170 ft. spans over the Route 6 expressway. Although the bridge spans over Route 6, vehicles travel under the bridge as part of Route 6 and circle around to travel on the bridge itself, still as part of Route 6 (Figure 54). This 8 girder composite bridge contains a steel girder superstructure and 7.75-inch concrete road deck (with concrete joint headers). A 2.5-inch bituminous concrete wearing surface and waterproofing membrane rests on top of the concrete deck. According to the 2013 Bridge Safety Inspection report, the anticipated daily traffic (ADT) for this bridge is 15,700 vehicles. The bearings are fixed at the pier, so each abutment joint accommodates movement over a temperature range of -10 degrees Fahreneheit to 110 degrees Fahrenheit, resulting in a theoretical movement of each joint of approximately 1.53 inches as per AASHTO specifications (AASHTO 2012). The speed limit on the bridge is 45 miles per hour. The state of Connecticut previously installed a silicone sealant which failed after an unknown period of time. Typically, they would install an asphaltic plug joint (APJ) to repair joints of this nature; however, the total movement of this bridge exceeds the capabilities of the asphaltic plug joint. Therefore, the silicone foam sealant joint was a good candidate for this bridge.

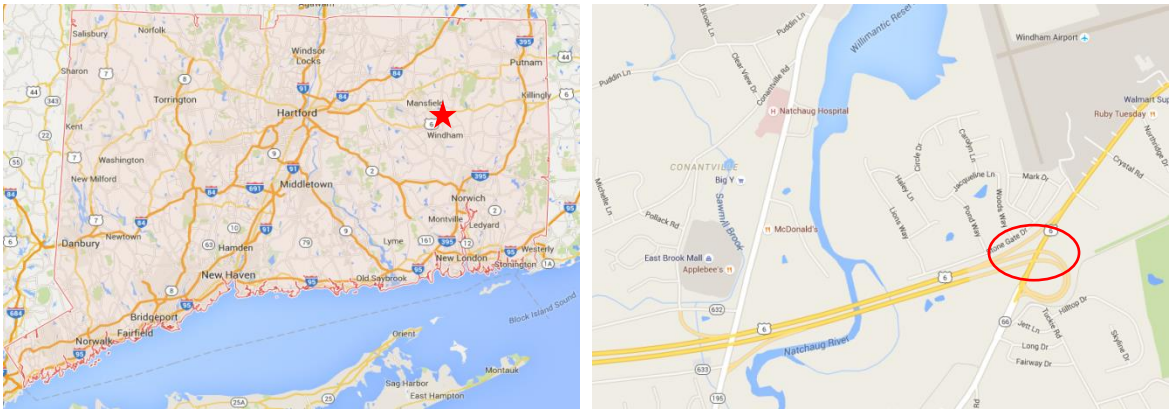

Figure 54: Map location of the Route 6 bridge in Windham, CT

(a) (b)

Figure 55: Span and center pier (a), support at abutment (b)

The full width of the bridge deck was sealed, amounting to a total of 106 feet (53 feet per joint). At the time of installation, the west joint had an average gap opening of 1.75 inches and the east joint had an average gap opening of 1.5 inches. However, due to imperfections of the concrete header, the gap width varied along the length of the joint by ± 0.25 inches.

The installation of the expansion joints of the Route 6 bridge was a two-day operation, conducted on Monday and Tuesday, September 14-15, 2015. Lane 1 and the south shoulder (shown in Figure 55) were installed on Monday, September 14. Weather conditions for Monday were

mostly sunny with some scattered clouds with a high temperature of 76 degrees Fahrenheit. Roadway temperatures and air humidity for this day ranged between 83-97 degrees and 18-26%, respectively. Lanes 2, 3 and the north shoulder were installed on Tuesday, September 15, 2015. Weather conditions for Tuesday were mostly sunny with some scattered clouds with a high temperature of 80 degrees Fahrenheit. Roadway temperatures and air humidity for this day ranged between 92-105 degrees Fahrenheit and 16-22%, respectively.

The Connecticut Department of Transportation provided two maintenance trucks for the installation of these new joints. For Monday's installation, a traffic pattern was established in such a way to allow for work on the East and West joint in the south shoulder and Lane 1. Using traffic cones, vehicles would travel in both directions using lanes 2, 3, and the north shoulder. For Tuesday's installation, two traffic patterns were set up. The first traffic pattern allowed for work on the East and West joint in lane 3 and the north shoulder. Traffic was diverted to travel in both directions using the south shoulder, lane 1, and lane 2. Once the sealant cured in lane 3 and the north shoulder, the traffic cones were redistributed to allow for work in lane 2 (the middle lane). Lane 3 and the north shoulder accommodated for westbound traffic, while lane 1 and the south shoulder accommodated for eastbound traffic.

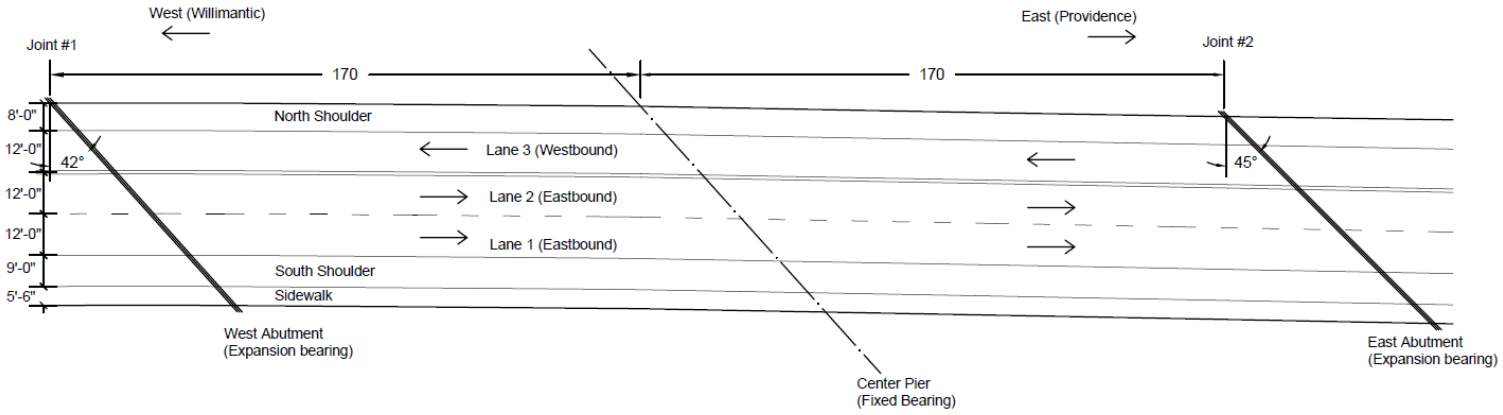

Figure 56: Plan schematic of the Route 6 bridge

The preparation of the joint (Figure 57) prior to actual installation of the sealant involved removing the existing joint and sand blasting the header to ensure any remnants of the previous joint were removed. Since this particular bridge was sealed using a poured silicone joint in the past, care was taken to ensure no remnants of the silicone joint were remaining on the substrate. This was to optimize the bond between the new foam sealant and the substrate. Once the surface was free of any loose material, a rag was used to apply a thin coating of acetone to the header of the bridge to remove any oils that may be present on the surface of the header.

Figure 57: Sandblasting and primer application onto the Route 6 bridge joint

After cleaning the joint from any loose debris or oils, primer was applied in locations as prescribed by the placing pattern shown in Figure 60. The top surface of the joint header was lined with duct tape to prevent any silicone from sticking to the roadway. This also allowed for a clean termination line between the edge of the substrate and the silicone sealant. A 3-inch backer rod was inserted 1 inch below the surface of the road using a T-shaped spacing tool. The vertical

portion of the spacing tool was exactly one inch, which allowed for a consistent recess of the backer rod along the joint. The backer rod was a 3-inch diameter closed cell, polyethylene extruded foam rod with excellent UV and moisture resistance. The joint was air blown after installation of the backer rod to remove any sand or debris that may have been carried into the joint after initial cleaning. Dividers were placed at the boundary sections (between the foam and solid sealant) to ensure the foam sealant did not spill over into the portion designated for solid sealant. The final configuration of the joint prior to pouring the silicone sealant is shown in Figure 58 (b).

Figure 58: Overview of the joint (a) before backer rod installation and (b) after installation

The placement of the sealants and the application of primer was chosen by following the Latin square method of randomly assigning variables to a field. This pattern was applied to one lane and then rotated clockwise for each adjacent lane to minimize bias of placement. It was assumed that any vehicle driving over the bridge stays in the same lane when it encounters both joints. This would allow for a straight forward comparison of the in-service behavior for the joint containing foam sealant with primer, foam sealant without primer, solid sealant with primer, and

solid sealant without primer. Each lane was split into two sections per joint; therefore, all four variables were included in each joint. It was assumed that the effect of the left tire onto the joint was the same as the effect of the right tire. Therefore, the effectiveness of the primer and the foam sealant could be easily observed when assessing each section of the lane.

Once the entire joint was prepared for pouring, appropriate amounts of each component were mixed to create the foam sealant formulation. Knowing the joint gap and sections of sealant needed as indicated in the placement plan, the components were pre weighed for lengths equivalent to half of a lane. Each component was sealed and stored in labeled syringes to allow facilitate the mixing process in the field without having to weigh out each component on site. Since the foam sealant is known to have a longer curing time, the foam sealant was placed first. The components were mixed on site in a bucket using a hand drill with an appropriate mixing attachment. Equal parts by volume of the Wabo white and Wabo black were combined and mixed in a bucket using the hand drill. Once a uniform color was established, the platinum was slowly added while continuously stirring the sealant. The addition of water followed. Once these four components were thoroughly mixed, the crosslinker was also added while continuously stirring the sealant. After a uniform texture was obtained, the sealant was carefully poured into the joint by hand. A leveling tool, also T shaped, was used to establish the appropriate recess from the roadway. The vertical portion of the T was exactly 0.5 inches in height, so the sealant was poured and shaped with a recess of 0.5 inches from the surface of the road.

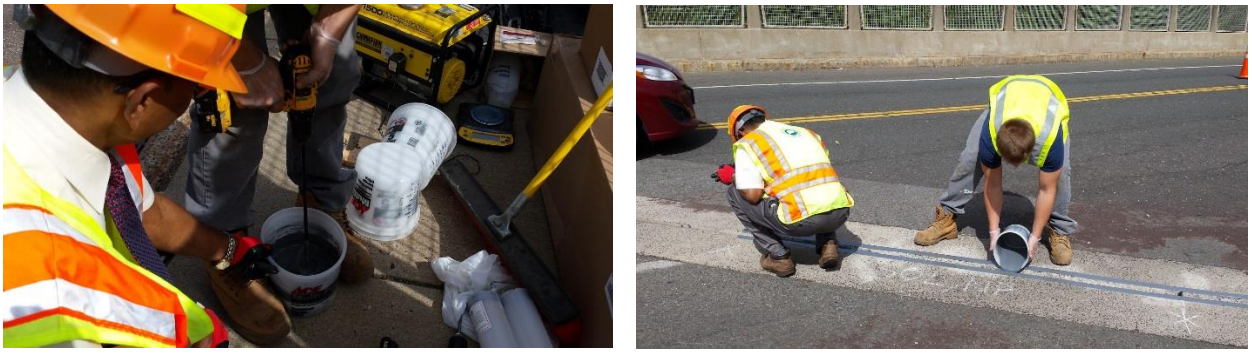

Figure 59: Installation of the sealant

The details of installation were meticulously recorded, as the curing of the sealant was time dependent. Tack free time for the foam sealant is approximately 1.5 hours, while tack free time for the solid sealant is about 1 hour. However, these times are highly dependent on the outside temperature and humidity. Silicone tends to cure quicker with higher temperatures. This difference in curing time motivated the group to install the foam sealant prior to installing the solid sealant at each lane. The average time for mixing, pouring and leveling one lane was approximately 35 minutes (both joints).

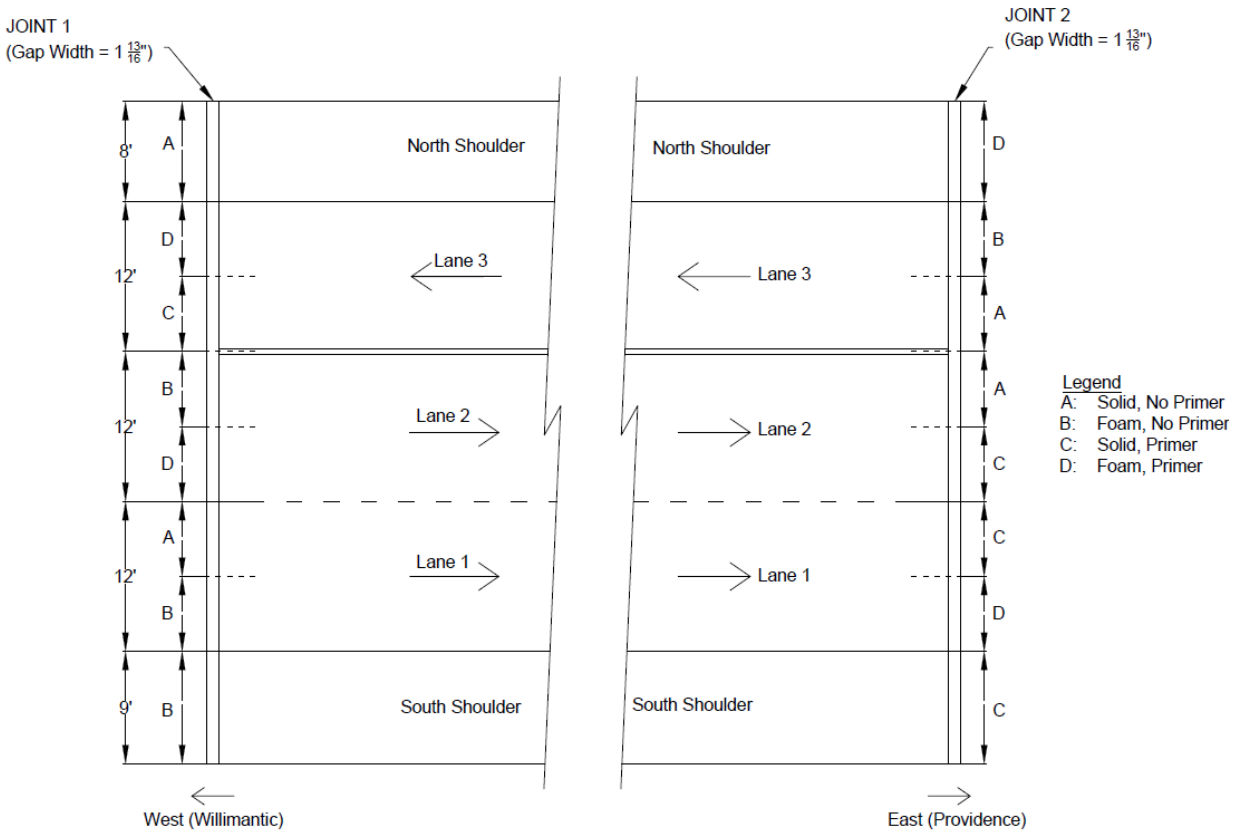

Figure 60: Sealant and primer placement plan

3.2 Route 291 Bridge

The second bridge selected for field implementation is located in Windsor, Connecticut as part of Route 291 spanning over Deerfield Road. The structure is a four span continuous, curved, multi-girder steel bridge carrying 4 lanes of traffic (2 in each direction). This 9 girder composite bridge contains a steel girder superstructure and 8.25-inch concrete road deck and 2.5 inch wearing surface with a waterproof membrane (with concrete joint headers). According to the 2014 Bridge Safety Inspection report by the Connecticut Department of Transportation, the anticipated daily traffic (ADT) for this bridge is about 52,600. The structure is supported at each abutment and at three intermediate piers spaced at 132, 124, 124, and 124 feet from west to east. The middle pier (pier 2) is fixed, while the exterior piers and abutments contain rollers to accommodate expansion.

Each abutment joint accommodates movement over a temperature range of -10 degrees Fahrenheit to 110 degrees Fahrenheit, resulting in a theoretical movement of each joint of approximately 2.44 inches as per AASHTO specifications. The speed limit on this bridge is 65 miles per hour. The state of Connecticut previously installed a poured silicone sealant joint which failed after two full years. This bridge was a good candidate to directly compare the longevity of the foam sealant in comparison to the previously installed commercially available product.

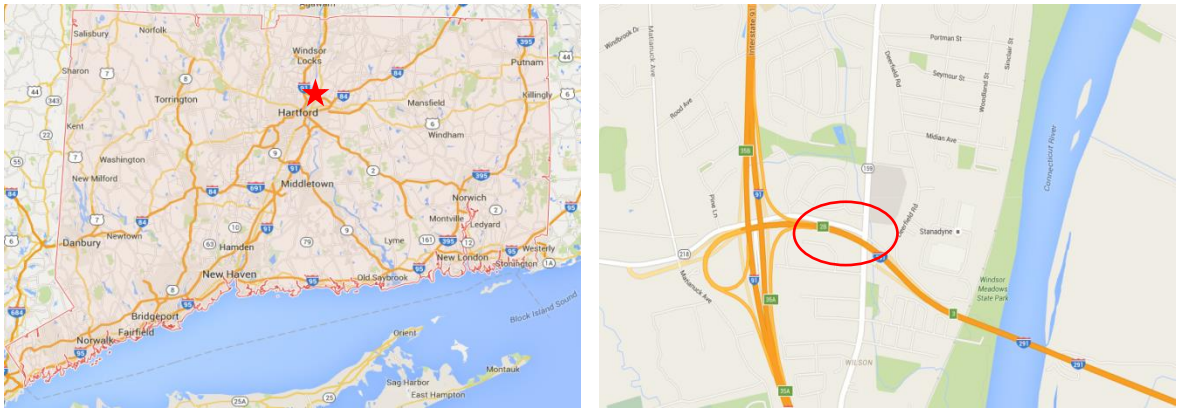

Figure 61: Location of Route 291 candidate bridge

Three joints, all located on the East-bound portion of the highway, were sealed on this bridge; two expansion joints at each abutment, and one static joint parallel to the west side joint. The static joint was included into the structure of the bridge when repairs were conducted in the past. The average width of the static joint is approximately 1” along the entire length. Since the bridge experienced some repair work in the past, the gaps were not a uniform width along the length of the joint. The west side joint gap varied between 3.125 – 3.375 inches. The west side joint gap varied between 2.625 – 3.5625 inches. The total length of expansion joints to be sealed amounted to 114 feet (3 joints of 38 feet each), as only the East-bound portion of the highway was sealed; the west-bound portion of the highway was not sealed.

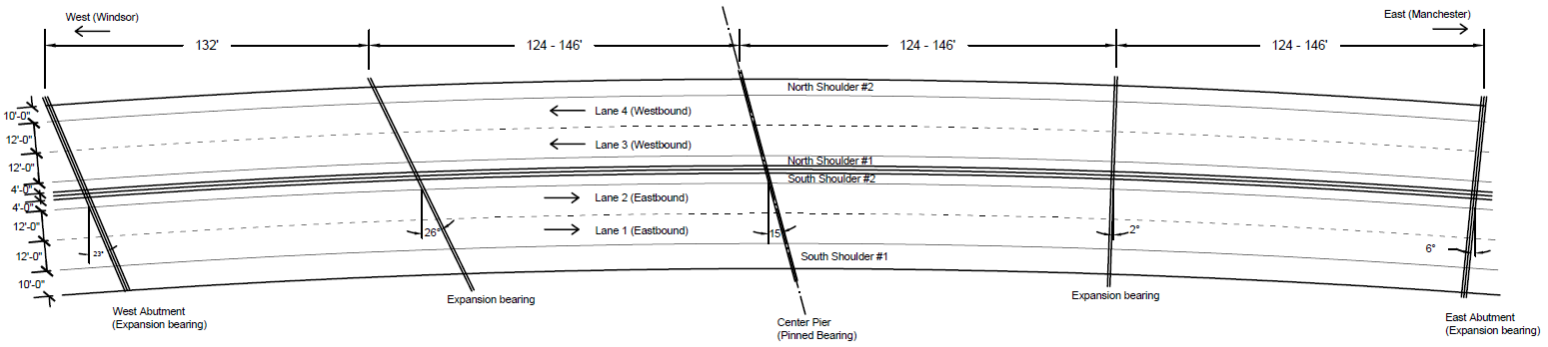

Figure 62: Plan schematic of Route 291 bridge

The installation of the expansion joints of the Route 291 bridge was a three-day operation; the Connecticut Department of Transportation provided conservative installation time gaps due to the importance of the route for commuters and its high volume traffic. The installation was conducted on Monday, Tuesday and Thursday, October 05, 06, and 08, 2015. Weather conditions for Monday, October 05 were mostly sunny with some scattered clouds with a high temperature of 60 degrees Fahrenheit. Roadway temperatures and air humidity at time of installation ranged between 71-77 degrees Fahrenheit and 37-44%, respectively. Weather conditions for Tuesday, October 06 were mostly sunny with some scattered clouds with a high temperature of 66 degrees Fahrenheit. Roadway temperatures and air humidity at time of installation ranged between 70-86 degrees Fahrenheit and 29-41%, respectively. Weather conditions for Thursday, October 08 were mostly sunny with some clouds with a high temperature of 72 degrees Fahrenheit. Roadway temperatures and air humidity at time of installation ranged between 64-70 degrees Fahrenheit and 51-63%, respectively.

The preparation of the joint prior to installation of the sealant involved removing the existing joint, which was coordinated by the Connecticut Department of Transportation as a night job conducted prior to installing the new expansion joint. This was done to save time and avoid

disrupting traffic on the day of installation. The header was thoroughly sand blasted to remove any loose material and remnants of the old joint. Additionally, a large blade saw was applied to the header to cut into the concrete and expose a fresh surface for optimal bond. Dividers were placed at the boundary sections (between the foam and solid sealant) to ensure the foam sealant did not spill over into the portion designated for solid sealant. Finally, a rag was used to apply a thin coating of acetone to remove any oils that may have potentially been left on the surface.

Figure 63: Joint preparation on the Route 291 bridge

After cleaning the joint from any loose debris or oils, primer was applied in locations as prescribed by the placing pattern shown in Figure 64. The placement of the sealants and the application of primer was chosen by following the Latin square method of randomly assigning variables to a field with minimal bias of placement. It was assumed that any vehicle driving over the bridge stays in the same lane when it encounters both joints. This would allow for a straight

forward comparison of the in-service conditions for the joint containing foam sealant with primer, foam sealant without primer, solid sealant with primer, and solid sealant without primer. Each lane was split into two sections per joint; therefore, all four variables were included in each joint. It was assumed that the effect of the left tire onto the joint was the same as the effect of the right tire. Therefore, the effectiveness of the primer and the foam sealant could be easily observed when assessing each section of the lane.

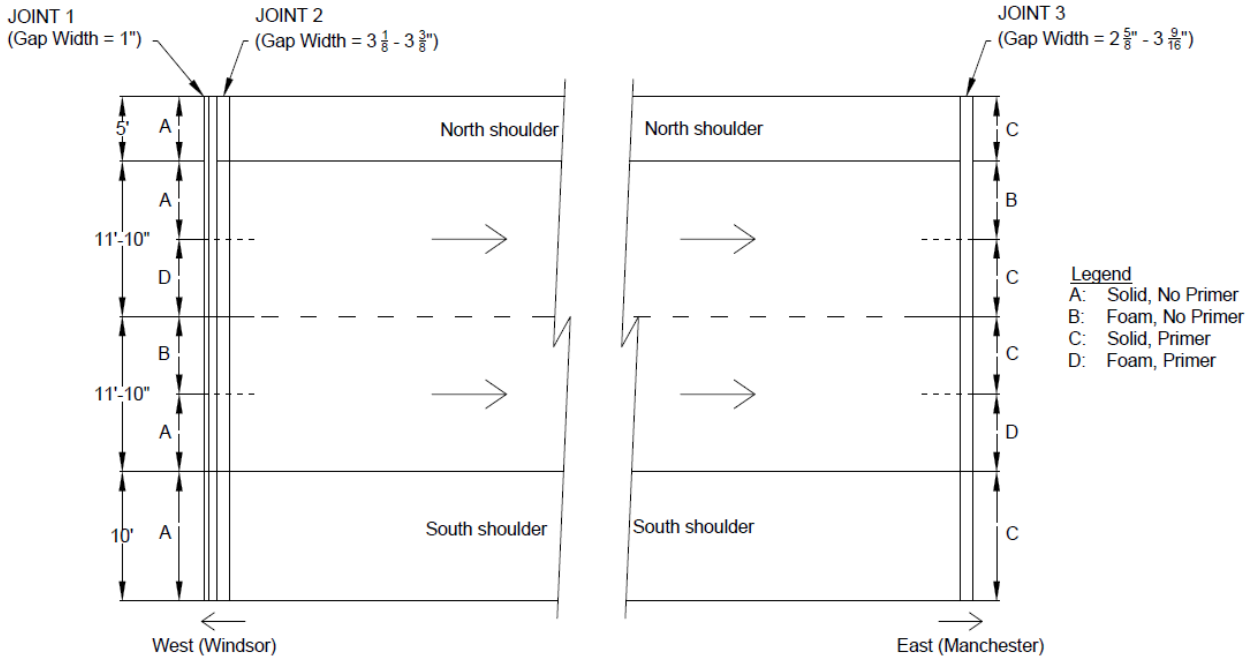

Figure 64: Sealant and primer placement plan

Once primer was applied to the appropriate locations, the top surface of the joint header was lined with duct tape to prevent any silicone from sticking to the roadway. A 5-inch backer rod was inserted 1 inch below the surface of the road using a T-shaped spacing tool. The vertical portion of the spacing tool was exactly one inch, which allowed for a consistent recess of the backer rod along the joint. The backer rod was a 5-inch diameter closed cell, polyethylene extruded foam rod with excellent UV and moisture resistance. The joint was air blown after installation of

the backer rod to remove any sand or debris that may have been carried into the joint after initial cleaning.

Figure 65: Installation of backer rod and duct tape lining

Once the entire joint was prepared and the appropriate amounts of each component were mixed to create the foam sealant formulation. Once again, the components were pre weighed for specified lengths of expansion joint to be sealed and stored in capsules for easy extraction. Since the foam sealant is known to have a longer curing time, the foam sealant was placed first. Dividers were placed at the boundary sections (between the foam and solid sealant) to ensure the foam sealant did not spill over into the portion designated for solid sealant.

3.3 Route 22 Bridge

The third bridge selected for field implementation in this project is located in North Haven, CT, comprising of two 141 ft. spans over Route 40. This 5 girder composite bridge contains a steel girder superstructure and 8-inch reinforced concrete deck (with concrete joint headers). A 2.5-inch

bituminous concrete wearing surface and waterproofing membrane rests on top of the concrete deck. According to the 2013 Bridge Safety Inspection report, the anticipated daily traffic (ADT) for this bridge is 6,100 vehicles. The bearings are fixed at the center pier, so each abutment joint accommodates movement over a temperature range of -10 degrees Fahrenheit to 110 degrees Fahrenheit, resulting in a theoretical movement of each joint of approximately 1.3 inches as per AASHTO specifications (AASHTO 2012). The speed limit on the bridge is 25 miles per hour. The previous joint on this bridge consisted of a poured silicone seal which showed signs of failure, as there was noticeable leaking of water onto the abutment and several rips and punctures throughout the length of the joint. The maintenance crew reported that the seal was installed approximately 4 years prior to the installation of the foam sealant. Therefore, this bridge allowed for a straight forward comparison of the in-service lifespan of the solid and foam sealant.

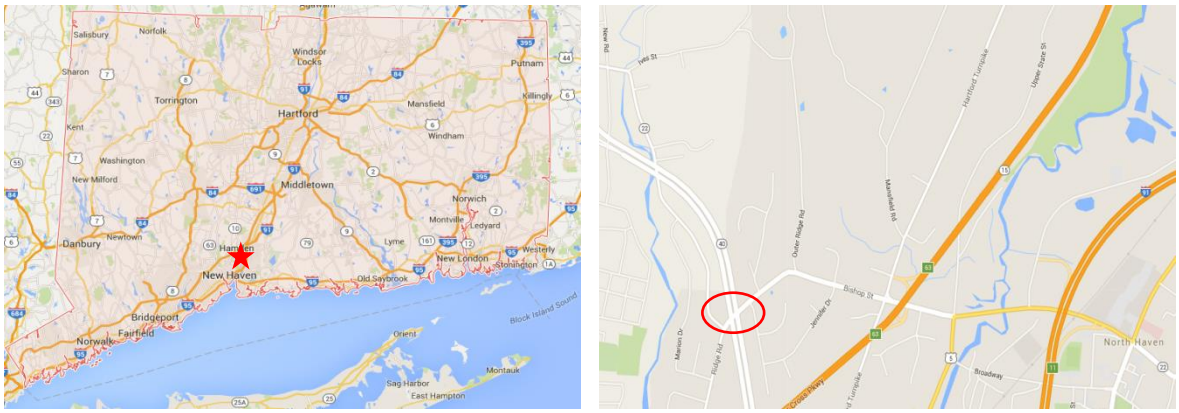

Figure 66: Map location of the Route 22 bridge in North Haven, CT

For this bridge, both joints were sealed for the full width of the bridge deck. This amounted to a total of 80 feet (approximately 40 feet per joint). At the time of installation, the west joint had an average gap opening of 1.00 inches and the east joint had an average gap opening of 2.00 inches. The east joint, however, had significant imperfections along the length of the joint which varied the gap width by ± 0.50 inches.

The installation of the expansion joints of the Route 22 bridge was a one-day operation, conducted on Tuesday, October 20, 2015. Weather conditions for that day were mostly sunny with an average temperature of 58 degrees Fahrenheit. Roadway temperatures and humidity ranged from 57.2-84 degrees Fahrenheit and 28-42%, respectively. The Connecticut Department of Transportation provided two maintenance trucks for the installation process. The traffic pattern consisted of shutting down Lane 1 and the south shoulder. This allowed for installation of the silicone sealants in these lanes for both joints. Since the west joint was sealed first, it was opened to traffic upon full curing of the sealant. However, the east joint was not fully cured. Therefore, traffic was routed in an S-shape to allow for installation of the sealant in lane 2 on the west joint. Once the sealant in lane 1 and the south shoulder cured on the east side, lane 2 was fully closed for installation and curing of the sealant of both joints. Finally, lane 3 and the north shoulder was closed to allow for installation in those locations for both joints. The entire bridge was sealed in approximately 4.5 hours with minimal traffic disruption.

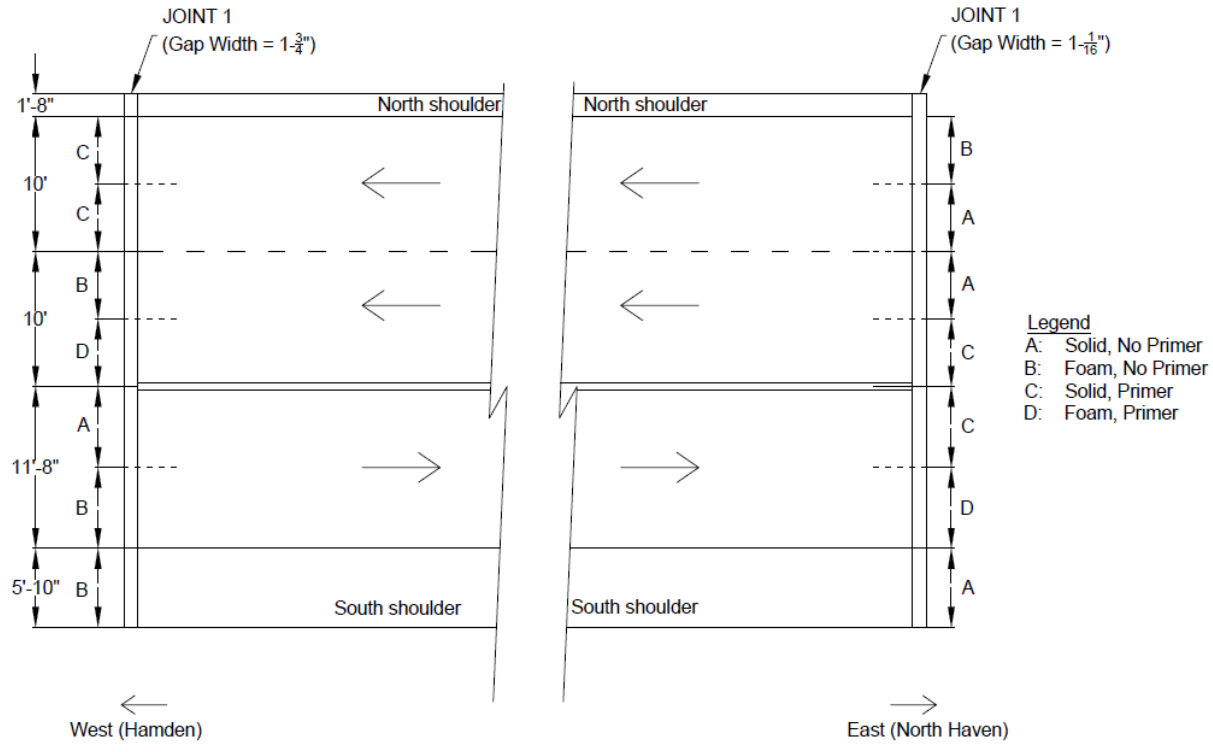

Figure 67: Sealant and primer placement plan

Similar to the installation procedure of the previous two bridges, the previous expansion joint (also a poured silicone seal) was first removed and the header of the deck was cleaned using a blade saw to remove any remnants of the old joint and expose a fresh surface of concrete. After this, the entire joint was blown with compressed air to remove any dust or loose particles from the header. This procedure ensured the best quality header since the blade saw exposed a brand new surface of concrete. The preparation of the joint is shown in Figure 68.

(a) (b)

Figure 68: Air blasting the joint (a) and cutting of the header surface (b)

Upon cleaning of the joint, a three-inch backer rod was inserted into the west joint along the length of the entire south shoulder and lane 1. The backer rod was inserted approximately 1 inch below the surface of the roadway. A recess tool was used to push the backer rod to the desired depth to ensure even placement along the entire joint. Once the backer rod was in place, primer

was applied at the appropriate locations. Stoppers were inserted in between areas where the solid sealant was terminated and the foam sealant was poured. Each sealant was poured so that, when a vehicle drove over the joint, one tire hit the solid sealant and the other tire hit the foam sealant. However, this was not always the case due to the Latin square rotation, since the foam sealant could have been located on the west joint and the solid sealant on the East joint.

3.4 Sealant Dispenser

One of the challenges faced when mixing the foam sealant is combining the small volumes of chemicals, such as platinum catalyst or crosslinker, without spilling or splashing them. In an attempt to resolve these issues and ensure an appropriate consistency to the foam sealant, a dispenser prototype was designed and fabricated. The main body of the dispenser was created out of 8-inch PVC pipe, which was capped on both ends. A hole was drilled in each cap; the top cap hole was used to send a piston through to the main body, which pushes the sealant through to the bottom cap hole. A nozzle was attached to the bottom cap to allow the foam sealant to travel through to the joint. Although the dispenser was not used for field installation during this research work, this prototype served as a conceptual design to facilitate mixing and pouring to optimize the field installation process. Figure 69 shows a schematic of the dispenser.

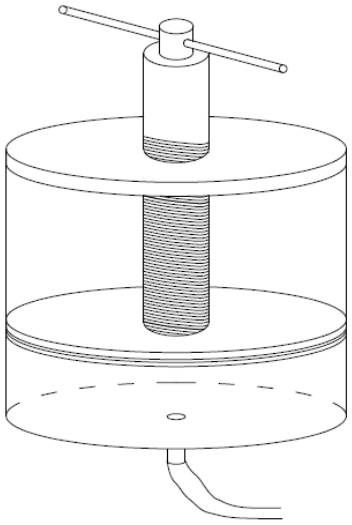

Figure 69: Dispenser showing piston and body assembly

4.0 FIELD MONITORING

This section outlines the measures taken to monitor the conditions of each bridge onto which the expansion joints were installed. Due to limitations such as seasonal weather, availability of crews, access to substructure, time window for work, and traffic conditions, each bridge was monitored using varying techniques.

4.1 Route 6 Bridge

The Route 6 bridge in Windham, CT was monitored with the most effort due to its proximity to the University of Connecticut, easy access to the substructure, and good relationship with the local maintenance crews. After installation of the sealant, several joint gap readings were recorded on a monthly basis. Additionally, the Connecticut Department of Transportation generously provided maintenance crews and equipment to assist with the installation of displacement measuring devices onto the east abutment. Through the efforts of the Connecticut Transportation Institute and the University of Connecticut, a traffic counter was installed to conduct continuous monitoring of the vehicles passing over the bridge. Finally, weather data (temperatures, humidity and precipitation) was recorded to examine the nature's effect on the joint gap.

4.1.1 Joint Gap History

Upon installation, the joint gap was measured at several locations along the joint. Since portions of the road were closed during the installation process, a detailed record of the joint gap widths were recorded. However, after installation of the joint, the gaps were measured at limited locations as moving traffic prevented measuring the joint gap due to safety precautions. During installation on Friday, August 14, 2015, the average joint gap for the west joint was 1.625 inches

for the west joint and 2.00 inches for the east joint with an average temperature of 82 degrees Fahrenheit. On Monday, September 14, 2015, the average joint gap for the west joint increased to approximately 1.685 inches. The east gap that day measured 2.0625 inches. These measurements were recorded at a temperature of 76 degrees Fahrenheit. On Tuesday January 12, 2016, the west joint gap measured about 2.0625 inches while the east joint gap measured 2.25 inches at a corresponding temperature of 29 degrees Fahrenheit. This large shift in joint gap corresponds to a 52 degree drop in temperature since the day of installation. According to equation 1, the theoretical change in the joint gap is 0.87 inches assuming the thermal coefficient of expansion (alpha) is 0.000008. Field measurements indicate that the joint gap increased by about 0.25 inches, much less than the movement calculated theoretically. This may be due to the condition of the bridge bearings, as significant rust and debris has accumulated near the supports over time. The time history of the joint gap is shown in Figure 70.

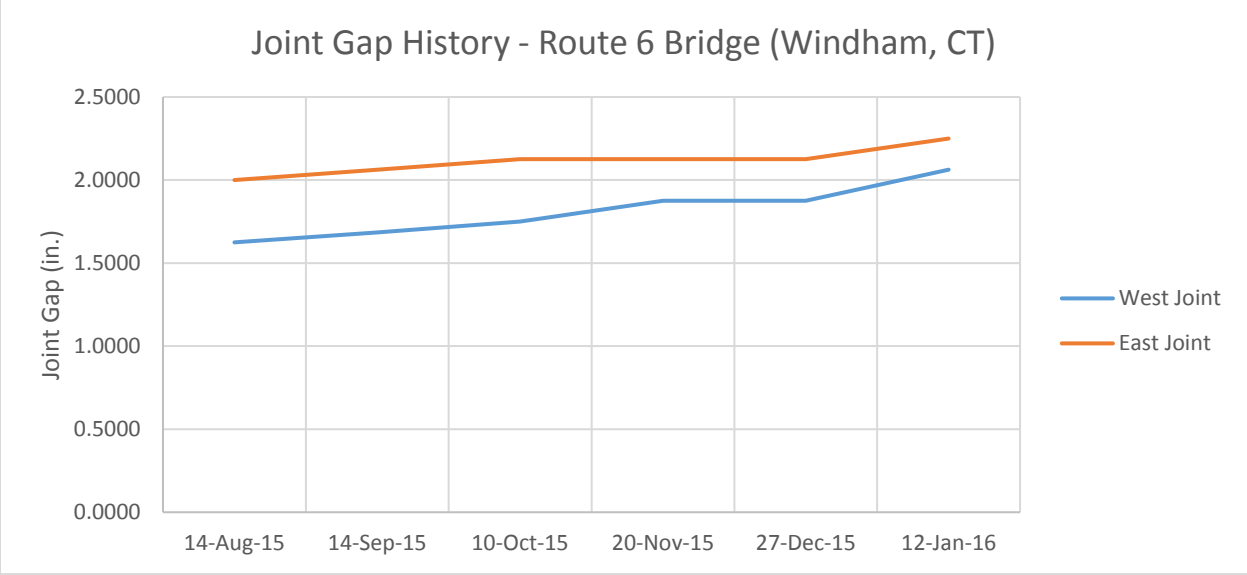

Figure 70: Joint gap history for Route 6 bridge

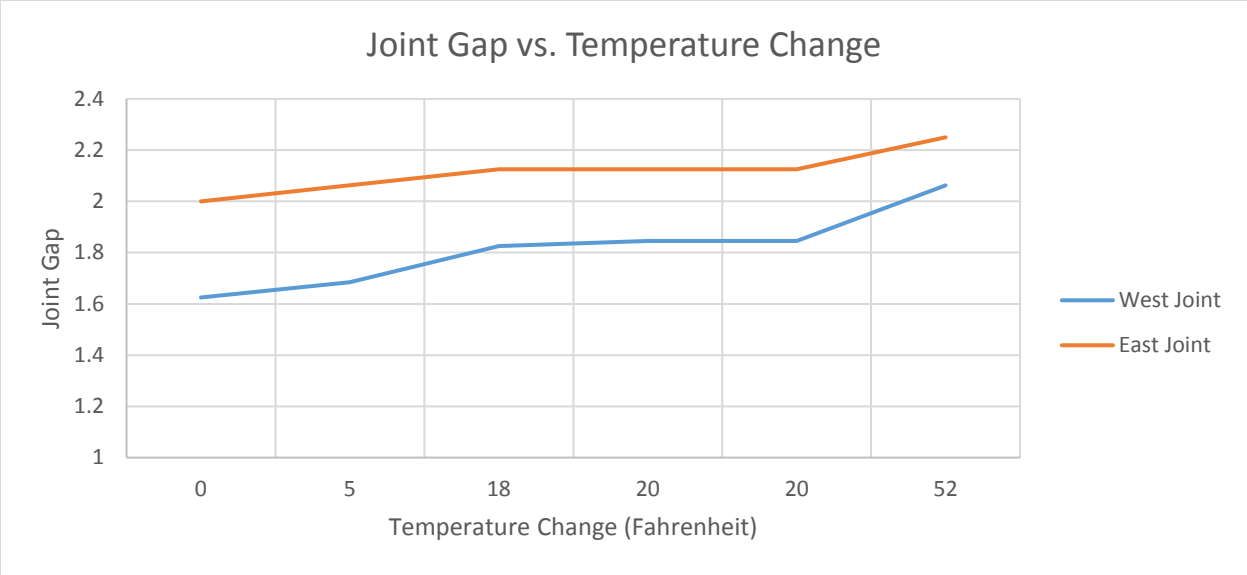

Figure 71: Joint gap as a function of temperature change for Route 6 bridge

4.1.2 Traffic Counter

Through the assistance of the Connecticut Transportation Institute, a traffic counter was installed approximately 100 feet away from the east expansion joint. The traffic counter could not be installed onto the bridge itself because there were no fixtures to secure the computer that recorded and stored the data. However, there are no turns or alternate routes between the bridge and the traffic counter, so the vehicle data was as accurate as possible. The traffic counter consisted of two portable, automatic, pneumatic tube counters spread across the entire width of the roadway. Tube counters have proven over the years to be inexpensive devices that are fairly easy to install and remove and that provide adequate accuracy for most applications (Transportation Engineering Handbook, 2008).

The tubes were installed by nailing metal clamps to road at the outer edges of the roadway. These clamps secured the tubes at each end, while a wire loop held the tube in place at the median.

The wire loop was installed to allow for some movement of the tubes as vehicles drive by; if the tubes were clamped at all three locations, vehicles could rip them off in between the two clamps. Therefore, the wire loop provided some flexibility when the vehicles drove over. The west tube was labeled “A” and the east tube was labeled “B”. This convention was established to determine the direction of vehicles travelling over the bridge. The tubes were spaced exactly 36 inches apart; this spacing is commonly used when speed data is also desired. An overview of the location of the traffic counter is shown in Figure 72.

Figure 72: Location of traffic counter

The traffic counter enabled recording of the number, direction, speed and classification of all vehicles driving over the bridge over a specified period of time. Two 6-day periods were chosen for monitoring. The first period monitored was from 8:23AM on Tuesday, November 24, 2015 to 2:54PM on Monday, November 30, 2015. This time period, which falls during Thanksgiving, gave a good indication of regular weekday traffic, holiday traffic, and also weekend traffic. The second

time period monitored was from 9:52AM on Thursday, December 17, 2015 to 6:48PM on Wednesday, December 23, 2015. This time period gave a good indication of the traffic flow during a regular week, including a typical weekend.

During time period from December 17 to December 23, 2015, the bridge experienced approximately 18,000 vehicles per day. The ADT measured by the Connecticut Department of Transportation was approximately 18,600, comparable to the data obtained during the joint gap monitoring process. Figure 73 shows the distribution of vehicle classes that the bridge experienced during that time span. Since this road is not a highway, there are very few trucks or heavy axle load vehicles (vehicles in classes 6-13). The most frequent vehicle types encountered were those in classes 2 and 3, which are passenger cars and pick-up trucks.

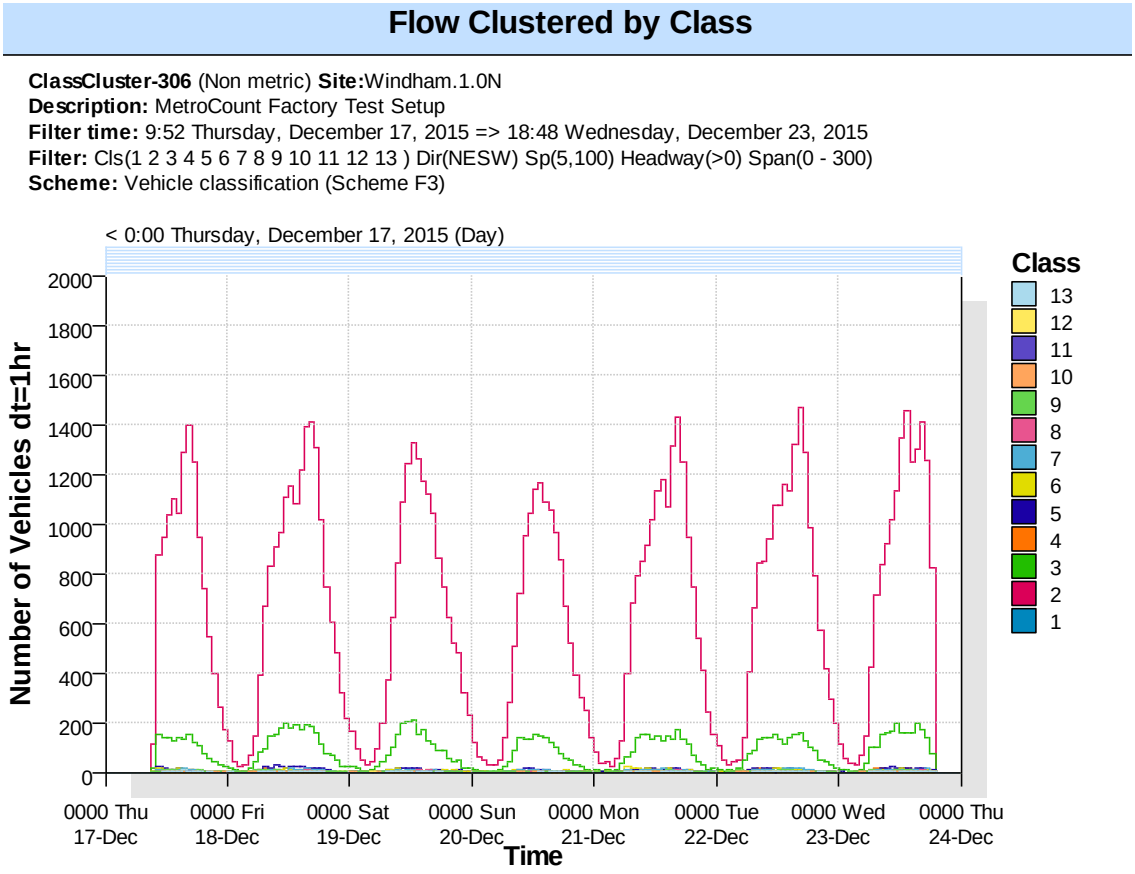

Figure 73: Classification of vehicles entering bridge over monitoring period

Throughout the course of the week dating December 17 through December 24, 2015, about 1400 passenger cars (class 2 vehicles) drove over the bridge per hour. Class 2 vehicles include all sedans, coupes, station wagons manufactured primarily for the purpose of carrying passengers and including those passenger cars pulling recreational or other light trailers (FHWA, 2014). Class 2 vehicles accounted for 85.3% of the total volume of traffic that the bridge experienced. The second highest class observed was class 3, which includes all two-axle, four-tire vehicle other than passenger cars. Since this route accommodates for bus traffic, about 0.4% of the volume accounted for passenger carrying buses with two axles and six tires or three or more axles. This route experienced truck traffic as well, which included classes 5-10. Class 11, 12 and 13 were rarely experienced, as these include multi trailer trucks. Since this route is not a highway or a major connecting route between large hubs, these classes were not observed as frequently. Motorcycles accounted for 0.1% of the total traffic volume (total of 142 motorcycles throughout the monitored period).

Class Bin Chart

ClassBin-307 (Non metric) **Site:**Windham.1.0N
Description: MetroCount Factory Test Setup
Filter time: 9:52 Thursday, December 17, 2015 => 18:48 Wednesday, December 23, 2015
Filter: Cls(1 2 3 4 5 6 7 8 9 10 11 12 13) Dir(NESW) Sp(5,100) Headway(>0) Span(0 - 300)
Scheme: Vehicle classification (Scheme F3)
Total=118336

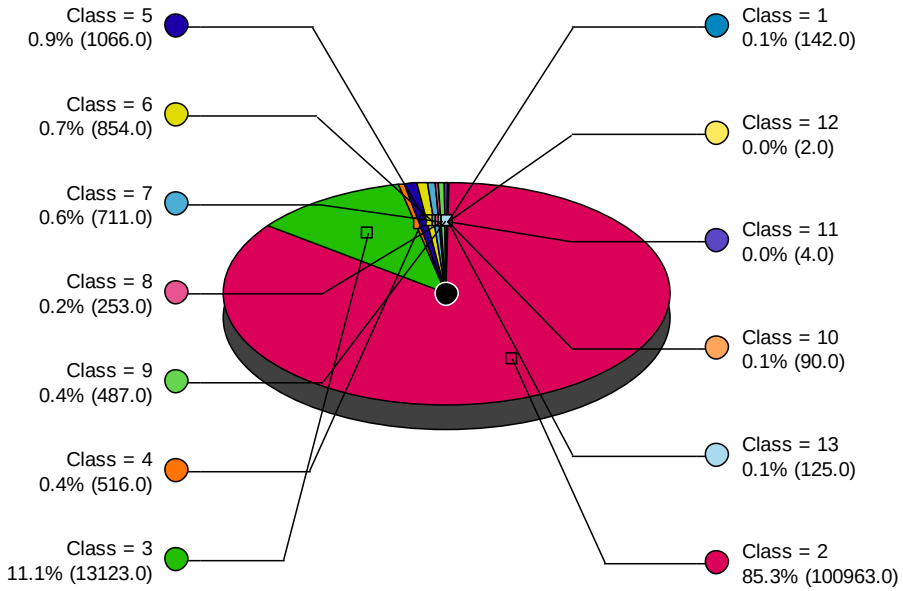

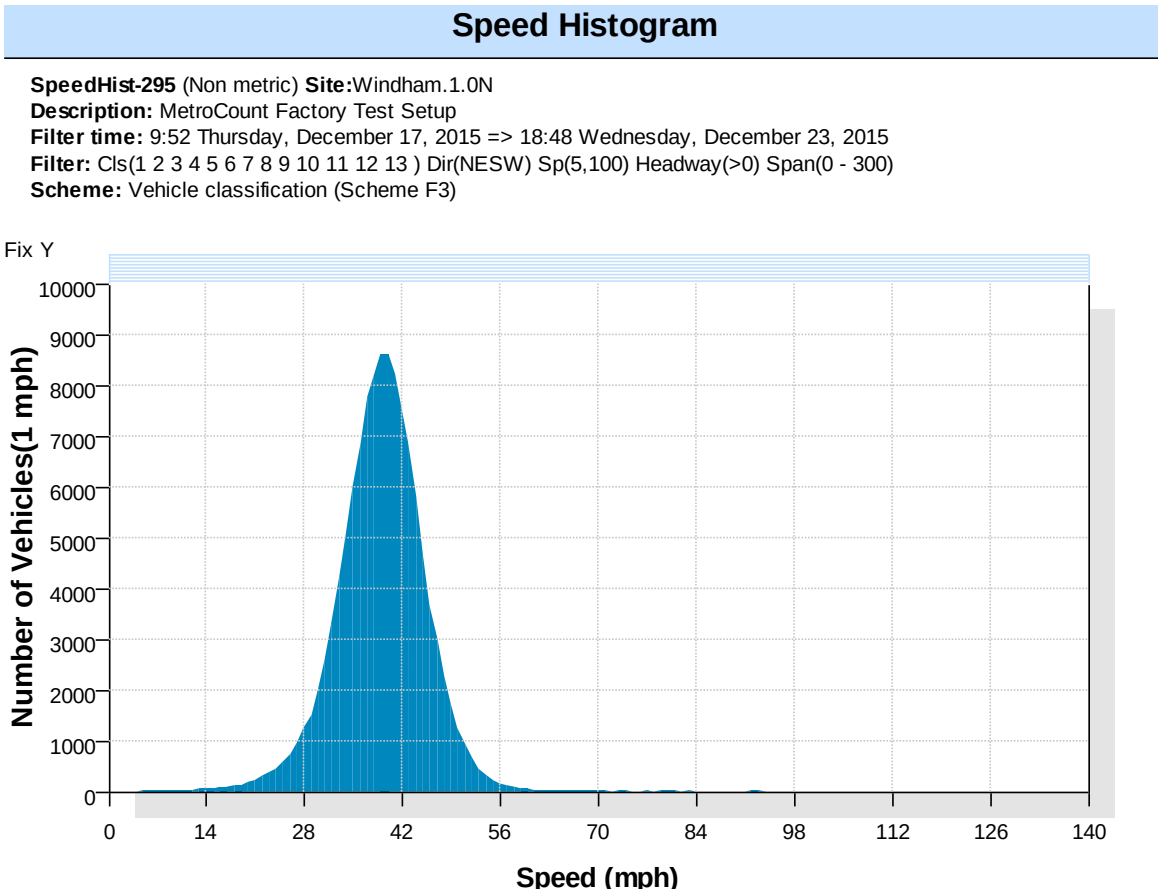

Figure 74: Number of vehicles traveling in specified speed ranges (Route 6 Bridge)

The next measure taken to monitor the Route 6 bridge was to record the axial displacement of the bridge as a function of vehicular movement. In order to do this, several Linear Variable Differential Transformers (LVDT's) were installed onto the girders of the bridge. The devices, supplied by TransTek, Inc., have a working range of ± 2 inches with an internal carrier frequency of 1500 Hz. The LVDT's were wrapped with plastic sheeting and duct tape to prevent any moisture from damaging the internal structure of the device. The distance between the end of the girder and the abutment was approximately 16 inches; therefore, the LVDT alone could not reach out to make contact with the abutment. In order to attach the devices to the girder and also rest the needle onto the abutment, a wooden angle was constructed and clamped to the girder in such a way so that it

extended to the abutment. Since the devices are spring loaded, they were mounted onto the girders with the needle placed against the abutment (Figure 75). The joints on this bridge are skewed (42 degrees for the west joint and 45 degrees for the east joint). To prevent the needle from slipping off of the abutment, a small hole was drilled into the abutment into which the needle was placed to ensure a proper mounting location. One LVDT was attached onto a girder at two different locations along the east joint. LVDT #1 was attached onto Girder 3 and LVDT #2 was attached onto Girder 6. This placement was designed to gather displacement data at symmetric locations from the edge of the deck, and also monitor the activity at the center of the east and westbound lanes.

Figure 75: Attachment of LVDT for axial displacement measuring

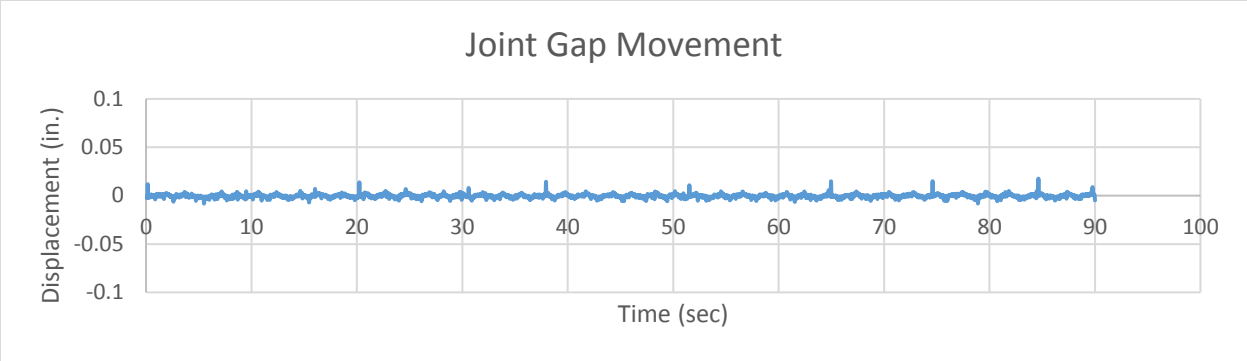

Table 9: Sample vehicle count output

Count ID	Date	Time	Direction	Speed	Headway	FHWA Class
00012bde	12/18/15	9:52:22	N1	42.98	1.7	2
00012be2	12/18/15	9:52:30	N1	38.95	7.6	2
00012be6	12/18/15	9:52:31	N1	38.14	1.3	2
00012bea	12/18/15	9:52:34	N1	36.1	2.7	2
00012bee	12/18/15	9:52:38	S0	44.44	26.3	2
00012bee	12/18/15	9:52:38	S0	44.44	0	2
00012bf5	12/18/15	9:52:40	S0	45.39	1.6	2
00012bf9	12/18/15	9:52:41	N1	39.23	6.9	2
00012bfd	12/18/15	9:52:41	N1	32.27	0.4	2
00012c01	12/18/15	9:52:42	S0	41.1	2.4	3
00012c05	12/18/15	9:52:43	N1	31.2	1.4	2
00012c09	12/18/15	9:52:44	N1	31.71	1.2	2
00012c0d	12/18/15	9:52:52	N1	54.15	7.8	2
00012c11	12/18/15	9:52:52	N1	50.41	0.7	2
00012c15	12/18/15	9:52:55	S0	47.98	13.1	2
00012c19	12/18/15	9:52:56	N1	49.32	3.3	3
00012c1d	12/18/15	9:52:56	N1	46.05	0.4	3
00012c21	12/18/15	9:52:59	N1	44.96	2.9	2
00012c25	12/18/15	9:53:00	N1	43.77	1.4	2
00012c29	12/18/15	9:53:02	N1	37.66	1.6	2
00012c2d	12/18/15	9:53:02	N1	50.73	0.4	2
00012c31	12/18/15	9:53:04	N1	42.13	1.2	2
00012c35	12/18/15	9:53:04	S0	41.13	8.5	2
00012c39	12/18/15	9:53:05	N1	48.45	0.9	2
00012c3d	12/18/15	9:53:08	S0	39.92	3.6	2
00012c41	12/18/15	9:53:12	N1	39.02	7.1	2
00012c45	12/18/15	9:53:15	N1	41.33	3.1	2
00012c49	12/18/15	9:53:16	S0	46.79	8.1	2
00012c4d	12/18/15	9:53:29	N1	44.23	14.6	2
00012c51	12/18/15	9:53:31	N1	39.24	1.9	7

4.1.3 Visual Inspection of Sealant

Visual inspections were performed on each date during which the joint gap was measured. No damage was observed during these dates. Another visit was conducted on March 23, 2016. The east and west joint gaps measured at 2.00 and 2.125 inches, respectively. No damage to the joint or the substrate was observed on this date. There was an accumulation of road salt and other road debris inside of the joint. The accumulation was more significant closer to the shoulder and in the shoulder itself.

4.2 Route 291 Bridge

The Route 291 bridge was monitored routinely for its joint gap opening as a function of thermal contraction and expansion, and also as a function of vehicular movement. Weather conditions such as temperature, precipitation and humidity were also recorded. However, due to the speed limit and high priority route, the Connecticut Department of Transportation did not support installing a traffic counter on the roadway. Therefore, exact traffic data regarding classifications and daily vehicle totals were not obtained.

4.2.1 Joint Gap History

Upon installation, the joint gap was measured at several locations along the joint. Since portions of the road were closed during the installation process, a detailed record of the joint gap widths were recorded. After the installation of the expansion joint, however, readings were only obtained from the shoulder because of the high speed of traffic and danger associated with measuring the gap at the center of the lanes. During installation on October 6, 2015, the joint gap measured approximately 3.125 inches for the east joint and 3.625 inches for the west joint with an average temperature of 72 degrees Fahrenheit. On October 17, 2015, the joint gap was measured

at 3.25 inches for the east joint and 3.75 inches for the west joint at a temperature of 55 degrees Fahrenheit. On Wednesday, November 25, 2015, the joint gap measured about 3.375 inches for the east joint. The west joint measured 3.875 inches that day. The corresponding temperature was 48 degrees Fahrenheit. By January 12, 2016, the temperature dropped to 29 degrees Fahrenheit; consequently, the joint gap increased to 3.875 inches for the east joint and 4.25 inches for the west joint. This large shift in joint gap corresponds to a 43 degree drop in temperature since the day of installation. According to equation 1, the theoretical change in the joint gap is 0.7 inches assuming the thermal coefficient of expansion (alpha) is 0.000008. Field measurements indicate that the joint gap increased by about 0.875 inches, which is more than the theoretically calculated value. This value, however, uses the thermal coefficient of expansion for concrete; since the structure is a composite, however, the steel may contract and thus carry the concrete deck further than what would be expected out of pure concrete. The time history of the joint gap is shown in Figure 76.

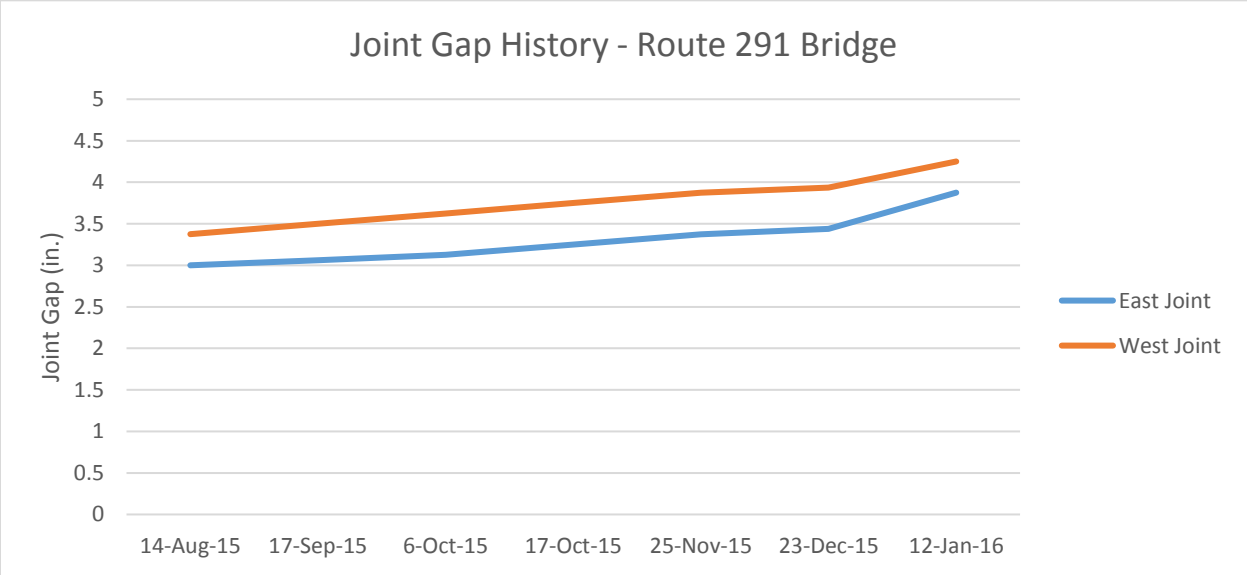

Figure 76: Joint gap history for Route 291 bridge

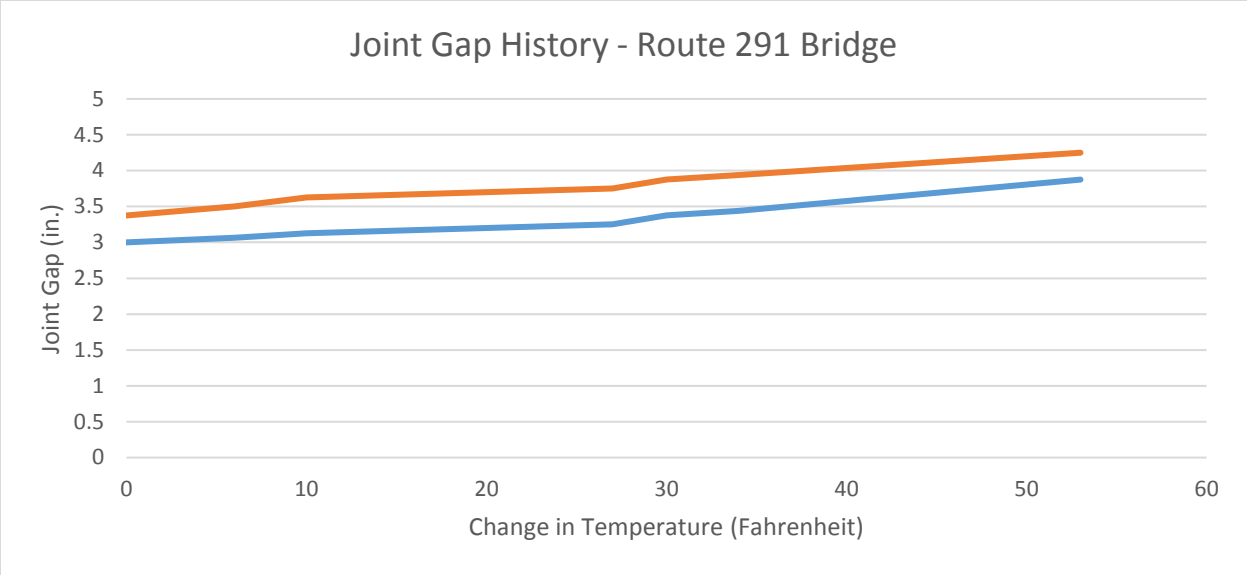

Figure 77: Joint gap vs. change in temperature for Route 291 bridge

4.2.2 Visual Inspection of Sealant (Route 291 Bridge)

A brief visual inspection of each joint was conducted on October 17, 2015, November 25, 2015, and January 12, 2016. During these dates, no visual damage was observed. However, during a site visit on March 23, 2016, some damage to the sealant was observed on both joints. Two ruptures (A and B) were observed on the west joint and one rupture (C) was observed on the east joint (shown in Figures 79-80). Rupture A was observed in the location where solid sealant was applied without primer. Rupture B was observed in the location where foam sealant was applied without primer. Finally, rupture C was observed in the location where foam sealant was applied with primer. All three ruptures were located at the same location along each joint (i.e. right side of the lane, close to the shoulder). Road salt was also accumulating inside the joint, especially towards the shoulder area.

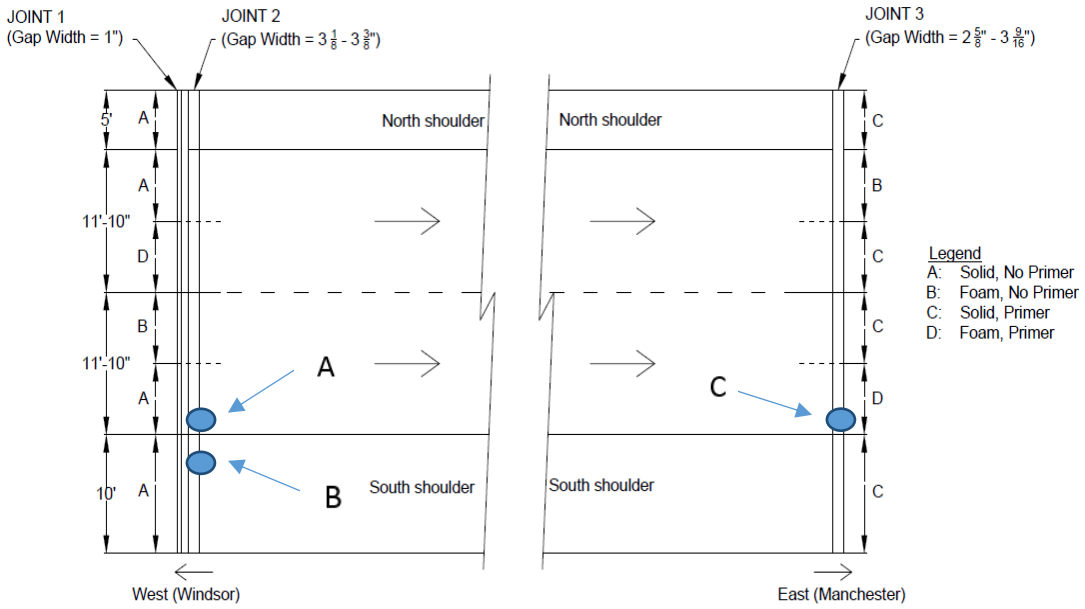

Figure 79: Location of damage on the Route 291 bridge

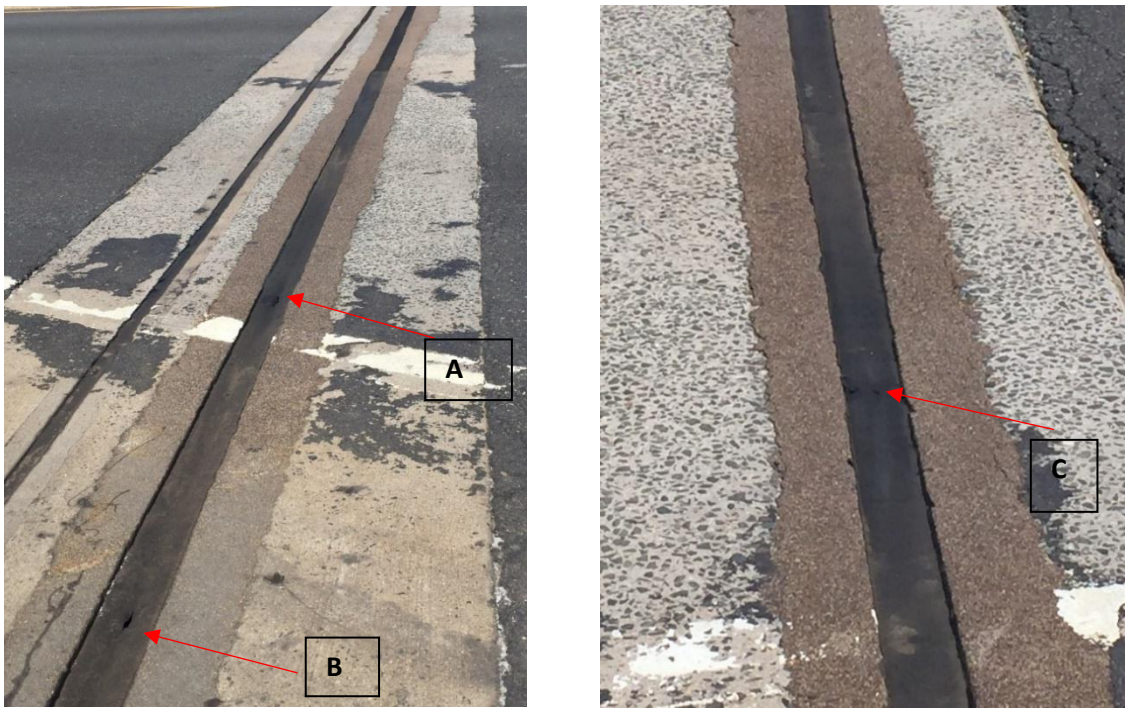

Figure 80: Visual observation of damage on the Route 291 bridge

4.3 Route 22 Bridge

The Route 22 bridge was also monitored routinely for its joint gap opening as a function of thermal contraction and expansion. No traffic data or joint gap movement as a function of vehicular loading was obtained for this bridge. The gap opening and the condition of the joint was regularly checked to ensure no premature or unexpected failing.

Weather conditions such as temperature, precipitation and humidity were also recorded. However, due to the speed limit and high priority route, the Connecticut Department of Transportation did not support installing a traffic counter on the roadway. Therefore, exact traffic data regarding classifications and daily vehicle totals were not obtained.

4.3.1 Joint Gap History

Upon installation, the joint gap was measured at several locations along the joint. Since portions of the road were closed during the installation process, a detailed record of the joint gap widths were recorded. After the installation of the expansion joint, however, readings were only obtained from the shoulder because of the high speed of traffic and danger associated with measuring the gap at the center of the lanes. During installation on October 6, 2015, the joint gap measured approximately 3.125 inches for the east joint and 3.625 inches for the west joint with an average temperature of 72 degrees Fahrenheit. On October 17, 2015, the joint gap was measured at 3.25 inches for the east joint and 3.75 inches for the west joint at a temperature of 55 degrees Fahrenheit. On Wednesday, November 25, 2015, the joint gap measured about 3.375 inches for the east joint. The west joint measured 3.875 inches that day. The corresponding temperature was 48 degrees Fahrenheit. By January 12, 2016, the temperature dropped to 29 degrees Fahrenheit; consequently, the joint gap increased to 3.875 inches for the east joint and 4.25 inches for the west joint. This large shift in joint gap corresponds to a 43 degree drop in temperature since the day of

installation. According to equation 1, the theoretical change in the joint gap is 0.7 inches assuming the thermal coefficient of expansion (alpha) is 0.000008. Field measurements indicate that the joint gap increased by about 0.875 inches, which is more than the theoretically calculated value. This value, however, uses the thermal coefficient of expansion for concrete; since the structure is a composite, however, the steel may contract and thus carry the concrete deck further than what would be expected out of pure concrete. The time history of the joint gap is shown in Figure 78.

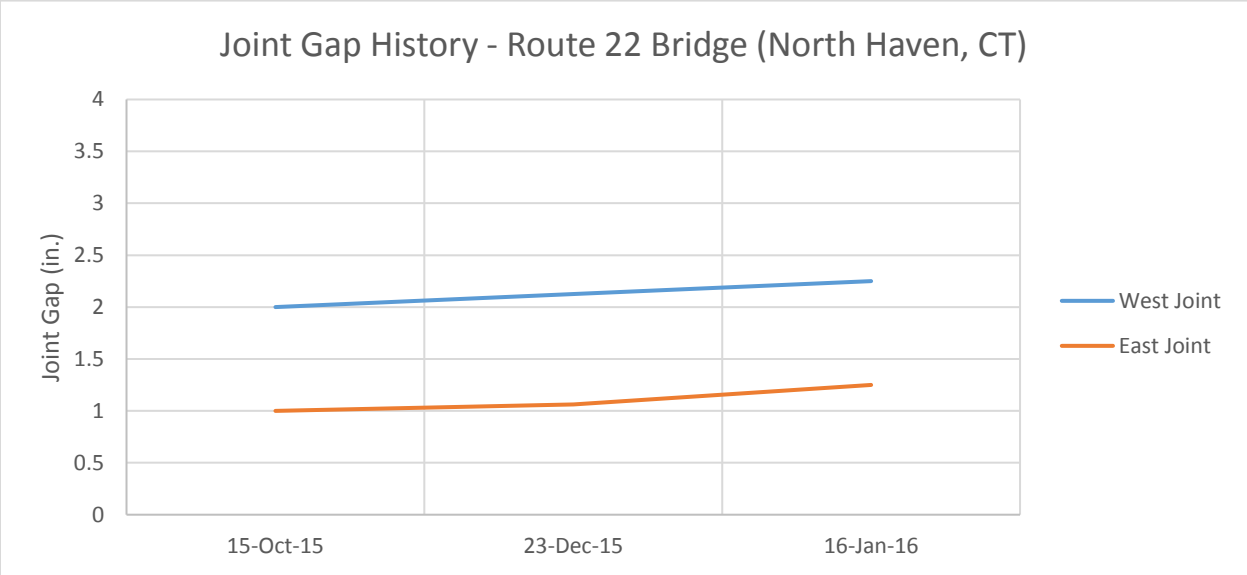

Figure 78: Joint gap history of the Route 22 bridge (North Haven, CT)

4.3.2 Visual Inspection

Several visual inspections were conducted on October 17, 2015, November 25, 2015, and January 12, 2016, and March 23, 2016. No damage to the joint or the substrate was observed on these dates. Accumulation of debris and some road salt was present on March 23, especially towards the shoulder area. However, this is expected as the winter season was coming to an end.

5.0 SUMMARY, CONCLUSIONS AND RECOMMENDATIONS FOR FUTURE WORK

5.1 Summary

The silicone foam sealant was developed and tested in the laboratory to gain a better understanding of the adhesion and bonding characteristics when compared to the solid sealant. Adhesion and tensile properties were obtained by pulling the specimens to failure. Expansion properties were characterized by observing expansion of various initial thicknesses of sealant. Finally, aging and road salt corrosion testing was conducted to determine the degradation of the bond and modulus of elasticity between the sealant and the substrate when subject to laboratory accelerated aging.

5.2 Conclusions

- Under a pure tensile load, the foam sealant exhibited a lower and a lower ultimate stress. This indicates smaller stresses being transferred between the sealant material and the bridge header. This characteristic may be considered favorable when aiming to improve the adhesion properties of poured silicone joints, as the most common mode of failure is detachment from substrate (material failure was much less common).
- The application of primer onto the specimens yielded no significant difference in tensile and adhesion performance. Although 2 out of 10 specimens containing solid sealant failed via cohesive failure under the influence of primer, it cannot be said that primer significantly improves the bonding as the ultimate elongation was comparable to the specimens with no primer. The foam sealant showed no change in performance, as all specimens failed cohesively.

- The expansion of the foam sealant varies depending on the initial thickness of the sealant applied. When applying a thick coating of 1″, the foam sealant expanded nearly 75%; meanwhile, a coating of 0.25″ produced a total expansion of approximately 50% for a final thickness of 0.375″. This may be attributed to the volume of additives in the foam sealant, as smaller quantities of foam sealant will contain less crosslinker. The hydrogen gas may tend to escape from the sealant as a whole, instead of creating bubbles within the bulk sealant. For sealants with a larger thickness, however, more time may be needed for the gas to diffuse from the sealant; this may result in an increased foaming effect as more bubbles may stay trapped inside the structure of the sealant.
- The stress at 100% strain (secant modulus) was observed to drop significantly for the solid sealant over an aging period of 5 months. The rate of deterioration of the solid sealant was on average 3 faster than that of the foam sealant. The specimens treated with primer did not show any noticeable change in secant modulus as a function of aging. Soaking in road-salt solution did not have a significant effect in the reduction of the modulus of either sealants
- The silicone foam sealant was installed onto three bridges throughout the state of Connecticut to monitor the in-service performance of the joints under realistic environmental and vehicular demands. The performance of these joints will be monitored regularly throughout the lifespan of the joint.

5.3 Recommendations for Future Work

Future work includes further development of an applicator that will make field installation easier and more efficient, as combining five ingredients (especially the small amounts of chemical

additives) can be difficult. In this regard, it is imperative to develop a two-component formulation, including variations for cold and hot temperature. Additionally, a fatigue test may be beneficial to understanding the behavior of each type of sealant when repeated impacts cause the material to slightly expand and contract due to the movement of the bridge deck. A larger sample size of bridges for field installation may be helpful to determine whether the sealant can adhere to bridges with different geometries, substrate headers, movement behavior, traffic patterns, and environmental conditions. Finally, quantitative or at least ordinal scoring of sealant field performance is needed. This might be done with a joint leak test.

APPENDIX A

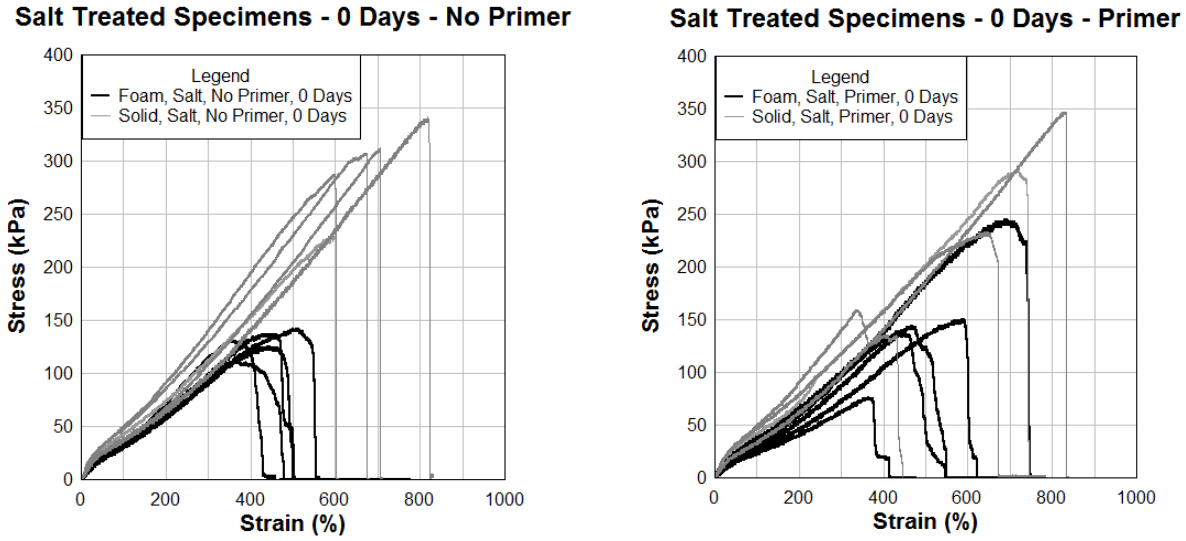

Figure B.1: Salt treated specimens at 0 days containing no primer (left) and primer (right)

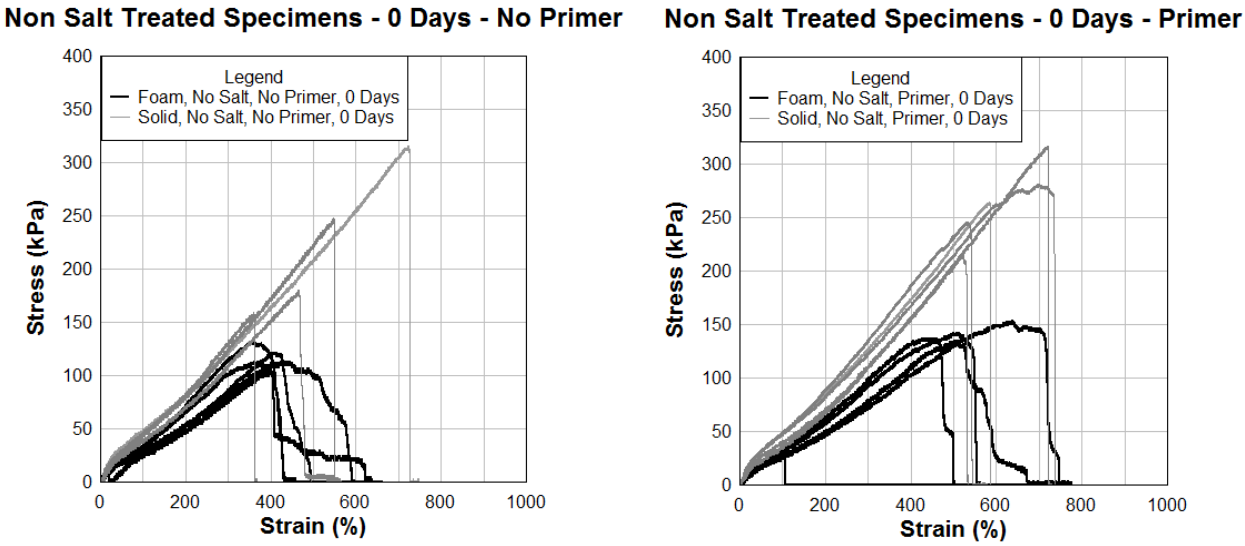

Figure B.2: Non salt treated specimens at 0 days containing no primer (left) and primer (right)

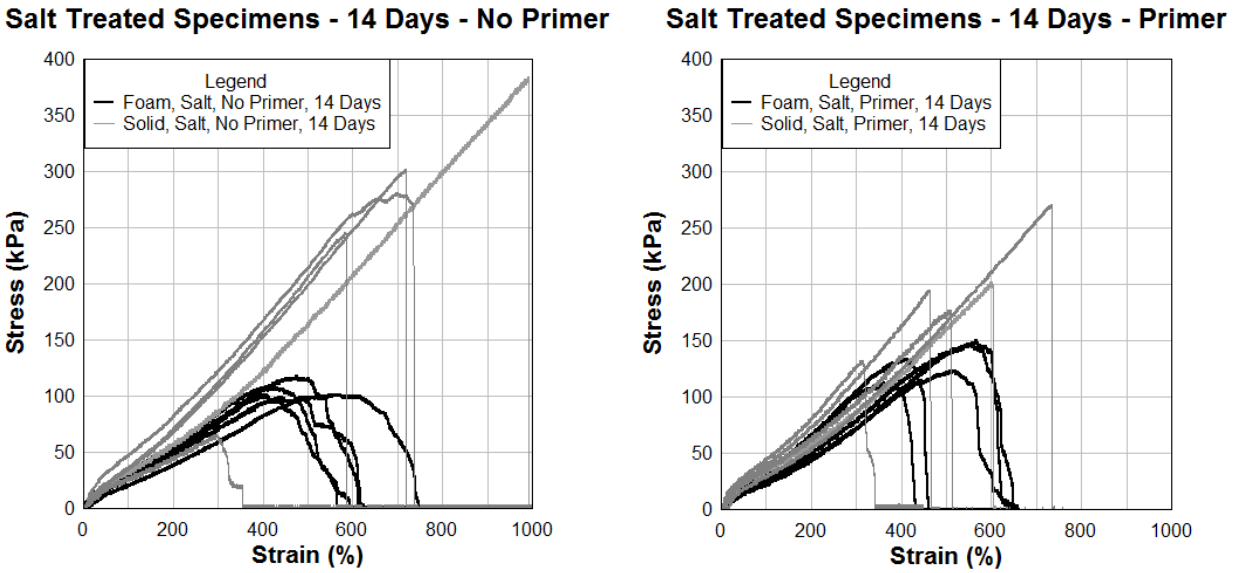

Figure B.3: Salt treated specimens at 14 days containing no primer (left) and primer (right)

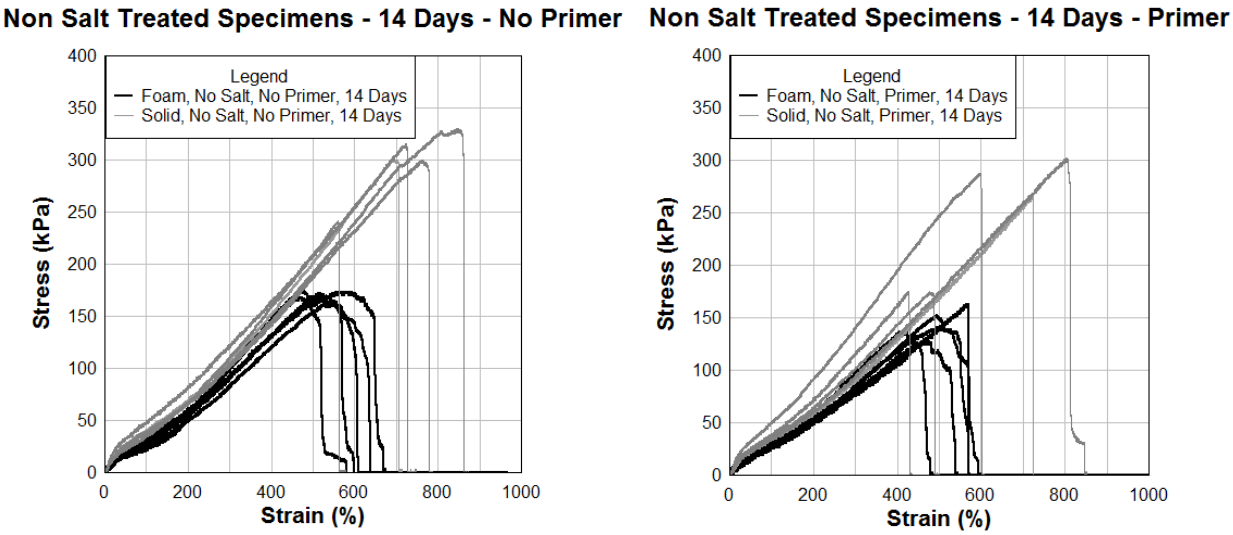

Figure B.4: Non salt treated specimens at 14 days containing no primer (left) and primer (right)

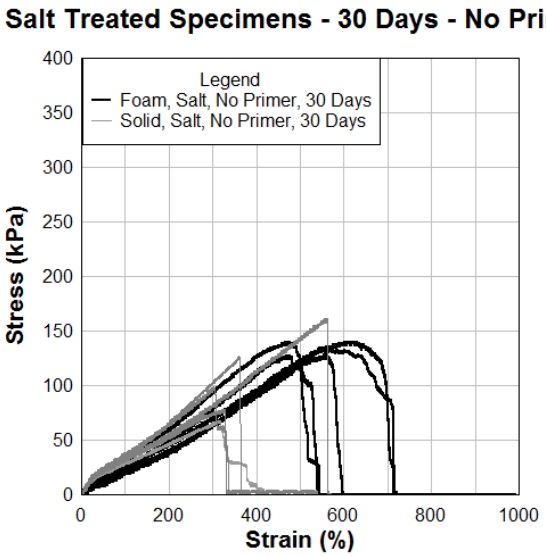

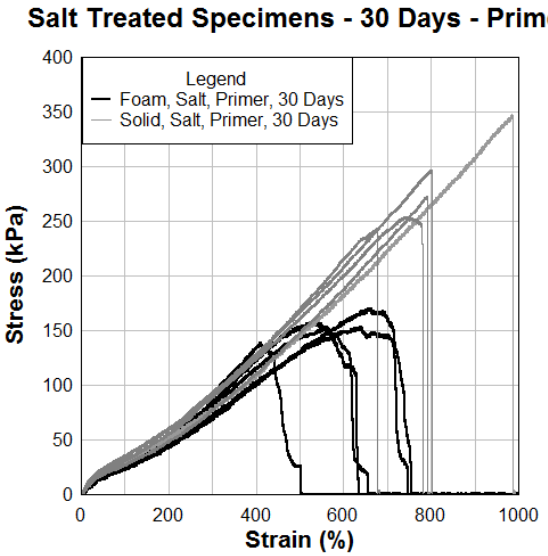

Figure B.5: Salt treated specimens at 30 days containing no primer (left) and primer (right)

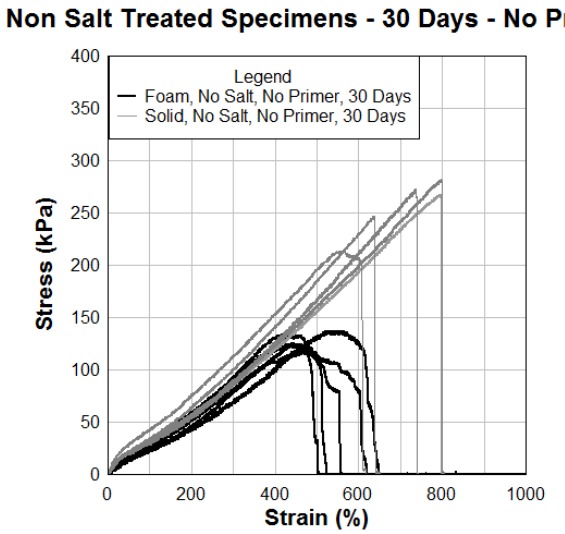

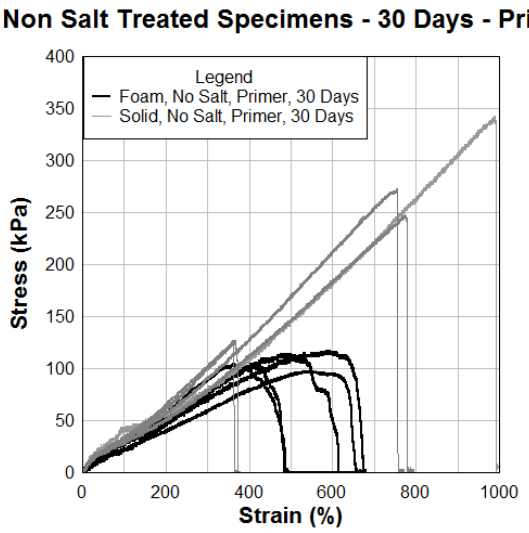

Figure B.6: Non salt treated specimens at 30 days containing no primer (left) and primer (right)

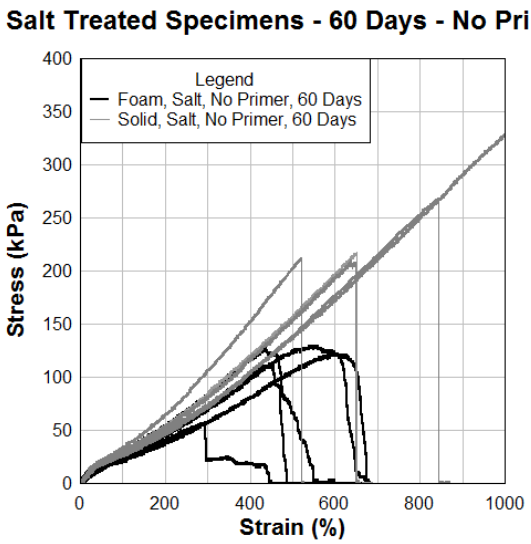

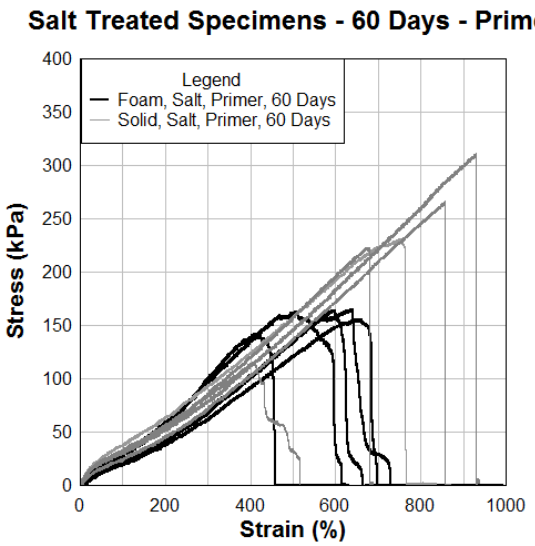

Figure B.7: Salt treated specimens at 60 days containing no primer (left) and primer (right)

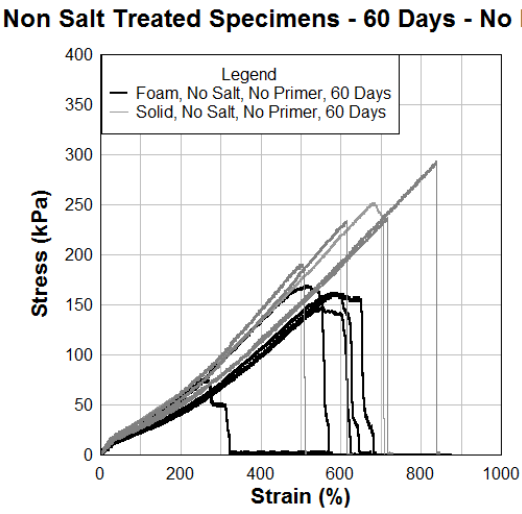

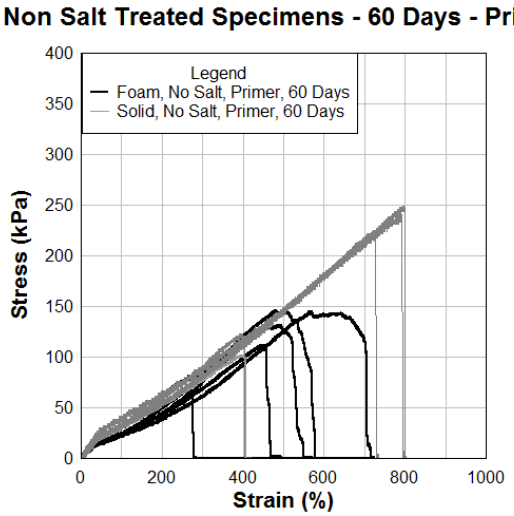

Figure B.8: Non salt treated specimens at 60 days containing no primer (left) and primer (right)

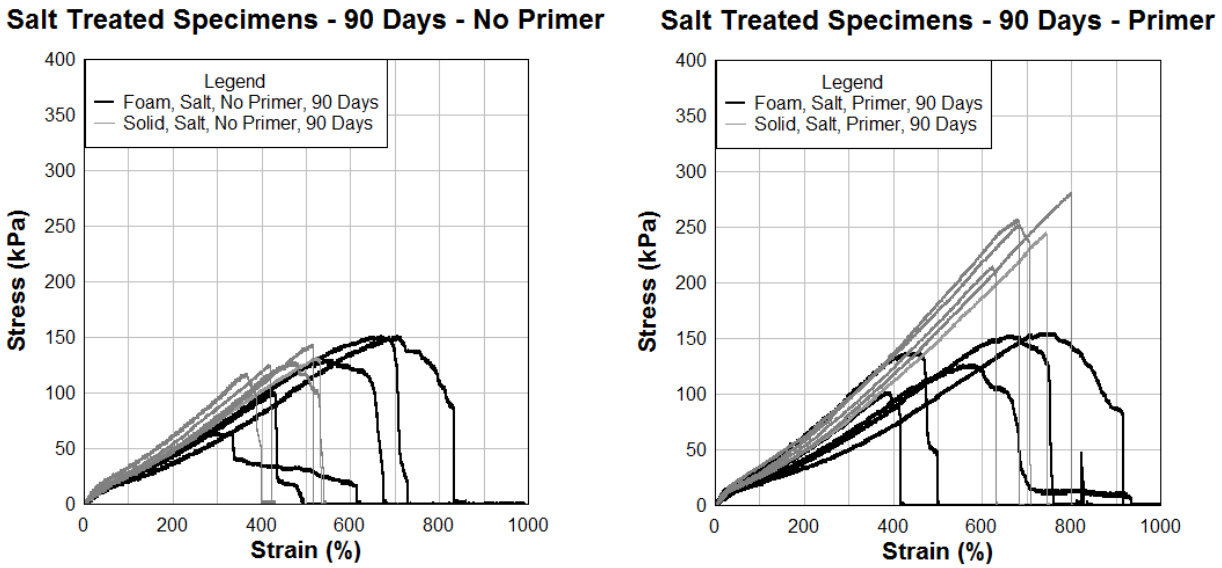

Figure B.9: Salt treated specimens at 90 days containing no primer (left) and primer (right)

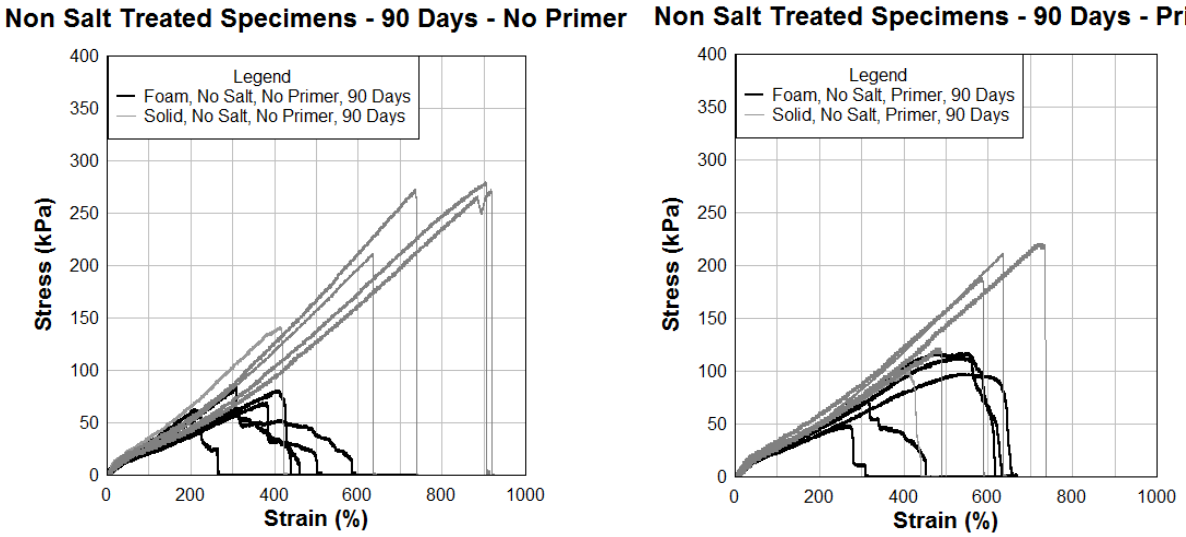

Figure B.10: Non salt treated specimens at 90 days containing no primer (left) and primer (right)

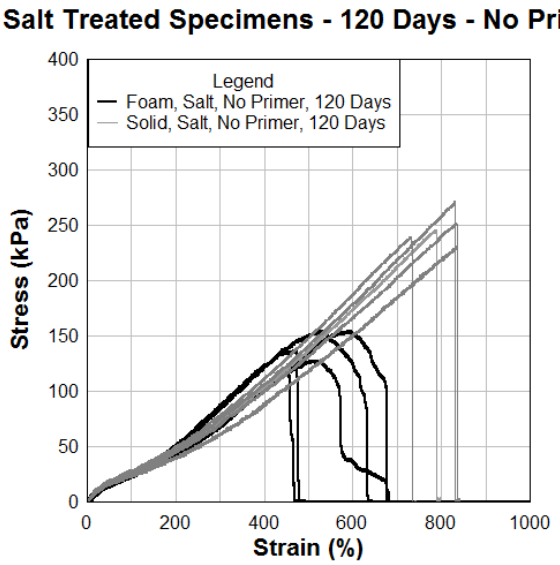

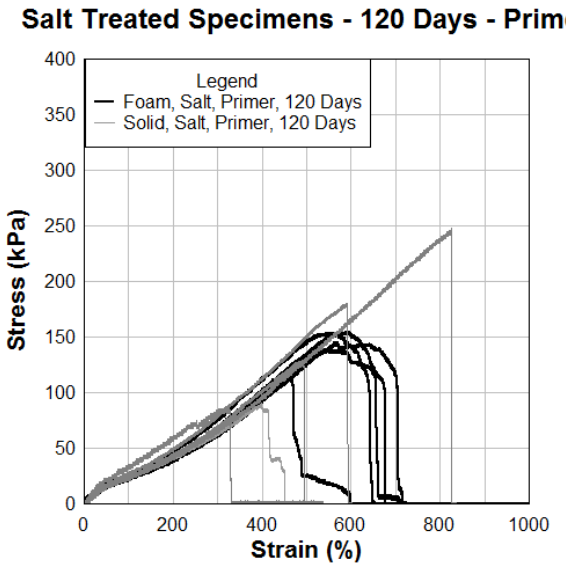

Figure B.11: Salt treated specimens at 120 days containing no primer (left) and primer (right)

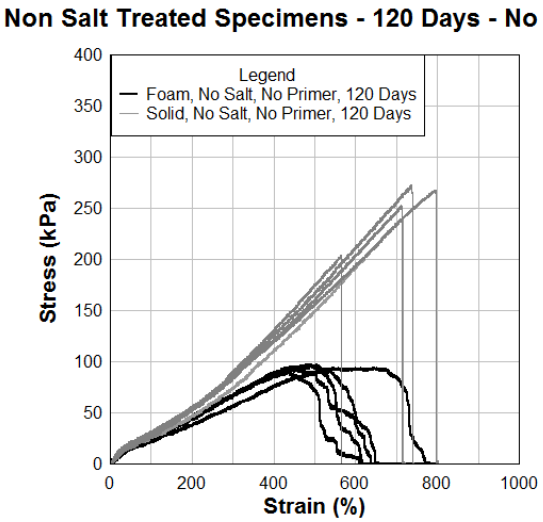

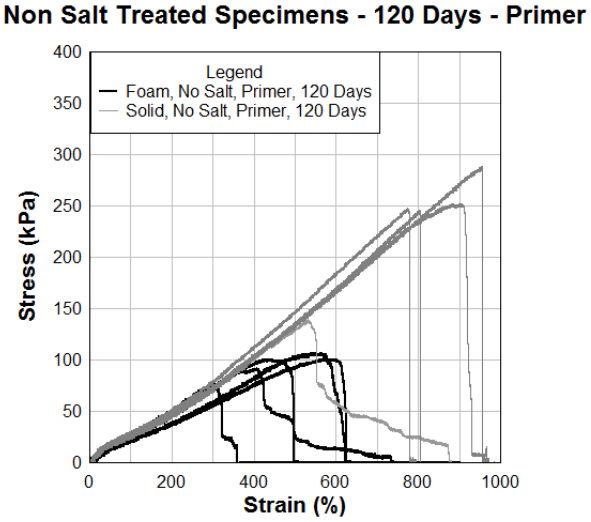

Figure B.12: Non salt treated specimens at 120 days containing no primer (left) and primer (right)

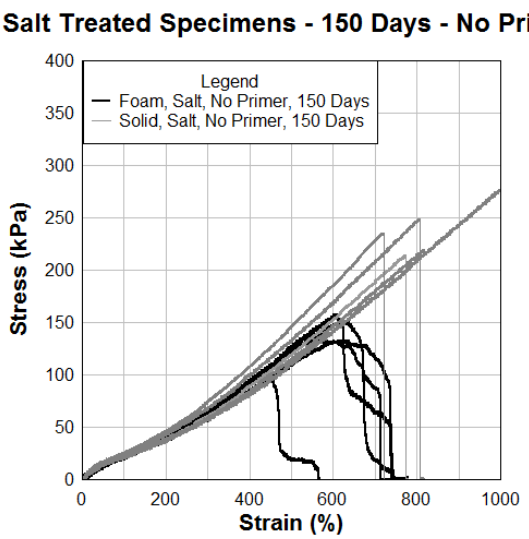

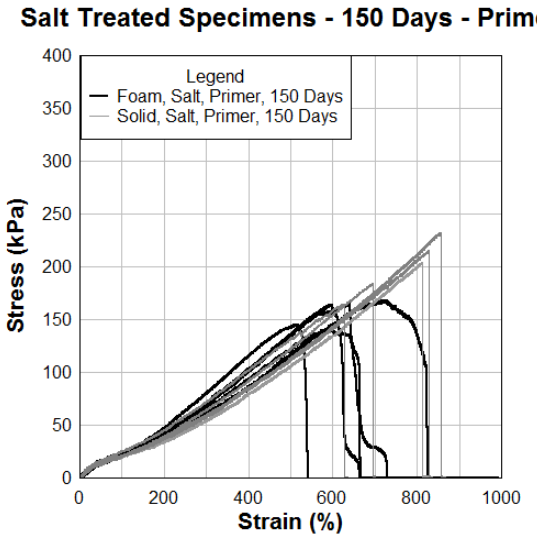

Figure B.13: Salt treated specimens at 150 days containing no primer (left) and primer (right)

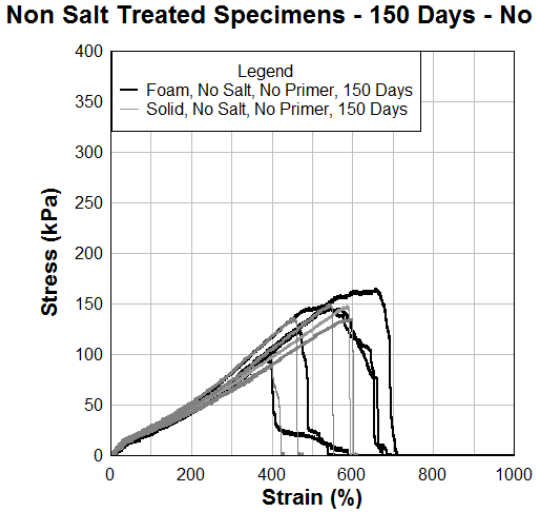

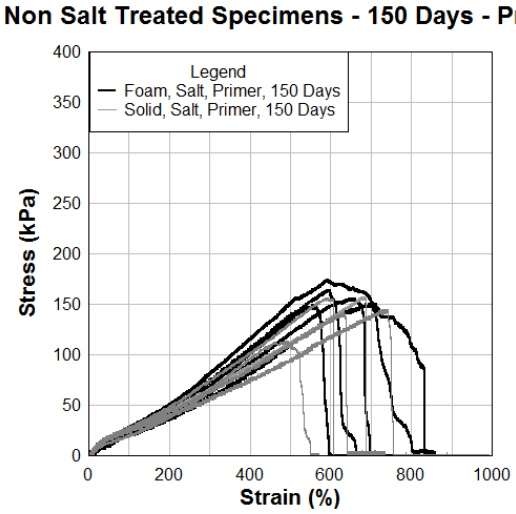

Figure B.14: Non salt treated specimens at 150 days containing no primer (left) and primer (right)

APPENDIX B

Table B.1: Stresses at 100% Strain for salt water/aging test

	Stress at 100% Strain (kPa)								
	Salt				No Salt				
Days	Specimen No.	Foam		Solid		Foam		Solid	
		Primer	No Primer	Primer	No Primer	Primer	No Primer	Primer	No Primer
0	1	29.9	30.86	41.3	42.2	26	28.5	47.7	46.9
	2	37.8	31.47	47	37.9	33.9	24.8	47.8	44.5
	3	23.43	24.22	32.3	47.3	30.5	27.4	40.4	38.8
	4	27.3	28.9	39.4	49.6	32.8	34.6	48.9	44.4
	5	25.9	25.46	49.9	36.4	26.7	32.1	37.3	46.2
14	1	21.1	25.7	25.7	32.2	29	24.4	40.8	34.75
	2	23.5	19.6	37	26.4	31.8	32.7	28.9	35.35
	3	26.5	29.11	38.9	36.1	27.2	22.4	38.5	35.2
	4	32.1	31.5	28	35.2	28	27.6	34.5	38.6
	5	32.2	27.7	44.4	48.7	24.8	28.9	46.9	49.6
30	1	26.8	21.9	30.5	27.6	22.9	27.8	30.1	41.7
	2	26.2	29.1	34.4	31.5	26.5	29.3	29.7	31.3
	3	31.4	24.7	34.5	31	22.5	29.6	33.2	34.4
	4	18.8	25.5	26.2	37.1	25	21.9	34.7	32.4
	5	21.8	26.1	32.3	34.3	31.4	22.3	42.9	29.8
60	1	23.7	29.1	37.9	29.4	21.6	27.2	29.8	35.5
	2	20.2	28.7	29.4	29.6	23.5	24.7	28.9	29.2
	3	24.2	21.9	32.4	25.13	24.3	24	31.8	26.8
	4	28.9	19.2	32.7	30.8	22	21.1	33.2	33.9
	5	25.6	22.4	25.3	34.5	30.5	26.9	32.8	30.1
90	1	25.7	21	25.4	27.6	19.3	22.38	29.2	36
	2	22.7	19.3	29.5	28.3	21.3	22.17	29.1	25.2
	3	24	22.1	27.7	29.6	31	27	32.7	26.3
	4	24.6	25.5	24.9	21.9	25.7	24.4	27.8	26.7
	5	20.1	32.8	34.5	22.3	23.5	24.4	26.7	29.7
120	1	21.44	24	25.1	21.8	21.9	21.5	25.8	26.5
	2	24.08	22	25.2	25.6	24.7	26.8	28.8	26.4
	3	25.38	22.9	28.7	23.9	24.4	20.9	27.2	28.44
	4	24.01	24.1	24.2	34	23.1	26.1	30.1	28.66
	5	21.69	25.2	24	22.6	24.2	23.7	29.7	24.2
150	1	21.8	23.1	21.2	20.4	20.9	23.1	28	26.2
	2	21.3	22.4	24	20.9	26.7	24.9	26.5	25.2
	3	23	20.8	26	21.1	19.2	22.4	24.6	25.1
	4	20.9	22.2	20.9	21.1	21.9	23.9	28	26.3
	5	21.2	21.9	23.2	25.8	21.9	21	19.7	27.9

Table B.2: Ultimate stresses for salt water/aging test

Ultimate Stresses (kPa)									
		Salt				No Salt			
Days	Specimen No.	Foam		Solid		Foam		Solid	
		Primer	No Primer	Primer	No Primer	Primer	No Primer	Primer	No Primer
0	1	168	152	264	229	163	162	348	301
	2	165	175	281	341	142	174	254	330
	3	142	156	215	307	164	172	296	300
	4	146	164	245	287	156	168	273	241
	5	164	150	317	312	165	174	243	315
14	1	163	139	267	384	170	170	293	245
	2	137	245	272	66	139	162	233	215
	3	153	77	282	245	152	162	347	256
	4	141	144	247	301	158	147	159	281
	5	128	151	215	281	154	76	211	251
30	1	134	114	217	241	118	165	246	214
	2	133	139	335	253	128	148	252	249
	3	157	154	268	204	155	96	239	235
	4	100	155	209	267	155	124	271	220
	5	152	145	212	272	137	147	231	289
60	1	141	153	267	139	150	137	142	251
	2	128	155	174	252	124	118	272	293
	3	140	126	301	288	147	124	280	237
	4	128	101	175	248	113	134	211	190
	5	134	137	287	245	134	125	272	234
90	1	129	154	231	315	114	145	342	204
	2	100	36	311	248	104	112	126	215
	3	152	142	115	179	121	146	126	232
	4	65	137	223	158	131	132	272	184
	5	152	135	266	199	113	81	248	164
120	1	112	57	90	102	99	118	100	201
	2	125	123	180	240	102	114	121	176
	3	111	111	129	249	101	105	188	194
	4	128	128	85	122	108	104	221	271
	5	101	129	247	224	118	98	211	132
150	1	69	101	156	149	95	98	131	68
	2	64	91	141	90	98	49	125	161
	3	63	107	144	135	96	118	117	78
	4	84	78	156	149	92	113	143	99
	5	81	100	113	136	94	73	128	126

Table B.3: Ultimate elongation for salt water/aging test

Ultimate Elongation (%)									
		Salt				No Salt			
Days	Specimen No.	Foam		Solid		Foam		Solid	
		Primer	No Primer	Primer	No Primer	Primer	No Primer	Primer	No Primer
0	1	380	480	420	600	425	380	550	370
	2	420	500	678	675	515	400	512	440
	3	430	520	740	700	510	400	585	572
	4	590	530	830	600	160	415	725	720
	5	686	490	715	820	645	440	745	570
14	1	375	400	450	300	410	480	420	580
	2	420	410	585	470	502	510	490	700
	3	520	465	710	510	506	520	730	780
	4	570	435	990	600	579	560	810	840
	5	582	610	741	730	566	600	720	770
30	1	465	410	685	310	440	390	566	380
	2	457	570	760	320	425	410	620	385
	3	620	560	800	300	490	490	731	765
	4	633	635	790	580	550	600	796	990
	5	520	650	980	390	510	540	799	625
60	1	290	460	410	520	290	280	400	515
	2	420	600	689	635	480	520	400	615
	3	415	550	770	635	510	550	720	700
	4	600	510	855	840	530	585	785	710
	5	490	520	930	1025	670	590	800	830
90	1	300	415	620	400	220	270	425	420
	2	420	580	680	420	305	300	490	620
	3	620	645	745	520	310	570	580	910
	4	720	780	800	535	390	580	730	922
	5	610	650	700	550	400	595	600	641
120	1	440	470	735	320	425	300	570	550
	2	585	475	790	400	430	421	710	780
	3	575	510	820	500	480	490	720	800
	4	600	520	825	597	485	600	625	920
	5	590	605	830	820	700	615	640	950
150	1	450	520	715	615	600	400	480	410
	2	590	590	775	685	630	490	610	460
	3	608	625	805	805	690	520	640	560
	4	629	720	820	820	720	540	700	590
	5	622	650	835	830	815	700	750	605

APPENDIX C

```
============================================================
            User Defined Fitting Report

            Data File Name: C:\Projects\Bridge\Adhesive-Failure-
Fraction.pdw
           Model File Name:
C:\Users\IMS\AppData\Roaming\PSIPlot\$PSFIT.EQN

============================================================

  Model Equation(s):
    X1=SALT
    X2=PRIMER
    X3=FOAM
    X4=AGE

Y=A0+A1*X1+A2*X2+A3*X3+A4*X4+A12*X1*X2+A13*X1*X3+A14*X1*X4+A23*X2*X3+A
24*X2*X4+A34*X3*X4

  Fitting Method: Levenberg-Marquardt LSQ

     Number of used data points:               56

  Initial Parameters:
                             A0=              0.4
                             A1=                0
                             A2=                0
                             A3=              0.5
                             A4=                0
                            A12=                0
                            A13=                0
                            A14=                0
                            A23=                0
                            A24=                0
                            A34=                0
  Save Options:
                       Save Data
                  Save Parameter


  Number of Function Calls:                4

  Fitted Parameters:
                            A0=       0.98214286
                            A1=     -0.107142857
                            A2=            -0.05
                            A3=      -0.93571429
                            A4=    -0.0285714286
```

```
                A12=      0.071428571
                A13=              0.1
                A14=    -0.0178571429
                A23=     0.0142857143
                A24=    -0.0035714286
                A34=     0.0142857143

             Chi-Sq:      0.213571429
             SumSqr:      0.213571429
             StdErr:      0.068891449
Covariance Matrix:

            cvm[1,1]:            0.125
            cvm[2,1]:     -0.107142857
            cvm[2,2]:      0.214285714
            cvm[3,1]:     -0.107142857
            cvm[3,2]:      0.071428571
            cvm[3,3]:      0.214285714
            cvm[4,1]:     -0.107142857
            cvm[4,2]:      0.071428571
            cvm[4,3]:      0.071428571
            cvm[4,4]:      0.214285714
            cvm[5,1]:  -1.9680261e-015
            cvm[5,2]:   5.0428765e-015
            cvm[5,3]:   3.0569368e-015
            cvm[5,4]:   1.0188845e-015
            cvm[5,5]:     0.0178571429
            cvm[6,1]:      0.071428571
            cvm[6,2]:     -0.142857143
            cvm[6,3]:     -0.142857143
            cvm[6,4]:   1.2180733e-014
            cvm[6,5]:   -5.493055e-015
            cvm[6,6]:      0.285714286
            cvm[7,1]:      0.071428571
            cvm[7,2]:     -0.142857143
            cvm[7,3]:   6.5072664e-015
            cvm[7,4]:     -0.142857143
            cvm[7,5]:  -2.7480852e-015
            cvm[7,6]:  -4.0022407e-014
            cvm[7,7]:      0.285714286
            cvm[8,1]:   1.9159844e-016
            cvm[8,2]:  -2.2875692e-015
            cvm[8,3]:  -1.4475382e-015
            cvm[8,4]:   4.1208533e-016
            cvm[8,5]:    -0.0089285714
            cvm[8,6]:   2.4538195e-015
            cvm[8,7]:   8.6155572e-016
            cvm[8,8]:     0.0178571429
            cvm[9,1]:      0.071428571
            cvm[9,2]:  -4.7671617e-015
            cvm[9,3]:     -0.142857143
            cvm[9,4]:     -0.142857143
```

```
                    cvm[9,5]:  -2.7613966e-016
                    cvm[9,6]:  -7.6854622e-015
                    cvm[9,7]:   9.3530625e-015
                    cvm[9,8]:  -1.5690397e-016
                    cvm[9,9]:      0.285714286
                   cvm[10,1]:   3.9867486e-015
                   cvm[10,2]:  -8.2850393e-015
                   cvm[10,3]:  -2.3175906e-015
                   cvm[10,4]:  -2.9344441e-015
                   cvm[10,5]:    -0.0089285714
                   cvm[10,6]:    6.672667e-015
                   cvm[10,7]:    6.050149e-015
                   cvm[10,8]:   5.4378271e-017
                   cvm[10,9]:  -1.2422036e-015
                  cvm[10,10]:     0.0178571429
                   cvm[11,1]:    3.174898e-016
                   cvm[11,2]:  -9.4312313e-016
                   cvm[11,3]:  -1.6959223e-015
                   cvm[11,4]:   3.3929775e-016
                   cvm[11,5]:    -0.0089285714
                   cvm[11,6]:   2.5914645e-015
                   cvm[11,7]:  -6.2308435e-017
                   cvm[11,8]:   5.7097184e-016
                   cvm[11,9]:   1.5860329e-016
                  cvm[11,10]:   2.2793558e-015
                  cvm[11,11]:     0.0178571429

Goodness of Fit Statistics ...

                      __ C O D:        0.9811701
                      __ Corrl:       0.99054031
                      __ M S C:       3.57945204
                      __ A I C:     -64.45190076

Parameter Statistics...


Parameter: A0= 0.98214286

                        StdErr:     0.0243568054
                        StdDev:       0.35355339
             Coeff. of Variance:      35.99816341

__95 % Confidence Interval

  __ Uninvariant ...
                          LOW:       0.93308573
                         HIGH:       1.03119998
  __ Supporting Plane ...
                          LOW:       0.86764705
                         HIGH:       1.09663866
```

```
Parameter: A1= -0.107142857

                      StdErr:      0.031890544
                      StdDev:       0.46291005
           Coeff. of Variance:    -432.04937989

__95 % Confidence Interval

  __ Uninvariant ...
                        LOW:      -0.17137371
                       HIGH:     -0.042912004
  __ Supporting Plane ...
                        LOW:     -0.257053057
                       HIGH:      0.042767343


Parameter: A2= -0.05

                      StdErr:      0.031890544
                      StdDev:       0.46291005
           Coeff. of Variance:    -925.82009977

__95 % Confidence Interval

  __ Uninvariant ...
                        LOW:     -0.114230853
                       HIGH:     0.0142308529
  __ Supporting Plane ...
                        LOW:       -0.1999102
                       HIGH:        0.0999102


Parameter: A3= -0.93571429

                      StdErr:      0.031890544
                      StdDev:       0.46291005
           Coeff. of Variance:     -49.47130304

__95 % Confidence Interval

  __ Uninvariant ...
                        LOW:      -0.99994514
                       HIGH:      -0.87148343
  __ Supporting Plane ...
                        LOW:      -1.08562449
                       HIGH:      -0.78580409


Parameter: A4= -0.0285714286

                      StdErr:     0.0092060071
```

```
                        StdDev:      0.133630621
           Coeff. of Variance:    -467.70717335

__95 % Confidence Interval

  __ Uninvariant ...
                          LOW:     -0.047113279
                         HIGH:    -0.0100295785
  __ Supporting Plane ...
                          LOW:     -0.071846776
                         HIGH:     0.0147039185


Parameter: A12= 0.071428571

                        StdErr:      0.036824028
                        StdDev:       0.53452248
           Coeff. of Variance:     748.33147735

__95 % Confidence Interval

  __ Uninvariant ...
                          LOW:   -0.00273882896
                         HIGH:     0.145595972
  __ Supporting Plane ...
                          LOW:     -0.101672817
                         HIGH:       0.24452996


Parameter: A13= 0.1

                        StdErr:      0.036824028
                        StdDev:       0.53452248
           Coeff. of Variance:     534.52248382

__95 % Confidence Interval

  __ Uninvariant ...
                          LOW:     0.0258325996
                         HIGH:        0.1741674
  __ Supporting Plane ...
                          LOW:     -0.073101388
                         HIGH:      0.273101388


Parameter: A14= -0.0178571429

                        StdErr:     0.0092060071
                        StdDev:      0.133630621
           Coeff. of Variance:    -748.33147735

__95 % Confidence Interval
```

```
  __ Uninvariant ...
                          LOW:     -0.036398993
                         HIGH:    0.00068470724
  __ Supporting Plane ...
                          LOW:      -0.06113249
                         HIGH:     0.0254182042


Parameter: A23= 0.0142857143

                       StdErr:      0.036824028
                       StdDev:       0.53452248
            Coeff. of Variance:     3741.6573868

__95 % Confidence Interval

  __ Uninvariant ...
                          LOW:     -0.059881686
                         HIGH:      0.088453115
  __ Supporting Plane ...
                          LOW:     -0.158815674
                         HIGH:      0.187387103


Parameter: A24= -0.0035714286

                       StdErr:     0.0092060071
                       StdDev:      0.133630621
            Coeff. of Variance:    -3741.6573868

__95 % Confidence Interval

  __ Uninvariant ...
                          LOW:    -0.0221132787
                         HIGH:     0.0149704215
  __ Supporting Plane ...
                          LOW:     -0.046846776
                         HIGH:      0.039703919


Parameter: A34= 0.0142857143

                       StdErr:     0.0092060071
                       StdDev:      0.133630621
            Coeff. of Variance:     935.41434669

__95 % Confidence Interval

  __ Uninvariant ...
                          LOW:    -0.0042561358
                         HIGH:      0.032827564
```

```
__ Supporting Plane ...
                        LOW:    -0.0289896328
                       HIGH:      0.057561061
```

6.0 REFERENCES

1. AASHTO. (2012) *Maintenance Manual for Roadways and Bridges*. American Association of State Highway and Transportation Officials. Washington, D.C.

2. ASTM (2003). "Standard Test Method for Hot Water Accelerated Aging of Glass-Fiber Reinforced Cement-Based Composites*," ASTM Standard C1560,* ASTM International, West Conshohocken, PA. www.astm.org (August 1, 2015)

3. ASTM (2000). "Tensile Adhesion Properties of Structural Sealants," *ASTM Standard C1135*. ASTM International, West Conshohocken, PA. www.astm.org (August 1, 2015)

4. ASTM (2009). "Standard Guide for Use of Joint Sealants," *ASTM Standard C1193*, ASTM International, West Conshohocken, PA. www.astm.org (August 1, 2015)

5. BASF. (2015). "Bridge and Highway Maintenance – Expansion Joint Systems," *Watson Bowman Acme Corp*, Amherst, NY.

6. Bramel, B.K., Dolan, C.W., Puckett, J.A., and Ksaibati, K.. (2000). "Asphalt Plug Joints: Refined Material Tests and Design Guidelines." *Transportation Research Record*, No. 1740, pp 126-134.

7. Burke, M.P. (1989). “Bridge Deck Joints.” NCHRP Synthesis 141, Transportation Research Board, Washington, D. C.

8. CT DOT (2015). “Winter Highway Maintenance Operations: Connecticut”. Connecticut Department of Transportation, Newington, CT./Connecticut Academy of Science and Engineering, Rocky Hill CT.

9. CT DOT. (2003). *Bridge Design Manual*. Connecticut Department of Transportation. Newington, CT.

10. CT DOT (2001). *Bridge Inspection Manual Version 2.1*. Connecticut Department of Transportation. Newington, CT.

11. Dornsife, R. J. (2000). Chapter 25: “Expansion joints.” *Bridge engineering handbook, W. F. Chen and L. Duan, eds., CRC,* Boca Raton, Fla.

12. DS Brown. (2015). “Expansion Joint Systems,” *D.S. Brown,* North Baltimore, Ohio, USA.

13. Febajoint. (2015). “Febajoint Highways Agency Type 2 Asphaltic Plug Joint,” *Universal Sealants Company,* United Kingdom.

14. FHWA. (1980).“Expansion Devices for Bridges,” *Technical Advisory T5140.15, U.S. Department of Transportation,* Washington, D.C.

15. Fincher, H. E. (1983). ‘‘Evaluation of rubber expansion joints for bridges.’’ *Rep. No. FHWA/IN/RTC-83/1*, Washington, D.C., 15–16.

16. Gelest. (2003). “Adhesives and sealants.” *Gelest Inc.*, Morrisville, PA. http://www.gelest.com (November 1, 2014)

17. Hamilton, C. D. (1985). “Bridge deck expansion joints final report.” *Rep. No. FHWA-ME-TP-84-04, Maine Department of Transportation*, Augusta, ME.

18. Lee, D. J. (1994). “Bridge bearings and expansion joint.” *Alden Press, Osney Mead*, Oxford, UK.

19. Lesa Systems. (2016). “Lesa G Joint System.” *Lesa Systems Ltd., Auckland, New Zealand.*

20. Malla, R., Shaw, M., Shrestha, M., and Boob, S. (2006). “Sealing small movement bridge expansion joints*.” NETCR-58, Final NETC 02-6 Project Rep.*, New England Transportation Consortium, Fall River, MA.

21. Malla, R. B., Shaw, M. T., Shrestha, M. R., and Brijmohan, S. B. (2007). “Development and laboratory analysis of silicone foam sealant for bridge expansion joints.” *J. Bridge Eng.*, 12(4), 438–448.

22. Malla, R., Shrestha, M., Shaw, M., and Boob, S. (2005). "Experimental evaluation of silicone foam sealant for bridge expansion joints." *Proc., SEM Annual Conf. and Exposition (CD-ROM),* Society for Experimental Mechanics (SEM), Bethel, CT.

23. Malla, R. B., Swanson, B., and Shaw, M. T. (2010). "Laboratory evaluation of a silicone foam sealant for field application of bridge expansion joints." *Proc., 2010 Society for Experimental Mechanics (SEM) Annual Conf. and Exposition*, SEM, Bethel, CT.

24. Malla, R. B., Shrestha, M. R., Shaw, M. T., and Brijmohan, S. B. (2011a). "Temperature aging, compression recovery, creep, and weathering of a foam silicone sealant for bridge expansion joints." *J. Mater. Civ. Eng.*, 23(3), 287–298.

25. Malla, R.B., Shaw, M.T., Swanson, B., and Gionet, T. (2011). " NETC 02-6: Sealing Small Movement Bridge Expansion Joints (Phase 2)– Field Demonstration and Monitoring," *Final Project Report*, *New England Transportation Consortium*, Fall River, MA July 31, 2011, 128 pages http://www.uvm.edu/~transctr/pdf/netc/netcr86_02-6_phase2.pdf (September 15, 2014)

26. Malla, R. B., Swanson, B., and Shaw, M. T. (2011b). "Laboratory evaluation of a silicone foam sealant bonded to various expansion joint header materials." *Constr. Building Mat.*, 25(11), 4132–4143.

27. Milner, M.H. (2014). “Survey of Past Experience and State of the Practice in the Design and Maintenance of Small Movement Expansion Joints in the Northeast”. *Transportation System Preservation Technical Services Program (TSP2).* University of Delaware, Newark, DE.

28. MM Systems. (2015). “Waterproof Expansion Joints.” *MM Systems Corporation,* Pendergrass, GA, USA.

29. Shrestha, M. R., Malla, R. B., Boob, S., and Shaw, M. T. (2006), “Laboratory evaluation of weathering and freeze-thaw effects on silicone foam bridge joint sealant.” *Proc., SEM Annual Conf. and Exposition (CD- ROM),* Society for Experimental Mechanics (SEM), Bethel, CT.

30. IDOT (2011). “Silicone Bridge Joint Sealer.” *Manuals, Guides and Handbooks*, Illinois Department of Transportation, IL.

31. Swanson, B. J. , Malla, R. B., and Shaw, M.T. (2013). "Laboratory Testing, Field Installation, and Monitoring of a Silicone Foam Sealant for Bridge Expansion Joints," *J. Bridge Engineering,* Vol. 18, Num. 8, ASCE, Reston, VA ; August. http://dx.doi.org/10.1061/%28ASCE%29BE.1943-5592.0000425

32. Swanson, H.N., (1983). ”Bridge Deck Expansion Devices” *Report No. COH-DTP-R-83-11*, Colorado Department of Highways.

33. Tremco. (2014). "Sealant Restoration Guide." *Guide to Commercial Sealants and Waterproofing*, Tremco Waterprooding. Beachwood, OH. http://www.thorosystem.com/Documents/SEALANT_RESTORATION_GUIDE_10-6-08.pdf (February 5, 2016).

34. Victor, R. (2013) Report Card for America's Infrastructure. *ASCE*, Reston, VA, 2013.

35. Voigt, G. F., and Yrjanson, W. A. (1992). "Concrete Joint sealant performance evaluation." *Final Rep*., Utah Department of Transportation, Salt Lake City.

36. Watson Bowman Acme. (2001). "WABO_SiliconeSeal installation procedure."

37. *Watson Bowman Acme Corp* Amherst, NY. http://www.wbacorp.com/Products/ProductInstallationProcedures.aspx?ProductlineID=48 (November 1, 2014).

38. Watson Bowman Acme. (2008a). "WABO_SiliconeSeal." *Watson Bowman Acme Corp*., Amherst, NY; https://wbacorp.com/products/bridge-highway/highwaysroads/wabo-siliconeseal-bridge/ (November 1, 2014).

39. Watson Bowman Acme. (2008b). "WABO_SiliconeSeal installation procedure." *Watson Bowman Acme Corp*., Amherst, NY; https://wbacorp.com/public/userfiles/WaboSiliconeSeal_Install.pdf (November 1, 2014).